
UNIVERSITY OF TASMANIA

# Multiplexed electrophoretic systems for the detection and identification of small ions

Adam John Gaudry B.Sc (Hons)

Submitted in fulfilment of the requirements for the Degree of

Doctor of Philosophy

School of Physical Sciences

University of Tasmania

September 2014

# Statements and declarations

*Declaration of originality*

This thesis contains no material which has been accepted for a degree or diploma by the University or any other institution, except by way of background information and duly acknowledged in the thesis, and to the best of my knowledge and belief no material previously published or written by another person except where due acknowledgement is made in the text of this thesis, nor does this thesis contain any material that infringes copyright.

_____ Date: _____

Adam J. Gaudry

*Statement regarding published work contained in this thesis and authority of access*

The publishers of the papers included as part of Chapters 2 to 4 hold the copyright for that content, and access to the material should be sought from the respective journals. The remaining non published content of the thesis may be made available for loan and limited copying and communication in accordance with the *Copyright Act*, 1968.

_____ Date: _____

Adam J. Gaudry

*Statement of co-authorship of published work*

The following people and institutions contributed to the publications of work undertaken as part of this thesis:

Adam J. Gaudry, School of Physical Sciences:

Candidate, primary author of all Chapters

Cameron Johns, University of Tasmania:

Co-author of paper included in Chapter 2.

Emily F. Hilder, University of Tasmania:

Co-author of paper included in Chapter 2.

Greg W. Dicinoski, University of Tasmania:

Co-author of paper included in Chapter 2.

Joseph P. Hutchinson, University of Tasmania:

Co-author of paper included in Chapter 2.

Michael C. Breadmore, University of Tasmania:

Co-author of papers included in Chapters 2, 3 and 4.

Mirek Macka, University of Tasmania:

Co-author of paper included in Chapter 2.

Paul R. Haddad, University of Tasmania:

Co-author of paper included in Chapter 2.

Pavel N. Nesterenko, University of Tasmania:

Co-author of paper included in Chapter 2.

Rosanne M. Guijt, University of Tasmania:

Co-author of papers included in Chapters 2, 3 and 4.

Yi Heng Nai, University of Tasmania:

Co-author of paper included in Chapter 4.

Gaudry, A. J.; Guijt, R. M.; Macka, M.; Hutchinson, J. P.; Johns, C.; Hilder, E. F.; Dicinoski, G. W.; Nesterenko, P. N.; Haddad, P. R.; Breadmore, M. C.; **On-line simultaneous and rapid separation of anions and cations from a single sample using dual-capillary sequential injection-capillary electrophoresis.** *Analytica Chimica Acta* **2013,** *781*, 80-87.

This paper comprises the majority of Chapter 2. Adam Gaudry was the primary author (70%) and conducted all experiments, engineering and programming, analysed all data, interpreted the results and wrote the manuscript. The co-authors contributed a total of 30% to the published work. Michael Breadmore, Rosanne Guijt and Mirek Macka contributed to the idea, its formalisation and development. Cameron Johns and Joseph Hutchinson offered general laboratory assistance. All co-authors assisted with refinement and presentation.

Gaudry, A. J.; Breadmore, M. C.; Guijt, R. M.; **In-plane alloy electrodes for capacitively coupled contactless conductivity detection in poly(methylmethacrylate) electrophoretic chips.** *Electrophoresis* **2013,** *34* (20-21), 2980-2987.

This paper comprises the majority of Chapter 3. Adam Gaudry was the primary author (75%) and conducted all experiments, engineering and programming, analysed all data, interpreted the results and wrote the manuscript. The co-authors contributed a total of 25% to the published work. Michael Breadmore and Rosanne Guijt contributed to the idea, its formalisation and development, offered general laboratory assistance and assisted with refinement and presentation.

Gaudry, A. J.; Nai, Y. H.; Guijt, R. M.; Breadmore, M. C.; **Polymeric microchip for the simultaneous determination of anions and cations by hydrodynamic injection using a dual-channel sequential injection microchip electrophoresis system.** *Analytical Chemistry* **2014,** *86* (7), 3380-3388.

This paper comprises the majority of Chapter 4. Adam Gaudry was the primary author (75%) and conducted all experiments, engineering and programming, analysed all data, interpreted the results and wrote the manuscript. The co-authors contributed a total of 25% to the published work. Rosanne Guijt contributed to the idea, its formalisation and development, assisted with data interpretation, refinement and presentation. Michael Breadmore contributed to the idea, its formalisation and development and assisted with refinement and presentation. Yi Heng Nai provided general laboratory assistance and assisted with refinement and presentation.

We the undersigned agree with the above stated proportion of work undertaken for each of the above published peer-reviewed manuscripts contributing to this thesis:

| | |
|---|---|
| _____ | _____ |
| Michael C. Breadmore | John Dickey |
| Primary Supervisor<br>School of Physical Sciences<br>University of Tasmania | Head of School<br>School of Physical Sciences<br>University of Tasmania |
| Date: _____ | Date: _____ |

# Acknowledgements

There are enough words in this document already. This part is short but be assured, the brevity in no way undermines the depth of my gratitude.

I sincerely thank my supervisors Prof. Michael Breadmore and Dr Rosanne Guijt for their work, guidance and patience over the course of these studies. I also thank Prof. Mirek Macka for his assistance during his time as my supervisor.

I thank the members of the Australian Centre for Research on Separation Science, the School of Chemistry (Physical Sciences) and the staff of the Central Science Laboratory, in particular John Davis, for helping me get this done. Additionally, I would like to thank my family; Mum, Dad and Dave.

Finally: Thanks to Chez, Chum, Guch, Hawkez, Molly, Tom, Troy, Wrighty, and both of the Orders for proving more than fair-weather friends.

# List of publications

1. Gaudry, A. J.; Guijt, R. M.; Macka, M.; Hutchinson, J. P.; Johns, C.; Hilder, E. F.; Dicinoski, G. W.; Nesterenko, P. N.; Haddad, P. R.; Breadmore, M. C., On-line simultaneous and rapid separation of anions and cations from a single sample using dual-capillary sequential injection-capillary electrophoresis. *Analytica Chimica Acta* **2013,** *781*, 80-87.

2. Gaudry, A. J.; Breadmore, M. C.; Guijt, R. M., In-plane alloy electrodes for capacitively coupled contactless conductivity detection in poly(methylmethacrylate) electrophoretic chips. *Electrophoresis* **2013,** *34* (20-21), 2980-2987.

3. Gaudry, A. J.; Nai, Y. H.; Guijt, R. M.; Breadmore, M. C., Polymeric microchip for the simultaneous determination of anions and cations by hydrodynamic injection using a dual-channel sequential injection microchip electrophoresis system. *Analytical Chemistry* **2014,** *86* (7), 3380-3388.

4. Gaudry, A.J.; Breadmore, M.C.; Guijt, R.M., Hydrodynamic Control For Non-Biased Injection And Simultaneous Complementary Analysis, Proceedings of the 17th International Conference on Miniaturized Systems for Chemistry and Life Sciences, 27-31 October **2013**, Frieburg, Germany, pp. 1857-1859. [Refereed Conference Paper]

5. Breadmore, M.C.; Gaudry, A.J.; Guijt, R.M., Electrophoretic separation of analytes, Patent number: WO2014026224 A1. February **2014**.

# List of Abbreviations

| | |
|---|---|
| AA | Acetic Acid |
| AC | Alternating Current |
| BFS | Bare Fused Silica |
| BGE | Background Electrolyte |
| $C^4D$ | Capacitively Coupled Contactless Conductivity Detection |
| CE | Capillary Electrophoresis |
| COTS | Commercial Off-The-Shelf |
| DC | Direct Current |
| EOF | Electroosmotic Flow |
| HDMB | Hexadimethrine bromide |
| HPLC | High Performance Liquid Chromatography |
| HVPS | High Voltage Power Supply |
| IC | Ion Chromatography |
| ICP-MS | Inductively Coupled Plasma Mass Spectrometry |
| LIF | Laser Induced Fluorescence |
| LOC | Lab on a Chip |
| LOD | Limit of Detection |
| LPA | Linear Polyacrylamide |
| ME | Microchip Capillary Electrophoresis |

| | |
|---|---|
| MES | 2-(N-morpholino)ethanesulfonic Acid |
| µTAS | Micro Total Analysis System |
| PDMS | Poly(dimethylsiloxane) |
| PEEK | Polyetheretherketone |
| PMMA | Poly(methylmethacrylate) |
| UV | Ultraviolet |

# Abstract

Capillary electrophoresis (CE) is regarded as a powerful separation technique that is an alternative or complementary technique to more traditional methods such as gel electrophoresis and liquid chromatography. When applied to the separation of inorganic species, capillary electrophoresis still continues to take second place to other competitive techniques such as ion chromatography (IC) and elemental mass spectrometry. CE is often touted as having several obvious advantages over chromatographic techniques (mostly IC) including high resolving power, speed, instrumental simplicity, flexibility and cost-efficiency. On the other hand, CE is frequently cited as having a number of comparative disadvantages such as poor reproducibility and sensitivity. The work undertaken in this thesis describes technical innovations to harness the inherent advantages of CE whilst minimising the disadvantages as part of the development of a system for the rapid determination of common small environmental anions and cations. It is unique in its capability to analyse directly from a sample flow, making it especially attractive for monitoring purposes. To enable a move from a capillary to a chip-based system, simple, low cost techniques for the manufacture of polymeric microchips and the incorporation of detection electrodes were developed using limited resources to provide further improvements in speed and reduce resource consumption. A multiplexed polymeric microchip system was developed employing a novel hydrodynamic injection mechanism to reduce sample matrix effects and injection bias, and to improve the quantitative performance of the system. Finally, a compact multipurpose microfluidic platform is developed to support future research interests.

# Table of contents

# Chapter 1: Introduction

## 1.1 Background

With the rapid advancement in computer processing power, so the capability of faster and increased data capture, processing and analysis has advanced. These advancements enable the possibility of near-real time monitoring to improve notification, warning and response times and assist in predictive modelling of complex processes. One important area of interest to analytical chemists with a wide potential for benefit from the aforementioned advancements is environmental monitoring. Environmental monitoring is an important tool for pollution control of paramount importance to human health and ecological sustainability, as well as economic prosperity. For example, real-time monitoring of highly toxic environmental pollutants such as (but not limited to) heavy metals, especially downstream of tailings mines or industrial areas can provide much improved warning and response times. Whilst investigative analytical demands may be satisfied by current technology, near-real time and predictive evaluations require faster, autonomous, in-situ analysis systems. In order to meet the demands of this application, some researchers have moved towards the use of micro total analysis systems (μTAS) which offer several inherent advantages which are discussed in recent reviews.[1, 2] These μTAS find uses in many different areas from analysis to drug delivery but in environmental monitoring they are most commonly employed in water quality evaluation.[3]

In this thesis, strategies to realise rapid, online water monitoring are examined with particular focus given to the determination of small common environmental anions and cations; a topic of interest to the research group. These analytes are predominately inorganic

but also include small organic ions and provide important environmental information in regards to pollutant and nutrient levels. These analytes are also important in other applications such as continuous monitoring of industrial chemical processes and determination of inorganic explosive residues for example.

## 1.2 Analysis of small ions by capillary electrophoresis (CE)

Over the last three and a half decades [4] CE has become a key separation technique for the analysis of a wide range of ions. It is a continually growing field in all areas including theory, instrumentation, separation modes and applications.[5] In the early 90s, the next evolutionary step in the development of CE occurred with its implementation being demonstrated in the microchip format (ME).[6, 7] This miniaturisation of the electrophoretic process resulted in the generation of a new field of research dedicated to making a μTAS or lab-on-a-chip. Several reviews of fundamental advances and applications of both CE [5, 8-11] and μTAS [12, 13] provide an excellent overview of both research fields. CE and ME can be considered to be a hybrid of more traditional methods such as slab gel electrophoresis and liquid chromatography and are frequently compared to these two methods.[14]

CE was first established as a method for the separation of inorganic ions (and small organic ions) in the early 1990's [15-18] and subsequently, the field has been covered by reviews focussing on many aspects such as detection,[19-23] speciation,[24-27] extension to microfluidic platforms,[28-31] and applications.[32, 33] The large amount of work conducted in this field clearly demonstrates the potential of this methodology, however, a number of perceived drawbacks of CE are consistently cited in these reviews. The most recent review of inorganic analysis using CE by Kubáň and Timerbaev highlights the comparatively tiny number of research

papers in analytical applications of CE to inorganic analysis over the period of review (January 2011 to December 2012) as opposed to the number of publications on applications based upon the analysis of organic or biomolecular analytes.[9] The reviewers state that whilst this trend may be partly attributable to commonly cited inherent disadvantages of CE such as poor repeatability and LODs, the main reason is due to a significant growth and acceptance of elemental mass spectrometry (MS), particularly HPLC-ICP-MS, over the same period. Whilst it is clear that the sensitivity, repeatability and sample throughput of HPLC-ICP-MS cannot be questioned in comparison to CE,[27] these are not always the most important characteristics of an applied analytical technique. In particular, where the application is for in-situ, automated and near-real time analysis and not for use in a laboratory setting, there are several inherent benefits of CE/ME that may provide considerable advantages for the technique, if the inherent disadvantages can be adequately managed.

## 1.3 Minimising the comparative disadvantages of CE/ME for online monitoring applications

In comparison to other LC methods, CE has a number of inherent advantages. These advantages however compete with the commonly accepted cons of CE: poor repeatability and sensitivity. The considerations for minimisation of the inherent disadvantages of CE/ME are first discussed, along with a discussion of detection modes in the context of on-line applications.

### 1.3.1 Repeatability

The issue of poor repeatability in CE/ME is quite complicated but is heavily influenced by sample introduction practices.[14, 34, 35] Obviously, variations in injection volume will effect peak height and area, but in CE/ME, variance in injection volume also effect the migration times of analytes as variations in length of the sample plug alter the electric field distribution along the capillary in relation to the relative conductivities of the BGE and sample. Broad strategies to minimise this contribution to variance include careful selection of injection mode (electro vs hydrodynamic), hardware component selection and optimisation of injection parameters.

Where electrokinetic injection is used another problem is encountered whereby any change in the sample matrix induces a change in the applied electric field applied to the sample which in turn impacts the number of ions that migrate into the capillary.[36, 37] This phenomena is further discussed in Chapters 2 and 4 but potential methods for minimising this contribution to variance include either extracting the analytes from the sample matrix prior to injection at the expense of time, system cost and complexity, or to prepare the sample in the separation BGE, again with the same disadvantages as well as a reduction in the capacity for field-amplified stacking.

Another factor affecting reproducibility in CE/ME is the requirement for a stable and repeatable EOF as both electromigration and electroosmosis transport the analytes through the capillary during separation. In fused silica capillaries with amorphous surface structures, it is common practice to flush new capillaries with 1M NaOH to charge saturate the capillary surface with as many silanol groups as possible to ensure a repeatable EOF. This may or may not be followed by flushing with water and/or acid prior to a final conditioning with the separation BGE. In between electrophoretic separations, conditioning step(s) may be

repeated. Inter-run conditioning adds to the effective run to run time and may also entail additional hardware and system complexity. Another requirement for obtaining a reproducible EOF is to ensure that no sample component adsorbs irreversibly onto the capillary surface which will affect the surface charge and hence EOF.[38] One very popular method for providing consistent and repeatable surface charge is through the use of surface coatings which is covered in recent reviews [39, 40] and examined in Chapter 2.

There are a number of other residual factors that cause changes in migration time between analyses, leading to a reduction in reproducibility. To account for these factors and factors relating to sample introduction and EOF, one may use an appropriate internal standard against which data can be normalised.

### 1.3.2 Sensitivity

Ultimately, the reduced sensitivity of CE/ME as compared to LC is due to the use of much narrower capillaries or channels. These narrow channels are necessary for dissipating the heat generated by the application of the high voltages required for highly efficient separations. With reduced channel volumes come lower injection volumes, meaning less analyte is present for detection in CE/ME as opposed to LC. Hence, the benefits of separation efficiency, and low chemical consumption in CE/ME are to some extent antithetical to sensitivity. Any number of sample pre-concentration methods may be used to increase sensitivity at the expense of time and cost, however manual pre-concentration methods are not suitable for autonomous monitoring applications and whilst on-line sample pre-concentration methods such as various stacking and sweeping techniques and ITP may greatly increase sensitivity, they may also increase hardware and reagent requirements and system complexity. The

subject of increasing sensitivity in electrophoresis, including on-line pre-concentration methods has been covered in a number of recent reviews.[41, 42]

#### *1.3.2.1 Detection*

System sensitivity is also fundamentally related to the detection mode and is a key aspect in the design of CE and ME systems. Optical detection methods, either label-based or label free are commonly used and present several advantages. They generally have good limits of detection, are isolated from the fluid, and can be used to detect a wide variety of compounds.[43, 44] Conventional optical detection systems however are costly, require precise alignment and generally do not translate well to microfluidic devices. Additionally, many optical detection principles such as absorbance and fluorescence perform poorly at smaller geometries due to shorter path lengths. This is certainly a problem in conventional CE and can be exacerbated by even smaller geometries and the material properties of microfluidic devices.[44]

Direct photometric detection is the most commonly used detection technique in CE due to its ready availability and wide applicability. However, this technique is not suitable for most inorganic ions because very few of the analytes exhibit substantial direct absorbance in the wavelengths available to CE instruments although advances in LED technology may provide improvements to sensitivity and significant reduction in size.[45, 46] Considerable work done by means of indirect photometric detection, described in several reviews [20, 22, 47] have led to enhancements in sensitivity for CE detection of small organic and inorganic ions. Laser-Induced Fluorescence is a frequently used optical detection method in microfluidic systems due to its low detection limits.[44] However, analytes that do not natively fluoresce need to be derivatized which may add to analysis time and instrumental complexity in an online monitoring context. The use of chemiluminescence detection (CLD) has been covered in

recent reviews in both capillary [48] and chip [49] format and may be employed without the use of a light source, although photo-initiated CLD has also been described.[50] The principal drawback with CLD as applied to small, on-line systems is its requirement for the conduct of chemical reactions that increase hardware and reagent requirements and system complexity.

Significant advances in the use of MS coupled to CE and ME have recently occurred and are covered in a number of reviews.[27, 51-56] The interfacing of CE and ME systems with MS probably provides the most potential for complex and universal detection for the method, however, whist miniaturised and portable mass spectrometers have already been described,[57, 58] interfacing requires considerable engineering, system complexity is increased and cost remains prohibitive.

Electrochemical (EC) detection techniques have found wide favour in CE and particularly ME techniques due to their small size, low cost, relative ease of incorporation into CE and ME formats and sensitivity. The fundamentals of amperometric, potentiometric and conductometric based detection are beyond the scope of this introduction but an excellent paper relating the basic principles of EC detection to electrophoresis has been produced by Kubáň and Hauser.[59] All EC detection modes have been demonstrated in both capillary and ME format as described in recent reviews.[60-62] Of these techniques, contactless conductivity detection, or more specifically, capacitively coupled contactless conductivity detection ($C^4D$), as applied to electrophoresis in the current common form, with two electrodes arranged axially along the separation channel, has experienced a considerable increase in popularity and progress.

Unlike other EC modes, $C^4D$ does not require direct contact between the detection electrodes and the solution which eliminates problems associated with interference of the separation field with detector electronics and corrosion and fouling of electrodes can be

eliminated. For online, continuous analysis, this places $C^4D$ in an excellent position as it means that the lifetime of the electrodes will be virtually unlimited, unless used in a highly corrosive environment. Additionally, $C^4D$ is a universal detection mode for CE/ME in that all charged species can be quantified. This makes $C^4D$ a useful tool for the determination of small inorganic and organic ions that do not possess chromophores and are not detectable by direct optical means. Several reviews describe the advances and applications of $C^4D$ as used in both the CE and ME format.[63-67] Numerous applications of CE and ME using $C^4D$ focussing on the determination of small anions and cations have been demonstrated [68-72] and it is generally considered that $C^4D$ offers greatly superior sensitivity with regards to these analytes as compared to indirect photometry. Similar analytes studied under optimised conditions report detection sensitivity improvements by factors of 8 [23] to 15 [73] using $C^4D$ over indirect photometric methods. Due to the advantages outlined above, $C^4D$ was chosen as the detection method for use during this thesis and is discussed further in Chapters 2 through 5.

## 1.4 Leveraging the comparative benefits of CE/ME for online monitoring applications

In relation to other LC methods, commonly cited strengths of CE include its high separation efficiency, relatively short analysis times, instrumental simplicity and flexibility, low consumption of chemicals, and cost-efficiency.[14] An overview of the considerations relating to the optimisation of these advantages are given in the context of online monitoring applications.

### 1.4.1 High separation efficiency and fast analysis times

For online monitoring applications both highly efficient separations and fast analysis times are very desirable properties in that they directly contribute to the quality and quantity of data generated. Both of these advantages of CE/ME are intrinsically related to the electric field strength and hence the magnitude of the applied voltage. Increasing the applied voltage will have a number of effects. Whilst it will increase both sample migration and EOF rate, as well as reducing analysis time, it may increase peak sharpness and improve resolution. These advantages may be lost however, if the ionic strength of the sample matrix is considerably greater than the ionic strength of the BGE so that the increased generation of Joule heat cannot be efficiently dissipated. Joule heating of the capillary will result in decreased solution viscosity which leads to further increases in ion mobility, EOF and analyte diffusion which may result in band broadening. This effect is governed by the electric field strength per unit length of capillary/channel so that alterations of capillary lengths need to take into account the applied voltage. Similarly, altering the internal dimensions of the capillary/channel alters the surface-volume ratio with the general rule that decreasing the internal diameter of the capillary, increases its Joule heat dissipation efficiency. Likewise, the temperature of the capillary/channel can be adjusted so as to effect solution viscosity and alter analysis times and separation efficiency. Careful optimisation of separation voltage, temperature, capillary length and internal dimensions can greatly improve the analytical performance of CE/ME as it relates to analysis time and separation efficiency. Modification of the capillary channel wall via coatings has the ability to drastically alter the magnitude and/or direction of the EOF which also impacts analysis time but must also be considered in the context of its effect upon reproducibility as discussed in Section 1.3.1 and other factors as examined in Chapter 2.

Another method of shortening analysis times is by the judicious application of hydrodynamic flow during separation.[74-76] Hydrodynamic flow however, may reduce efficiency by effectively shortening the separation space and reducing the number of theoretical plates available to the electrophoretic process for a fixed separation length. Hydrodynamic flow may also impart a parabolic flow profile to the sample plug and/ or separation flow which may result in band broadening and a reduction in efficiency. The importance of the sample plug geometry is further discussed in Chapter 4. Finally, the choice of BGE is critical to nearly all performance parameters of a CE/ME system including analysis time and is discussed further in Chapter 2.

### 1.4.2 Instrumental simplicity and flexibility

The inherent simplicity of instrumentation required for electrophoretic separations automatically lends itself to the potential for miniaturisation and low capital cost in terms of hardware. Miniaturisation may in turn enhance the benefits of low chemical consumption and cost-efficiency. Whilst the main thrust towards miniaturisation in electrophoresis is towards chip-based systems, considerable work has been conducted towards the development of field-deployable or portable capillary-based (non-chip) electrophoresis which is covered in an excellent review by Ryvolová *et al*.[77]

The practical advantages of field-deployable or portable instrumentation include the ability to conduct analysis in close proximity to where the sample is taken, reducing the likelihood of sample decomposition and reducing the time and cost of analysis. These benefits apply particularly to environmental,[72, 78] point-of-care,[79-81] forensic [82, 83] and military applications [84] where this chemical information is often required in a short period of time. Whilst portability is an important consideration for many applications, the trend towards

miniaturisation of analytical instrumentation also achieves the goals of reducing sample and reagent consumption, power usage and cost.

CE has a number of different separation modes allowing for analytes to be separated in a number of different ways including zone electrophoresis, electrokinetic chromatography (EKC), electrochromatography (EC), isotachophoresis (ITP) and isoelectric focusing (IEF) amongst others. Whilst LC has a number of different separation modes as well, it is much simpler to change from one mode to the other in CE. In all CE and ME modes, except for EC, all that is required to change from one mode to another is a change in the composition of the background electrolyte. Where several separation modes are required to be combined, for example, pre-concentration via ITP followed by zone electrophoresis, the benefits of this flexibility may be leveraged by CE and ME. Where multiple sample processing steps are required to be performed such as sample extraction, pre-concentration and separation, the opportunities exists for all the functions to be incorporated onto µTAS devices. Additionally, where multiple separations are required to be run simultaneously, the instrumental and design simplicity and inherent flexibility of CE and ME may be leveraged to reduce analysis times. The degree to which these functions are performed on or off-chip necessarily involves a complex trade-off between system complexity, hardware requirements and analytical performance and is further discussed in Chapter 5.

### 1.4.3 Low consumption of chemicals and cost-efficiency.

Ultimately, it is of very little practical benefit to develop systems, no matter how good, whose costs prohibit them from ever being used. These costs include capital costs involving research

and design, hardware and construction costs as well as ongoing costs principally associated with manning, consumables, waste disposal and maintenance.

The microscale dimensions involved in fluidic manipulation in CE and ME automatically work in favour of reduced chemical consumption, but design consideration given to minimise feeder tubing and channels can significantly reduce consumption levels, and hence reduce ongoing costs. Alhusban et al. quote using less than 9 µL of sample and approximately 1.1 ml of BGE per analysis running a three-day near-real time monitoring of extracellular lactate in cell culture flasks.[85] Effective storage of perishable reagents so as to maximise their effective working life is another important consideration. As compared to LC, not only the quantity of waste but the nature of most BGEs lends itself to lower costs relating to disposal as most are water-based solutions as compared to the organic mobile phases typically employed in LC.

In an on-line, autonomous monitoring method, the costs associated with manning are nearly eliminated, with the exception of back-end data analysis (if required) and maintenance. Maintenance may be reduced by clever instrumental design focussed on robust, repeatable performance. The system should be as simple as possible, because the simpler the system, the less that can go wrong. The trade off with regards to simplicity (and lower costs) is system capability and performance. All of the considerations relating to the inherent advantages and disadvantages of CE/ME have been taken into account during the conduct of work undertaken in this thesis.

## 1.5 Aims

The core aim of this work was to develop multiplexed electrophoretic separation systems for the determination of small anions and cations. The specific application driving this research was the development of a rapid technique for autonomous, near-real time monitoring of common small environmental items including inorganic and small organic analytes. To this end, three primary objectives were identified;

1. The development of a multiplexed electrophoretic separation system in the CE format for the simultaneous, rapid and autonomous determination of common small environmental anions and cations,

2. The development of a simple, low cost method for developing robust hard-polymer microchips and associated detection and interfacing components using available resources, and

3. The transfer of techniques and instrumentation developed in the CE format to the ME format.

## 1.6 References


1. Jokerst, J. C.; Emory, J. M.; Henry, C. S., Advances in microfluidics for environmental analysis. *Analyst* **2012,** *137*, 24-34.

2. Campos, C. D. M.; Da Silva, J. A. F., Applications of autonomous microfluidic systems in environmental monitoring. *RSC Advances* **2013,** *3*, 18216-18227.

3. Ríos, Á.; Zougagh, M.; Avila, M., Miniaturization through lab-on-a-chip: Utopia or reality for routine laboratories? A review. *Analytica Chimica Acta* **2012,** *740*, 1-11.

4. Jorgenson, J. W.; Lukacs, K. D., ZONE ELECTROPHORESIS IN OPEN-TUBULAR GLASS CAPILLARIES. *Analytical Chemistry* **1981,** *53*, 1298-1302.

5. Geiger, M.; Hogerton, A. L.; Bowser, M. T., Capillary electrophoresis. *Analytical Chemistry* **2012,** *84*, 577-596.

6. Harrison, D. J.; Manz, A.; Fan, Z.; Lüdi, H.; Widmer, H. M., Capillary electrophoresis and sample injection systems integrated on a planar glass chip. *Analytical Chemistry* **1992,** *64*, 1926-1932.

7. Harrison, D. J.; Fluri, K.; Seiler, K.; Fan, Z.; Effenhauser, C. S.; Manz, A., Micromachining a miniaturized capillary electrophoresis-based chemical analysis system on a chip. *Science* **1993,** *261*, 895-897.

8. Tubaon, R. M. S.; Rabanes, H.; Haddad, P. R.; Quirino, J. P., Capillary electrophoresis of natural products: 2011-2012. *Electrophoresis* **2014,** *35*, 190-204.

9. Kubáň, P.; Timerbaev, A. R., Inorganic analysis using CE: Advanced methodologies to face old challenges. *Electrophoresis* **2014,** *35*, 225-233.

10. Zhao, J.; Hu, D. J.; Lao, K.; Yang, Z. M.; Li, S. P., Advance of CE and CEC in phytochemical analysis (2012-2013). *Electrophoresis* **2014,** *35*, 205-224.

11. Kašička, V., Recent developments in capillary and microchip electroseparations of peptides (2011-2013). *Electrophoresis* **2014,** *35*, 69-95.

12. Nge, P. N.; Rogers, C. I.; Woolley, A. T., Advances in microfluidic materials, functions, integration, and applications. *Chemical Reviews* **2013,** *113*, 2550-2583.

13. Culbertson, C. T.; Mickleburgh, T. G.; Stewart-James, S. A.; Sellens, K. A.; Pressnall, M., Micro total analysis systems: Fundamental advances and biological applications. *Analytical Chemistry* **2014,** *86*, 95-118.

14. Breadmore, M. C., Capillary and microchip electrophoresis: Challenging the common conceptions. *Journal of Chromatography A* **2012,** *1221*, 42-55.

15. Jones, W. R.; Jandik, P., Controlled changes of selectivity in the separation of ions by capillary electrophoresis. *Journal of Chromatography A* **1991,** *546*, 445-458.

16. Jandik, P.; Jones, W. R., Optimization of detection sensitivity in the capillary electrophoresis of inorganic anions. *Journal of Chromatography A* **1991,** *546*, 431-443.

17. Romano, J.; Jandik, P.; Jones, W. R.; Jackson, P. E., Optimization of inorganic capillary electrophoresis for the analysis of anionic solutes in real samples. *Journal of Chromatography A* **1991,** *546*, 411-421.

18. Weston, A.; Brown, P. R.; Jandik, P.; Jones, W. R.; Heckenberg, A. L., Factors affecting the separation of inorganic metal cations by capillary electrophoresis. *Journal of Chromatography A* **1992,** *593*, 289-295.

19. Doble, P.; MacKa, M.; Haddad, P. R., Use of dyes as indirect detection probes for the high-sensitivity determination of anions by capillary electrophoresis. *Journal of Chromatography A* **1998,** *804*, 327-336.

20. Doble, P.; Haddad, P. R., Indirect photometric detection of anions in capillary electrophoresis. *Journal of Chromatography A* **1999,** *834*, 189-212.

21. Coufal, P.; Pacáková, V.; Štulík, K., An evaluation of the experimental approaches to detection of small ions in CE. *Electrophoresis* **2007,** *28*, 3379-3389.

22. Doble, P.; Macka, M.; Haddad, P. R., Design of background electrolytes for indirect detection of anions by capillary electrophoresis. *TrAC - Trends in Analytical Chemistry* **2000,** *19*, 10-17.

23. Johns, C.; Breadmore, M. C.; Macka, M.; Ryvolová, M.; Haddad, P. R., Recent significant developments in detection and method development for the determination of inorganic ions by CE. *Electrophoresis* **2009,** *30*, S53-S67.

24. Timerbaev, A. R., Element speciation analysis by capillary electrophoresis. *Talanta* **2000,** *52*, 573-606.

25. Timerbaev, A. R., Element speciation analysis by capillary electrophoresis: What are the hints on becoming a standard analytical methodology? *Analytica Chimica Acta* **2001,** *433*, 165-180.

26. Dabek-Zlotorzynska, E.; P.C. Lai, E.; R. Timerbaev, A., Capillary electrophoresis: The state-of-the-art in metal speciation studies. *Analytica Chimica Acta* **1998,** *359*, 1-26.

27. Timerbaev, A. R., Element speciation analysis using capillary electrophoresis: Twenty years of development and applications. *Chemical Reviews* **2013,** *113*, 778-812.

28. Willauer, H. D.; Collins, G. E., Analysis of inorganic and small organic ions with the capillary electrophoresis microchip. *Electrophoresis* **2003,** *24*, 2193-2207.

29. Evenhuis, C. J.; Guijt, R. M.; Macka, M.; Haddad, P. R., Determination of inorganic ions using microfluidic devices. *Electrophoresis* **2004,** *25*, 3602-3624.

30. Li, X. A.; Zhou, D. M.; Xu, J. J.; Chen, H. Y., Determination of chloride, chlorate and perchlorate by PDMS microchip electrophoresis with indirect amperometric detection. *Talanta* **2008,** *75*, 157-162.

31. Masár, M.; Bomastyk, B.; Bodor, R.; Horčičiak, M.; Danč, L.; Troška, P.; Kuss, H. M., Determination of chloride, sulfate and nitrate in drinking water by microchip electrophoresis. *Microchimica Acta* **2012,** *177*, 309-316.

32. Timerbaev, A. R., Inorganic analysis of biological fluids using capillary electrophoresis. *Journal of Separation Science* **2008,** *31*, 2012-2021.

33. Crevillén, A. G.; Hervás, M.; López, M. A.; González, M. C.; Escarpa, A., Real sample analysis on microfluidic devices. *Talanta* **2007,** *74*, 342-357.

34. Huang, X.; Luckey, J. A.; Gordon, M. J.; Zare, R. N., Quantitative analysis of low molecular weight carboxylic acids by capillary zone electrophoresis/conductivity detection. *Analytical Chemistry* **1989,** *61*, 766-770.

35. Jones, W. R.; Jandik, P., Various approaches to analysis of difficult sample matrices of anions using capillary ion electrophoresis. *Journal of Chromatography A* **1992,** *608*, 385-393.

36. Huang, X.; Gordon, M. J.; Zare, R. N., Bias in quantitative capillary zone electrophoresis caused by electrokinetic sample injection [2]. *Analytical Chemistry* **1988,** *60*, 375-377.

37. Van Der Moolen, J. N.; Boelens, H. F. M.; Poppe, H.; Smit, H. C., Origin and correction of bias caused by sample injection and detection in capillary zone electrophoresis. *Journal of Chromatography A* **1996,** *744*, 103-113.

38. Liu, C.; Kang, J., Improved capillary electrophoresis frontal analysis by dynamically coating the capillary with polyelectrolyte multilayers. *Journal of Chromatography A* **2012,** *1238*, 146-151.

39. Lucy, C. A.; MacDonald, A. M.; Gulcev, M. D., Non-covalent capillary coatings for protein separations in capillary electrophoresis. *Journal of Chromatography A* **2008,** *1184*, 81-105.

40. Huhn, C.; Ramautar, R.; Wuhrer, M.; Somsen, G. W., Relevance and use of capillary coatings in capillary electrophoresis-mass spectrometry. *Analytical and Bioanalytical Chemistry* **2010,** *396*, 297-314.

41. Breadmore, M. C.; Shallan, A. I.; Rabanes, H. R.; Gstoettenmayr, D.; Abdul Keyon, A. S.; Gaspar, A.; Dawod, M.; Quirino, J. P., Recent advances in enhancing the sensitivity of electrophoresis and electrochromatography in capillaries and microchips (2010-2012). *Electrophoresis* **2013,** *34*, 29-54.

42. Kitagawa, F.; Otsuka, K., Recent applications of on-line sample preconcentration techniques in capillary electrophoresis. *Journal of Chromatography A* **2014,** *1335*, 43-60.

43. Mogensen, K. B.; Kutter, J. P., Optical detection in microfluidic systems. *Electrophoresis* **2009,** *30*, S92-S100.

44. Myers, F. B.; Lee, L. P., Innovations in optical microfluidic technologies for point-of-care diagnostics. *Lab on a Chip - Miniaturisation for Chemistry and Biology* **2008,** *8*, 2015-2031.

45. Rodat-Boutonnet, A.; Naccache, P.; Morin, A.; Fabre, J.; Feurer, B.; Couderc, F., A comparative study of LED-induced fluorescence and laser-induced fluorescence in SDS-CGE: Application to the analysis of antibodies. *Electrophoresis* **2012,** *33*, 1709-1714.

46. Enzonga, J.; Ong-Meang, V.; Couderc, F.; Boutonnet, A.; Poinsot, V.; Tsieri, M. M.; Silou, T.; Bouajila, J., Determination of free amino acids in african gourd seed milks by capillary electrophoresis with light-emitting diode induced fluorescence and laser-induced fluorescence detection. *Electrophoresis* **2013,** *34*, 2632-2638.

47. Johns, C.; Macka, M.; Haddad, P. R., Enhancement of detection sensitivity for indirect photometric detection of anions and cations in capillary electrophoresis. *Electrophoresis* **2003,** *24*, 2150-2167.

48. García-Campaña, A. M.; Lara, F. J.; Gámiz-Gracia, L.; Huertas-Pérez, J. F., Chemiluminescence detection coupled to capillary electrophoresis. *TrAC - Trends in Analytical Chemistry* **2009,** *28*, 973-986.

49. Mirasoli, M.; Guardigli, M.; Michelini, E.; Roda, A., Recent advancements in chemical luminescence-based lab-on-chip and microfluidic platforms for bioanalysis. *Journal of Pharmaceutical and Biomedical Analysis* **2014,** *87*, 36-52.

50. Zhang, X.; Zhang, J.; Wu, X.; Lv, Y.; Hou, X., Light-emitting-diode-induced chemiluminescence detection for capillary electrophoresis. *Electrophoresis* **2009,** *30*, 1937-1942.

51. Pantůčková, P.; Gebauer, P.; Boček, P.; Kílvánková, L., Electrolyte systems for on-line CE-MS: Detection requirements and separation possibilities. *Electrophoresis* **2009,** *30*, 203-214.

52. He, X.; Chen, Q.; Zhang, Y.; Lin, J. M., Recent advances in microchip-mass spectrometry for biological analysis. *TrAC - Trends in Analytical Chemistry* **2014,** *53*, 84-97.

53. Krenkova, J.; Foret, F., On-line CE/ESI/MS interfacing: Recent developments and applications in proteomics. *Proteomics* **2012,** *12*, 2978-2990.

54. Stalmach, A.; Albalat, A.; Mullen, W.; Mischak, H., Recent advances in capillary electrophoresis coupled to mass spectrometry for clinical proteomic applications. *Electrophoresis* **2013,** *34*, 1452-1464.

55. Klepárník, K., Recent advances in the combination of capillary electrophoresis with mass spectrometry: From element to single-cell analysis. *Electrophoresis* **2013,** *34*, 70-85.

56. Lee, J.; Soper, S. A.; Murray, K. K., Microfluidic chips for mass spectrometry-based proteomics. *Journal of Mass Spectrometry* **2009,** *44*, 579-593.

57. Yang, M.; Kim, T. Y.; Hwang, H. C.; Yi, S. K.; Kim, D. H., Development of a Palm Portable Mass Spectrometer. *Journal of the American Society for Mass Spectrometry* **2008,** *19*, 1442-1448.

58. Malcolm, A.; Wright, S.; Syms, R. R. A.; Moseley, R. W.; O'Prey, S.; Dash, N.; Pegus, A.; Crichton, E.; Hong, G.; Holmes, A. S.; Finlay, A.; Edwards, P.; Hamilton, S. E.; Welch, C. J., A miniature mass spectrometer for liquid chromatography applications. *Rapid Communications in Mass Spectrometry* **2011,** *25*, 3281-3288.

59. Kubáň, P.; Hauser, P. C., Fundamentals of electrochemical detection techniques for CE and MCE. *Electrophoresis* **2009,** *30*, 3305-3314.

60. Matysik, F. M., Advances in amperometric and conductometric detection in capillary and chip-based electrophoresis. *Microchimica Acta* **2008,** *160*, 1-14.

61. Mark, J. J. P.; Scholz, R.; Matysik, F. M., Electrochemical methods in conjunction with capillary and microchip electrophoresis. *Journal of Chromatography A* **2012,** *1267*, 45-64.

62. Gencoglu, A.; Minerick, A. R., Electrochemical detection techniques in micro- and nanofluidic devices. *Microfluidics and Nanofluidics* **2014**.

63. Kubáň, P.; Hauser, P. C., A review of the recent achievements in capacitively coupled contactless conductivity detection. *Analytica Chimica Acta* **2008,** *607*, 15-29.

64. Kubáň, P.; Hauser, P. C., Ten years of axial capacitively coupled contactless conductivity detection for CZE - A review. *Electrophoresis* **2009,** *30*, 176-188.

65. Kubáň, P.; Hauser, P. C., Capacitively coupled contactless conductivity detection for microseparation techniques - recent developments. *Electrophoresis* **2011,** *32*, 30-42.

66. Mai, T. D.; Hauser, P. C., Contactless conductivity detection for electrophoretic microseparation techniques. *Chemical Record* **2012,** *12*, 106-113.

67. Kubáň, P.; Hauser, P. C., Contactless conductivity detection for analytical techniques: Developments from 2010 to 2012. *Electrophoresis* **2013,** *34*, 55-69.

68. Kubáň, P.; Evenhuis, C. J.; Macka, M.; Haddad, P. R.; Hauser, P. C., Comparison of different contactless conductivity detectors for the determination of small inorganic ions by capillary electrophoresis. *Electroanalysis* **2006,** *18*, 1289-1296.

69. Neaga, I. O.; Iacob, B. C.; Bodoki, E., The analysis of small ions with physiological implications using capillary electrophoresis with contactless conductivity detection. *Journal of Liquid Chromatography and Related Technologies* **2014,** *37*, 2072-2090.

70. Wan, Q. J.; Kubáň, P.; Tanyanyiwa, J.; Rainelli, A.; Hauser, P. C., Determination of major inorganic ions in blood serum and urine by capillary electrophoresis with contactless conductivity detection. *Analytica Chimica Acta* **2004,** *525*, 11-16.

71. Nguyen, H. T. A.; Kubáň, P.; Pham, V. H.; Hauser, P. C., Study of the determination of inorganic arsenic species by CE with capacitively coupled contactless conductivity detection. *Electrophoresis* **2007,** *28*, 3500-3506.

72. Mai, T. D.; Pham, T. T. T.; Pham, H. V.; Sáiz, J.; Ruiz, C. G.; Hauser, P. C., Portable capillary electrophoresis instrument with automated injector and contactless conductivity detection. *Analytical Chemistry* **2013,** *85*, 2333-2339.

73. Blanco, G. A.; Nai, Y. H.; Hilder, E. F.; Shellie, R. A.; Dicinoski, G. W.; Haddad, P. R.; Breadmore, M. C., Identification of inorganic improvised explosive devices using sequential injection capillary electrophoresis and contactless conductivity detection. *Analytical Chemistry* **2011,** *83*, 9068-9075.

74. Mai, T. D.; Hauser, P. C., Anion separations with pressure-assisted capillary electrophoresis using a sequential injection analysis manifold and contactless conductivity detection. *Electrophoresis* **2011,** *32*, 3000-3007.

75. Mai, T. D.; Hauser, P. C., Study on the interrelated effects of capillary diameter, background electrolyte concentration, and flow rate in pressure assisted capillary electrophoresis with contactless conductivity detection. *Electrophoresis* **2013,** *34*, 1796-1803.

76. Mai, T. D.; Hauser, P. C., Pressure-assisted capillary electrophoresis for cation separations using a sequential injection analysis manifold and contactless conductivity detection. *Talanta* **2011,** *84*, 1228-1233.

77. Ryvolová, M.; Macka, M.; Brabazon, D.; Preisler, J., Portable capillary-based (non-chip) capillary electrophoresis. *TrAC - Trends in Analytical Chemistry* **2010,** *29*, 339-353.

78. Sáiz, J.; Mai, T. D.; Hauser, P. C.; García-Ruiz, C., Determination of nitrogen mustard degradation products in water samples using a portable capillary electrophoresis instrument. *Electrophoresis* **2013,** *34*, 2078-2084.

79. Shallan, A. I.; Gaudry, A. J.; Guijt, R. M.; Breadmore, M. C., Tuneable nanochannel formation for sample-in/answer-out devices. *Chemical Communications* **2013,** *49*, 2816-2818.

80. Guihen, E., Recent advances in miniaturization-The role of microchip electrophoresis in clinical analysis. *Electrophoresis* **2014,** *35*, 138-146.

81. Gervais, L.; De Rooij, N.; Delamarche, E., Microfluidic chips for point-of-care immunodiagnostics. *Advanced Materials* **2011,** *23*, H151-H176.

82. Hutchinson, J. P.; Evenhuis, C. J.; Johns, C.; Kazarian, A. A.; Breadmore, M. C.; Macka, M.; Hilder, E. F.; Guijt, R. M.; Dicinoski, G. W.; Haddad, P. R., Identification of inorganic improvised explosive devices by analysis of postblast residues using portable capillary electrophoresis instrumentation and indirect photometric detection with a light-emitting diode. *Analytical Chemistry* **2007,** *79*, 7005-7013.

83. Hutchinson, J. P.; Johns, C.; Breadmore, M. C.; Hilder, E. F.; Guijt, R. M.; Lennard, C.; Dicinoski, G.; Haddad, P. R., Identification of inorganic ions in post-blast explosive residues using portable CE instrumentation and capacitively coupled contactless conductivity detection. *Electrophoresis* **2008,** *29*, 4593-4602.

84. da Costa, E. T.; Neves, C. A.; Hotta, G. M.; Vidal, D. T. R.; Barros, M. F.; Ayon, A. A.; Garcia, C. D.; Do Lago, C. L., Unmanned platform for long-range remote analysis of volatile compounds in air samples. *Electrophoresis* **2012,** *33*, 2650-2659.

85. Alhusban, A. A.; Gaudry, A. J.; Breadmore, M. C.; Gueven, N.; Guijt, R. M., On-line sequential injection-capillary electrophoresis for near-real-time monitoring of extracellular lactate in cell culture flasks. *Journal of Chromatography A* **2014,** *1323*, 157-162.

# Chapter 2: Dual Capillary Sequential Injection Capillary Electrophoresis (DCSI-CE) studies

## 2.1 Introduction

Simultaneous analysis of anions and cations negates the requirement for two separate analyses, thus reducing sample consumption and decreasing the time required. Technically however, this can be difficult to achieve. It can be done by ion chromatography, through for example, the use of a zwitterionic functionalised surface, called electrostatic ion chromatography or by direct coupling of two columns.[1-4] The only other viable chromatographic approach is the use of two separate instruments coupled together in some way. In most instances, separations of less than 10 anions and cations are achieved with separation times from 10-30 min.

An alternative approach is to use capillary electrophoresis (CE). In conventional CE, simultaneous analysis of anions and cations is difficult because one of the charged species must migrate against the electroosmotic flow (EOF). It is possible to separate both anions and cations but only when the EOF is greater than the electrophoretic mobility of all of the target analytes having opposite polarity to the separation electrode,[5] and the closer in magnitude of the EOF with the analyte of highest mobility, the longer is the total analysis time. The practical drawback of this approach is that it is not suitable for the separation of the complete range of inorganic ions. With a cathodic EOF, this approach can separate the full range of cations, but is only suitable for low mobility anions. With an anodic EOF the reverse is true in that the full range of anions can be separated but only the low mobility cations. The peak capacity of the ions separated in a co-EOF manner is also compromised due to the speed at which they reach the detector.

A clever method designed to overcome this problem was demonstrated in 1998 by Kubáň and Karlberg [6] and Padarauskas *et al.*[7] This approach, termed "Dual-Opposite end Injection" (DOI-CE), relies upon the injection of positively and negatively charged species from opposite ends of the capillary. This injection may occur simultaneously (electrokinetic injection) or sequentially (electrokinetic or hydrodynamic injection). During electrophoretic analysis which occurs under conditions of reduced EOF, analytes migrate from each end of the capillary, and in opposite directions towards the detector located near the centre of the capillary. A number of papers [8-10] have been published on the successful application of this technique in conjunction with UV or $C^4D$ detection for the simultaneous determination of small anions and cations. Whilst simple, the compromise with this approach is that the separation space is reduced so there must be precise control of the timing to ensure that anions and cations do not reach the detector at the same time.

Haumann *et al.* compared both approaches for the simultaneous determination of anionic and cationic species.[11] Initially, a high pH was used to maximise the EOF in an uncoated fused-silica capillary; however, this resulted in the formation of insoluble alkaline earth metal hydroxides. This was overcome by separating at pH 6.0, but in order to separate all the anions, the addition of a hydrodynamic pressure was required, which resulted in an increase in zone broadening, especially for high mobility anions, and a loss in resolution of cationic species. A third method studied was a DOI-CE approach using hydrodynamic injection and this was found to be superior to the other methods. During the course of this work, Mai and Hauser examined the use of hydrodynamic injection in narrower diameter (10 μm i.d.) capillaries with the result that Taylor dispersion was minimal due to the narrow capillary diameter.[12] They also introduced additional approaches in which the sample was

injected and hydrodynamically positioned in the centre of the capillary before application of the voltage and with anions and cations detected at opposite ends of the capillary.

An alternative approach for simultaneous CE separation of anions and cations involves the use of an anionic complexing agent that also serves as the anionic indirect detection probe.[13-15] Metal ions are converted to their chelated forms with EDTA [13] or 2,6-pyridinedicarboxylate [14, 15] and separated from other anionic components under conventional anion separation conditions. Whilst this simplifies the experimental set-up, it is only applicable to metals that can form a strong, anionic complex and is not suitable for all alkali and alkaline earth metals.

An entirely different approach was introduced by Bächmann *et al.* based on a single pressure injection to introduce the sample onto two different capillaries, using the same background electrolyte (BGE) in both capillaries, with detection performed using two fluorescence detectors operated in the indirect mode.[16] Recently, in a very similar method, Reschke *et al.* [17] demonstrated the simultaneous separation of cations and anions on a microfluidic device with suppressed EOF and a single injection point. In this method, a single pressure-driven sample injection stream was simultaneously siphoned in two directions into separate microchannels for electrophoretic separation. Hydrodynamic restrictors at the entrance to the electrophoretic separation channels allowed the achievement of high separation efficiencies. The methods of Bächmann *et al.* and Reschke *et al.* have similarities to the technique presented in the present study. Here, hydrodynamic suppression is achieved solely through the optimisation of channel geometry and flow-rates and is constructed from simple commercially available components, while injection is achieved by simultaneously applying equal and opposite potential differences at the outlet end of each capillary and grounding at the approximate centre of the separation interface. This method

also does not require splitting the sample as was required to generate the hydrodynamic flow in the device proposed by Reschke *et al*.[17]

## 2.2 Experimental

### 2.2.1 Apparatus

A DCSI-CE system was developed in-house, based upon a modified design of the instrument designed for the rapid separation of inorganic explosive anions by Blanco Heras *et al.*[18] A schematic representation of the bench-top system is depicted at Figure 2.1 (a).

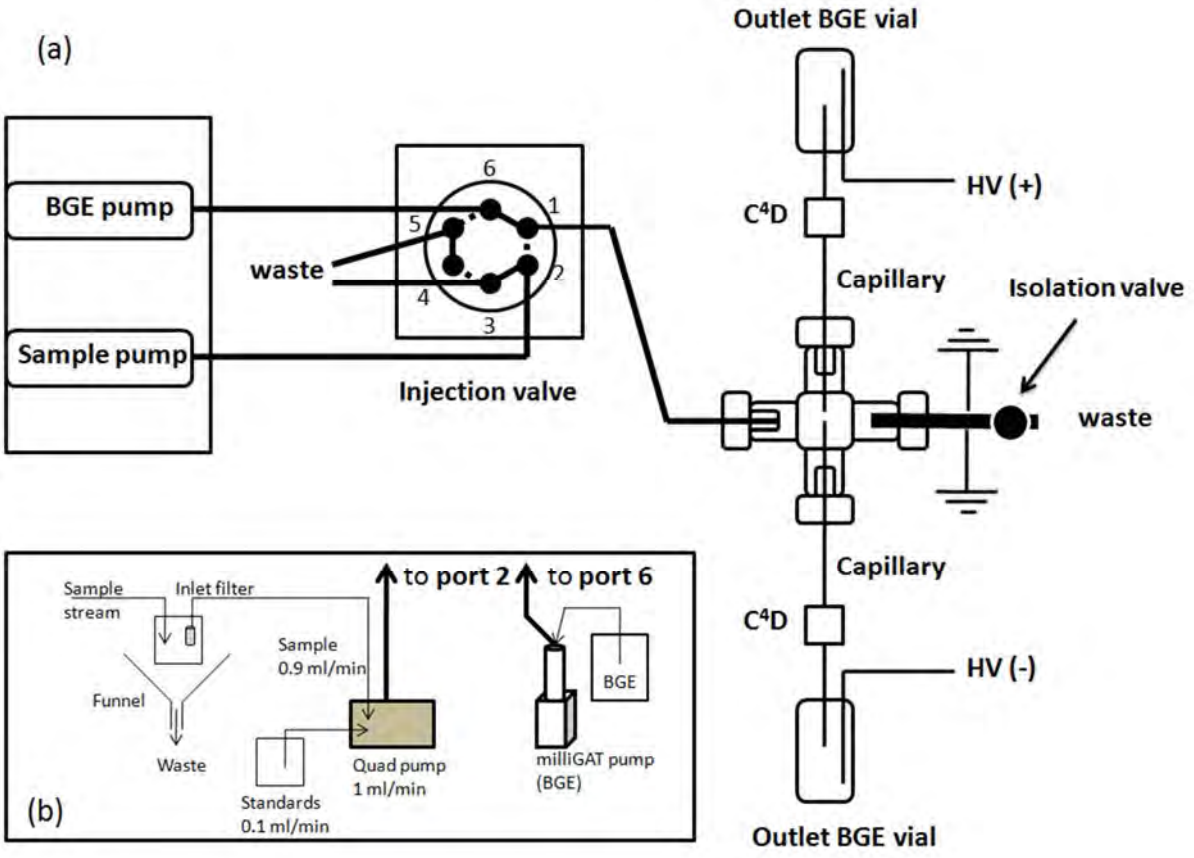


**Figure 2.1:** (a) Schematic diagram of the SI-CE bench top system. HV: High Voltage electrodes, $C^4D$: capacitively-coupled contactless conductivity detectors. (b) Schematic diagram of the SI-CE system adapted for on-line sampling.

A double syringe pump (Harvard Apparatus, Model 33, Holliston, MA, USA) was used to deliver sample and BGE to the system. Two 20 mL plastic syringes (Livingstone, Holliston, MA, USA) or glass syringes (Hamilton, Reno, NV, USA) were used. A two-position injector valve (MXP-7980, Rheodyne, Oak Harbor, WA, USA) enabled the alternate delivery of sample or BGE to the separation interface. A PEEK cross-piece connection (P-729, Upchurch Scientific, Oak Harbor, WA, USA) of 500 µm i.d. was used to interface the two capillaries to the flow system. A 20 mm stainless steel tube cut from a syringe needle (0.51 mm i.d.) served as a waste outlet and ground electrode. An isolation valve (HP225K021, NResearch, West Caldwell, NJ, USA) mounted on the cross-piece outlet line allowed for the on-line flushing of capillaries for equilibration and cleaning.

Two separate fused-silica capillaries of 50 µm i.d. (Polymicro, Phoenix, AR, USA) were utilised for the anion and cation separations. The distance between the two capillary tips within the interface was fixed by utilising a piece of capillary (360 µm o.d.) inserted through the flow-through arm of the crosspiece and by resting the two separation capillaries against opposite sides of the central capillary. The outlet sides of both separation capillaries were inserted into a 20 mL glass vial containing 15 mL of BGE.

For on-line sampling, the outlet line from a quaternary gradient HPLC pump (Alltech 727, Grace Division Discovery Science, Archerfield, QLD, AUS) was connected to the two-position valve instead of the sample syringe. This quaternary pump sampled directly from an overflow container on one inlet line and an internal standard container on a second inlet line. BGE was delivered to the system via a milliGAT pump/MForce controller (MG-5, GlobalFIA, Fox Island, WA, USA) to overcome the volume limitations of the syringe pump. The on-line sampling configuration is illustrated in Figure 2.1(b).

Two commercial $C^4D$ detectors (Tracedec, Innovative Sensor Technologies, Strassahof, Austria) were used; one detector per capillary. Detection parameters used for the study were: frequency high; voltage -6 dB; gain 100%, offset 000; filter: frequency 1/3 and cut-off 0.02. An Agilent 35900E A/D converter (Agilent Technologies, Waldbronn, Germany) was used to interface the $C^4D$ signals with the Agilent Chemstation software employed to record and analyse the signal. Separation on each capillary was driven by either a Spellman CZE2000 or CZE1000 high voltage power supply (Hauppage, NY, USA) working under normal polarity (+) for the cation separation or reversed polarity (-) for the anion separation, respectively. Electrodes were immersed in their respective outlet vials.

The system was controlled from a personal computer using an RS232 serial connection for the syringe pump and a RS422 serial connection for the milliGAT pump. The injection valve, isolation valve and high voltage power supplies were interfaced to the computer using a NI USB-6212 data acquisition device (National Instruments, Austin, TX, USA). Total system control, except for data acquisition, was achieved using in-house software written utilising Labview 8.1 (National Instruments, Austin, TX, USA). The system was not thermally controlled and all experiments were performed at ambient room temperature.

### 2.2.2 System operation

Sample injection was made sequentially and typical separation sequence steps are detailed in Table 2.1.

**Table 2.1:** Typical operation sequence of the dual capillary SI-CE system.

| Step | Operation | Valve position | Volume dispensed (µL) | Time (s) | Flow-rate (µLmin$^{-1}$) | Solenoid valve |
|---|---|---|---|---|---|---|
| 1 | Sample introduction | 2 | 83 | 5 | 1000 | Open |
| 2 | Injection | 2 | N/A | 1 | 1000 | Open |
| 3 | Flushing of interface | 1 | 42 | 5 | 500 | Open |
| 4 | Electrophoretic Separation | 1 | 150 | 180 | 50 | Open |
| 5 | Capillary and interface flush | 1 | 42 | 5 | 500 | Closed |
| 6 | Pressure equilibration | 1 | 0 | 5 | 0 | Open |

Commencing from a primed condition with the interface and capillaries completely filled with BGE, the interface was filled with sample followed by an application of +/- 5 kV for 1 s to electrokinetically inject sample anions and cations onto their respective separation capillaries. After injection, the sample was flushed from the interface at 500 µL min$^{-1}$ and the flow-rate was reduced to 50 µL min$^{-1}$ when the separation voltage was applied (+/- 30kV for anions and cations, respectively). These conditions were selected to minimise injection time and the consumption of reagents. Migration times of the analytes were not affected by the flow-rate of BGE during separation in the range 50-500 µL min$^{-1}$ when utilising 55 / 50 cm x 50 µm i.d. capillaries under the optimal separation conditions.

A hydrodynamic flush sequence was incorporated to physically clean and re-equilibrate the capillary surface between runs. This was achieved by closing the isolation valve and flowing BGE at 500-1000 µL min$^{-1}$ for 5 s to build sufficient pressure in the cross piece interface to flush the capillaries. Following the high flow flush of the capillaries, the isolation valve was reopened and a 5 s pause period was observed to allow the system to equilibrate to ambient pressure prior to the next sample injection. This flush step provided three benefits. Firstly it enabled the analysis time to be reduced by flushing unwanted analytes from the capillary past the detector so that they did not interfere with subsequent

runs. Secondly, it provided a physical cleaning of the capillaries to remove partial blockages and air bubbles and finally, it re-equilibrated the capillary surface between runs, which significantly increased baseline stability.

### 2.2.3 Reagents

All reagents were analytical reagent grade obtained from Sigma-Aldrich (Sydney, AUS) and were used as supplied unless stated otherwise. Solutions were prepared in Milli-Q water (Millipore, Bedford, MA, USA). Given that separations of both anions and cations were conducted simultaneously, standard solutions were prepared from available salts to achieve an approximately equal concentration of all 12 analytes of interest. Anion standard solutions of 1000 ppm were prepared by the dissolution of $NaClO_4$, $KClO_3$, $Mg(NO_3)_2$, NaF, $KH_2PO_4$ (BDH, VIC, AUS), $CaCl_2{\cdot}2H_2O$ (Ajax, NSW, AUS), and $(NH_4)_2SO_4$ (H&W, Essex, UK). Analytes were selected to allow a broad and general study of common inorganic ions of interest to water monitoring, explosive analysis and common environmental background ions. In order to achieve this aim, a standard analyte mixture comprising $PO_4^{3-}$, $F^-$, $SO_4^{2-}$, $ClO_3^-$, $ClO_4^-$, $Ca^{2+}$, $K^+$ (all 5 ppm), $Cl^-$ (9 ppm), $Na^+$ (7 ppm), $NH_4^+$ (2 ppm) and $Mg^{2+}$ (1 ppm) was prepared. Sodium methanesulfonate and $Li_2CO_3$ were used as internal standards. Apart from filtration, no sample pre-treatment prior to injection was performed.

The three studied BGEs were 70 mM (tris(hydroxymethyl)aminomethane (Tris)) / 70 mM *N*-Cyclohexyl-2-aminoethanesulfonic acid (CHES) at pH 8.6, 50 mM 2-(*N*-morpholino)ethanesulfonic acid (MES) / 50 mM L-histidine (His) at pH 6.1, and 50 mM acetic acid (AA) / 10 mM His at pH 4.2. Hexadimethrine bromide (HDMB) was employed to coat the walls of the fused-silica capillaries in order to reverse the EOF when required.

### 2.2.4 Electrophoretic procedures

Prior to first use, all bare fused-silica capillaries were conditioned off-line by flushing at 0.5 µL $min^{-1}$ with 1 M NaOH for 5 min and Milli-Q water for 5 min. Where HDMB coatings were employed, these capillaries were then coated with a 5% aqueous solution of HDMB for 5 min, followed by flushing with Milli-Q water for 5 min. After both of the separation capillaries were conditioned and/or coated, they were assembled into the cross-piece and equilibrated with BGE in order to avoid cross contamination of any cationic surfactant onto the bare fused silica capillary used for the cation separation. Linear polyacrylamide (LPA) coated capillaries of 50 µm i.d. was purchased from Polymicro Technologies. These capillaries were conditioned by flushing at 0.5 µL $min^{-1}$ with Milli-Q water for 10 min. In all cases, capillary equilibration was achieved by flushing with BGE for 30 min at 5 µL $min^{-1}$ after assembly of the separation interface.

## 2.3. Results and discussion

The previous work by Reschke *et al.* demonstrated the simultaneous separation of anions and cations on a microfluidic device from a single injection point, although the sample needed to be placed in two separate reservoirs to electrophoretically fill a double-tee channel profile which was subsequently mobilised with pressure.[17] The EOF was suppressed in both microchannels and flow restrictors were fabricated at the entrance of each microchannel to restrict the influence of hydrodynamic flow used to load the sample. Taking this work as a starting point, we modified a previously developed SI-CE system [18] to allow the simultaneous injection and separation of anions and cations. A commercial cross piece was used to interface the separation capillaries, and capillaries with an i.d. of 50 µm were

used as these had sufficient backpressure to restrict any hydrodynamic flow through the separation capillaries. The functionality of the system was increased in comparison to Reschke's microchip system by inclusion of an isolation valve which could be shut in order to divert flow into the separation capillaries for flushing.

The results of the above approach are demonstrated in Figure 2.2, showing the simultaneous separation of 5 cations ($K^+$, $NH_4^+$, $Ca^{2+}$, $Na^+$, $Mg^{2+}$) and 8 anions ($Cl^-$, $NO_3^-$, $SO_4^{2-}$, $ClO_4^-$, $ClO_3^-$, $F^-$, $PO_4^{3-}$, $CO_3^{2-}$). Figure 2.2 also shows the comparison of three BGEs previously reported for inorganic analysis by CE with $C^4D$ detection.

The first BGE, comprising 10 mM His and 50 mM AA at pH ≈ 4, has been used previously for the separation of various cations [8, 19] and anions.[20] The second buffer comprised of 20 mM MES/ 20 mM His at pH 6.1 is popular for the separation of cations and has been used in microchip CE separations of both anions and cations.[21] Here, the buffer concentration was optimised at 50 mM MES/ 50 mM His to improve the detection limits of the system. The third and final BGE consisted of 70 mM Tris and 70 mM CHES at pH 8.6, that has been demonstrated to be effective for the separation of inorganic anions [19] and low molecular weight organic acids. As can be seen from Figure 2.2, excellent separations can be achieved for both the anions and the cations. However, the same BGE chemistry must be used for both anions and cations, making the selection of the most appropriate BGE dependent on the specific application. The selection of the BGE for the target analytes in the present study will be discussed in Section 2.3.2.

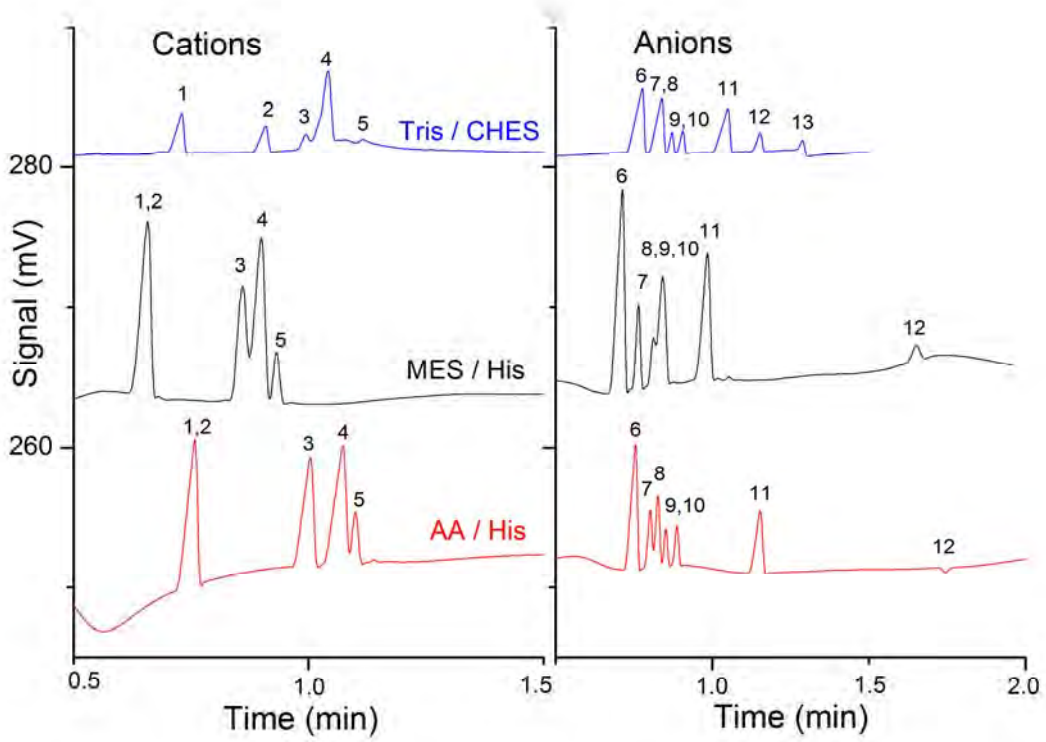


**Figure 2.2:** Simultaneous separations of cations (left) and anions (right) under suppressed-EOF conditions using LPA-coated capillaries. Injection sequence as per Table 2.1. CE conditions (both): capillary 50 µm id, total length of 40 cm (25 cm to detector), +/- 30kV cation / anion separation, respectively. Background electrolytes: Tris / CHES = 70 mM Tris/ 70 mM CHES at pH 8.6, MES/ His = 50 mM MES/ 50 mM His at pH 6.1, AA/ His = 50 mM AA acid / 10 mM His at pH 4.2. (1) $K^+$, (2) $NH_4^+$, (3) $Ca^{2+}$, (4) $Na^+$, (5) $Mg^{2+}$, (6) $Cl^-$, (7) $NO_3^-$, (8) $SO_4^{2-}$, (9) $ClO_4^-$, (10) $ClO_3^-$, (11) $F^-$, (12) $PO_4^{3-}$, and (13) $CO_3^{2-}$.

### 2.3.1. Capillary wall coatings

The main difference between the approach described here and that of the DOI-CE method is that two separation capillaries are used instead of one. This enables the use of different wall coatings on each separation capillary, leading to different EOF conditions for the anion and cation separations. This offers a degree of flexibility which can be used to optimise both separations. To evaluate the influence of the EOF in each separation capillary, separations of the target analytes were carried out in the three BGEs detailed above under three EOF conditions: (i) normal EOF in unmodified fused silica, (ii) low EOF in an LPA-coated capillary, and (iii) reversed EOF in a HDMB-coated capillary. Cation separations are only reported in fused silica and LPA-coated capillaries because the counter-EOF study of cation separations showed that HDMB was drawn into the separation interface (since the EOF was greater than the mobility of HDMB), contaminating the interface and the anion separation capillary.

The ability to use a capillary with a different surface charge will have the most pronounced effect on the separation of the anions at high pH as demonstrated in Figure 2.3. The migration time of $Cl^-$ changes from 120 s in the unmodified fused silica capillary, to 45 s in the LPA-coated capillary and 35 s in the HDMB-coated capillary. The migration time for the lowest mobility target analyte (phosphate, peak 12), changed from 530 s to 120 s and finally to 46 s, respectively. The use of HDMB-coated capillaries for the separation of anions and unmodified fused silica for cations presents the unique ability to simultaneously separate both anions and cations from the same injection point in a co-EOF manner. It is important to note this is not possible by any other approach in conventional or microchip CE. Figure 2.4 shows the results of the simultaneous co-EOF separation of the standard mixture of anions and cations in the three different BGEs.

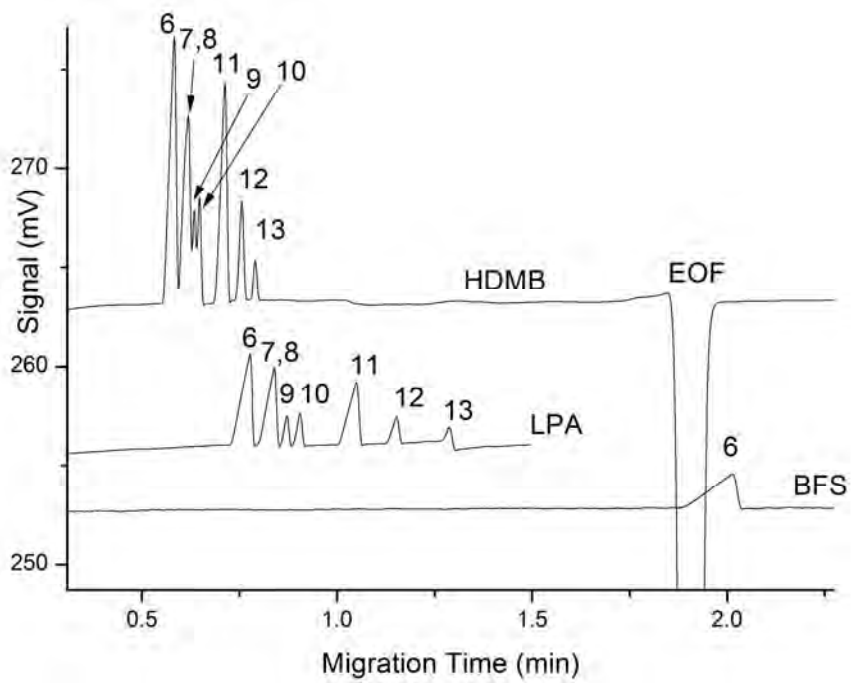


**Figure 2.3:** Anion separations in Tris/CHES buffer in HDMB-coated, LPA-coated and bare fused-silica (BFS) capillaries. All other separation conditions and analyte identities as for Figure 2.2.

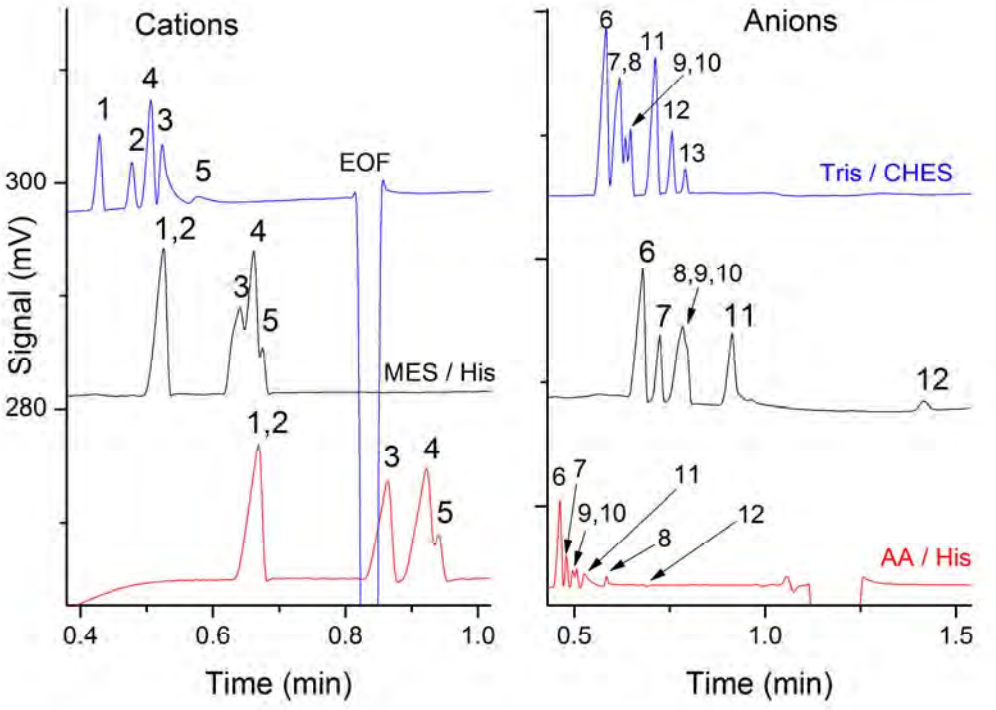


**Figure 2.4:** Simultaneous co-EOF separations conducted on bare fused-silica capillaries for cations and HDMB-coated capillaries for anions. All other separation conditions and analyte identities as for Figure 2.2.

As expected, the migration times of all cations decreased with increasing buffer pH due to an increase in the magnitude of the EOF. Only minor influences of pH on the migration times of the anions were expected, but this was not always the case. When performing co-EOF separations in both capillaries, variation in migration times (especially anions) was observed when capillaries were replaced. This variation was most noticeable in the Tris/CHES BGE where the EOF for the cation separation was the greatest (and the EOF in the anion separation capillary was also substantial). It was found that variations in migration times of cations after capillary replacement were relatively small (<15%) in comparison to the variations in migration times for anions (up to 30%). Whilst hydrodynamic, electrodynamic and EOF forces exist at the injection interface during injection and separation, these results indicated that the dominant force affecting migration times was the competition between two EOFs moving in opposite directions. In the case of the co-EOF Tris/CHES system, the EOF generated by the bare fused silica capillary was significantly greater than the pH-independent EOF generated by the HDMB-coated capillary. With suppressed EOF conditions in both capillaries, or co-EOF conditions in the cation capillary and suppressed EOF conditions in the anion capillary, reassembly of the cross-piece interface led to no significant change in the migration times of either anions or cations. These results indicated that precise capillary alignment at the interface was critical only under conditions of high EOF in both directions. Once the capillary assembly had been constructed, migration times were found to be repeatable over the lifetime of the capillary wall coating, with inconsistencies occurring only when capillaries needed to be replaced. Improvements in methodology for physically defining the positions of the capillaries may alleviate this issue, but were not studied further in this work.

### 2.3.2 Optimum conditions for simultaneous separation

As demonstrated in Figure 2.4, good separation selectivity was observed for the cations in Tris/CHES, with $K^+$ and $NH_4^+$ being separated without the use of an additive because of the partial deprotonation of $NH_4^+$ at pH values above 8.[22] The same separation of the test cations could be accomplished in the AA/His and MES/His BGEs by the addition of 18-crown-6 ether (which forms a complex with potassium) without affecting the anion separation, an approach which was not included here in order to simplify comparison of the separation systems. The drawback of the Tris/CHES system for cations was the significant tailing observed for both $Ca^{2+}$ and $Mg^{2+}$ which was attributed to the formation of their respective hydroxides. The separation selectivity of the cations was improved slightly in AA/His and this would be the BGE of choice if the separation of cations was the only consideration.

With regard to separation of the anions, the Tris/CHES buffer provided short migration times, good signal response and the most stable baseline of all three buffers, but satisfactory resolution between $NO_3^-$ and $SO_4^{2-}$ was not achieved within the required maximum run time of 3 min. Further, the HDMB coating was found to last no more than 80 runs before a 10% decrease (relative to the first run) in the migration time of $PO_4^{3-}$ occurred. Eventually, the EOF signal in the anion separation would disappear completely, accompanied by a significant increase in migration times for all anions, indicating a significant degradation of the surface coating. This required a replacement of the capillary so as to avoid contamination of the interface and the cation separation capillary with HDMB. The long-term instability of HDMB coatings was most prominent at high pH but was observed for all BGEs, and is not surprising as HDMB coatings are known to be dynamic in nature. In practical terms, the observed instability of the coated capillaries limited the appeal of a HDMB coating for long-term use.

In the MES/His buffer, anion selectivity was unsatisfactory over the required maximum separation time of 3 min. The AA/His buffer provided suitable resolution of all anionic species although the migration time of phosphate was significantly greater than that of the next migrating analyte ($SO_4^{2-}$) and significant tailing of the $F^-$ ion occurred for HDMB-coated capillaries, suggesting a wall interaction with the positively charged HDMB coating. The selectivity of $SO_4^{2-}$ was also altered from the same separation carried out in either fused-silica or LPA-coated capillaries (compare to Figure 2.4), presumably due to interaction with the HDMB.

Whilst co-EOF conditions for both anions and cations promised the fastest separations, the short lifetime of the capillary wall coating in the anion channel precluded the use of HDMB coatings for extended operation. Given that the total separation time was ultimately governed by the migration time of the analyte with lowest mobility (phosphate) it was decided that the slower migration time afforded for the cationic separation in the LPA-coated capillary would help to better resolve $Na^+$ and $Mg^{2+}$. Therefore, a suppressed EOF system (obtained with LPA-coated capillaries) utilising an AA/His/18-crown-6 ether BGE was chosen to evaluate the analytical performance of the system

### 2.3.3 Sequential Injection analysis of environmental samples

To fully resolve all target analytes in the LPA-coated capillaries using a BGE with 50 mM AA, 10 mM His and 2.5 mM 18-crown-6 ether, the capillary lengths were extended to 55 cm (35 cm effective length) for the cation separation and 50 cm (28 cm effective length) for the anion separation. To improve the analytical performance for applications, two internal standards (IS) were used to correct for bias that occurs with electrokinetic injection and to account for sample matrix variability. The IS selected for the cation separation was $Li^+$

(5 ppm), as $Li_2CO_3$, with the benefit that the $CO_3^{2-}$ ion would be protonated at pH 4.2 and not be seen in the anion separation. Methanesulfonate ($CH_3SO_3^-$) (10 ppm) added as the sodium salt was selected as the anionic IS. A representative electropherogram for the separation of the standard set of analytes is presented in Figure 2.5(a).

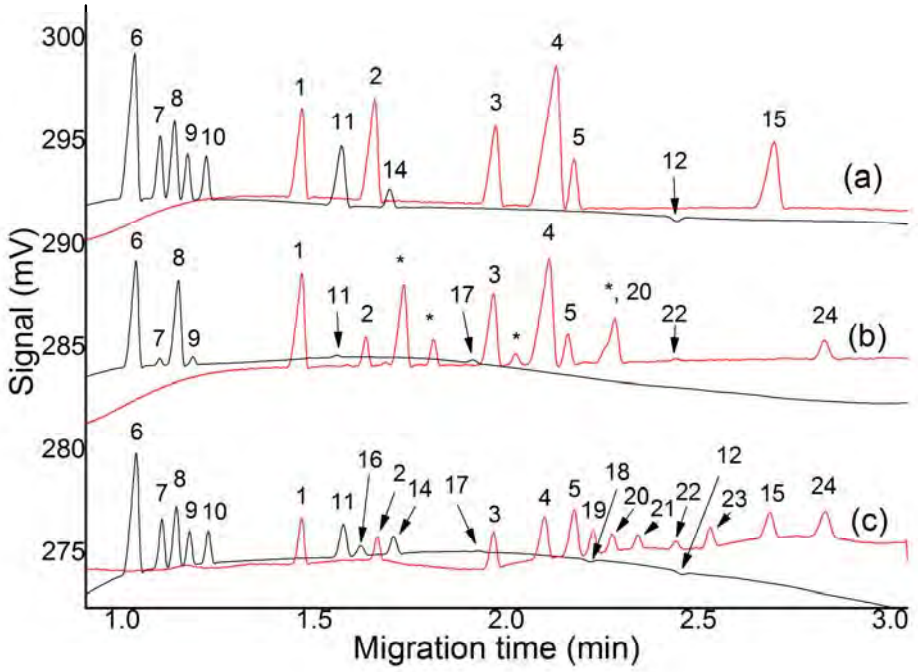


**Figure 2.5:** Separations of (a) standard analyte mixture plus internal standards, (b) process water from a zinc manufacturing plant and (c) 23 small ions. In all electropherograms, anion signals (black) are overlaid with corresponding cation signals (red). CE conditions for a, b and c: Cation capillary 50 µm i.d LPA-coated, I/L = 35/55 cm, Anion capillary 50 µm i.d LPA-coated, I/L = 28/50 cm, V= -/+ 30 kV (Cation/Anion respectively). Background electrolyte: 50 mM Acetic acid/ 10 mM His/ 2.5 mM 18-Crown-6 ether at pH 4.2. Analyte identities: (1) $NH_4^+$, (2) $K^+$, (3) $Ca^{2+}$, (4) $Na^+$, (5) $Mg^{2+}$, (6) $Cl^-$, (7) $NO_3^-$, (8) $SO_4^{2-}$, (9) $ClO_4^-$, (10) $ClO_3^-$, (11) $F^-$, (12) $PO_4^{2-}$, (14) $CH_3SO_3^-$ [IS], (15) $Li^+$ [IS], (16) $(CrO_4)^{2-}$, (17) $MoO_4^{2-}$, (18) $C_3H_8SO_3^-$, (19) $Mn^{2+}$, (20) $Zn^{2+}$, (21) $Sr^{2+}$, (22) $Cd^{2+}$, (23) $Cr^{3+}$, (24) $Be^{2+}$, and *: unidentified ion.

These developed separation conditions allowed for good separations of various environmental samples including tap water (shown in Figure 2.6) and zinc processing plant water samples taken from various stages of production, one of which is shown in Figure 2.5(b). Within a total separation time of 3 min, Figure 2.5(c) demonstrates the simultaneous separation of 23 anions and cations, which is approximately half the time required by DOI-CE, and considerably quicker than could be achieved with two sequential analyses of the same sample. This has applications beyond those discussed here, particularly when it is necessary to analyse both anions and cations rapidly, for example, for the development of rapid screening technology for homemade inorganic explosives.[19]

Migration time and peak area reproducibility data are given in Table 2.2 and are based upon the analysis of every $10^{th}$ run from a total of 101 consecutive separations of the standard analyte solution (n=10) performed sequentially and in an automated manner over a 6 h period. Limits of detection (LODs) were calculated from injection of a 10 times diluted sample of the standard analyte solution (≈ 0.5 ppm for most analytes) and are calculated at a signal: noise ratio of 3.

Values in the range 0.005- 0.061 mg $L^{-1}$ were determined and these were significantly better than the 0.1–1.7 mg $L^{-1}$ values obtained by indirect absorbance detection [23-25] and slightly better than the 0.04-0.08 mg $L^{-1}$ values obtained using a CE system using $C^4D$ detection. [19] These LODs agree well with the results published by Blanco *et al.* Considerable variation in individual analyte LODs could be observed (compare sulphate at 0.005 mg/L to phosphate at 0.061 mg/L) primarily due to the difference in mobilities between the individual analytes and the BGE counter ion, in this case acetate. Phosphate

**Table 2.2:** Analytical figures of merit for the DCSI-CE system.

| | Migration time (n = 10) | | peak area (n = 10) | Range | | LOD (S/N = 3, |
|---|---|---|---|---|---|---|
| | (min) | RSD (%) | RSD (%) | (ppm) | Calibration $R^2$ | mg/L) |
| $NH_4^+$ | 1.44 | 0.59 | 4.87 | 0.1 - 5 | 0.998 | 0.016 |
| $K^+$ | 1.62 | 0.51 | 6.35 | 0.1 - 5 | 0.998 | 0.040 |
| $Ca^{2+}$ | 1.93 | 0.51 | 4.06 | 0.1 - 5 | 0.991 | 0.030 |
| $Na^+$ | 2.09 | 0.33 | 1.48 | 0.1 - 5 | 0.999 | 0.035 |
| $Mg^{2+}$ | 2.13 | 0.47 | 3.53 | 0.1 - 5 | 0.991 | 0.013 |
| $Li^{2+}$ | 2.65 | 0.46 | 3.71 | 0.1 - 5 | 0.994 | 0.032 |
| $Cl^-$ | 1.02 | 0.23 | 3.83 | 0.1 - 5 | 0.996 | 0.022 |
| $NO_3^-$ | 1.09 | 0.23 | 7.17 | 0.1 - 1 | 0.995 | 0.006 |
| $SO_4^{2-}$ | 1.12 | 0.26 | 6.81 | 0.1 - 1 | 0.992 | 0.005 |
| $ClO_4^-$ | 1.16 | 0.26 | 2.84 | 0.1 - 1 | 0.995 | 0.010 |
| $ClO_3^-$ | 1.20 | 0.27 | 4.41 | 0.1 - 1 | 0.995 | 0.009 |
| $F^-$ | 1.54 | 0.36 | 5.97 | 0.2 - 5 | 0.992 | 0.005 |
| $CH_3SO_3^-$ | 1.67 | 0.43 | 4.73 | 0.2 - 5 | 0.996 | 0.033 |
| Phosphate | 2.41 | 0.74 | 3.71 | 0.5 - 10 | 0.996 | 0.061 |

appears as a negative peak in the AA/His BGE (Figure 5) due to the fact that it has a lower mobility than acetate. This is a common restriction in C4D, exacerbated here by the use of a compromise BGE for determining both anionic and cationic species.

### 2.3.4 On-line autonomous analysis

Using the system configuration described in Figure 2.1(b), a two day on-line continuous analysis of Tasmanian Southern Water tap water was conducted as part of a laboratory analysis. This consisted of 900 consecutive analyses of 3.5 min per run (approximately 17 analyses/h) where samples were aspirated from a running reservoir of tap water to the quaternary pump. Figure 2.6 shows the results from one separation every 5 h over this period.

The internal standards (100 ppm $CH_3SO_3^-$, 50 ppm $Li^+$) were drawn from a reservoir via a second pump inlet line. The sample and IS were mixed at a flow-rate ratio of 0.1 mL/min IS: 0.9 mL/min sample. This resulted in a 10 % dilution of the sample and provided IS concentrations of 5 ppm for $Li^+$ and 10 ppm for $CH_3SO_3^-$. The sample/IS outlet line was

plumbed directly to the sample injection port. The experiment was conducted over a weekend period during winter during which heating to the building was turned off before being turned on again. Significant variations in migration times were observed over the period of analysis and were attributed to the change in temperature as the migration times of the final few hours of the experiment correlated well to those of the initial runs where the temperatures were similar. The migration times were normalised to the respective anionic and cationic IS as shown in figure 2.6(a) and demonstrate very good repeatability (< 1 % RSD for all species based on corrected migration times). The variations in migration times appeared to have negligible effect on the variation of IS peak areas, as shown in Figure 2.6(b) (%RSD < 3 % for both standards calculated from the 12 sampled values) over the period examined. These results indicated that variations seen in analyte peak areas were not due to system errors. Indeed, the final two data points showed a significant percentage increase in the $Fe^{2+}$ peak area as work resumed on Monday morning and building occupants began to use water throughout the building, increasing the concentration of $Fe^{2+}$ moving through the plumbing. With further consideration given to thermal insulation of the system and the development of automated data processing software, these results indicate that the system was stable and reproducible and that it could be adapted readily to a wide range of autonomous monitoring applications.

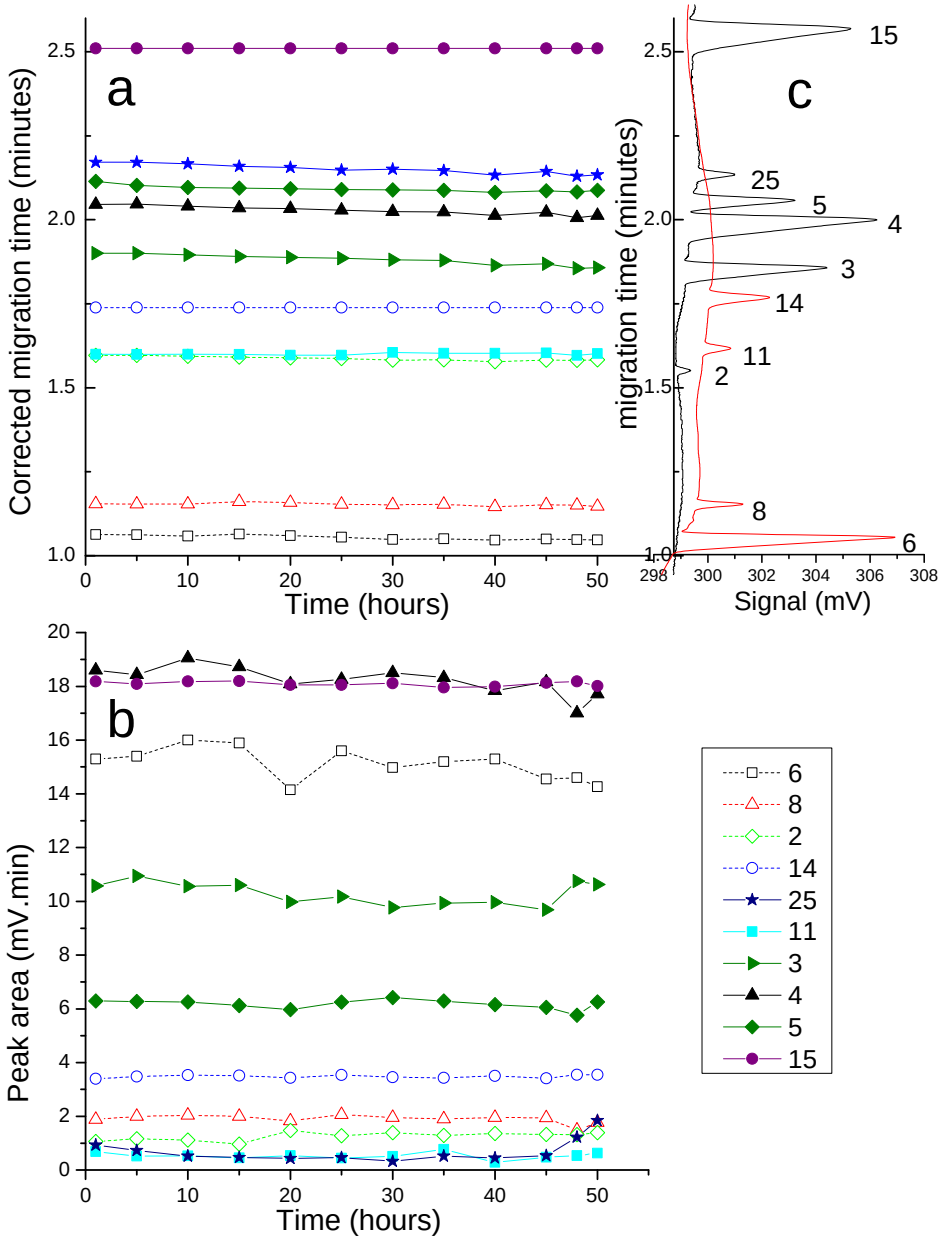


**Figure 2.6:** (a) Reproducibility of corrected migration times of tap water analytes over a 50 h period. (b) Reproducibility of uncorrected peak areas of tap water analytes over a 50 h period. $Li^+$ and $CH_3SO_3^-$ are cation and anion IS respectively. (c) A representative electropherogram of the separation. Analyte identities as for figure 2.5 except 25 which is $Fe^{2+}$.

## 2.4 Concluding remarks

In this work we have demonstrated a novel approach for the simultaneous separation of anions and cations by CE from a single injection point. Whilst the use of a single BGE for the separation of both anions and cations remains a potential drawback, the ability to vary the wall coatings and effective separation lengths of each capillary simplifies optimisation of the separation of both anions and cations. This approach is therefore more flexible than dual-opposite end injection CE. The system is suitable for a range of applications and is capable of simultaneously separating at least 11 anions and 12 cations within a total analysis time of 3.5 min. The ability to sample directly on-line make this a potentially useful system for the simultaneous analysis of anions and cations in both laboratory and extended automated monitoring applications, as demonstrated for the analysis of tap water samples in the laboratory on-line over a period of 50 h.

## 2.5 References

1. Nakatani, N.; Kozaki, D.; Mori, M.; Tanaka, K., Recent progress and applications of ion-exclusion/ion-exchange chromatography for simultaneous determination of inorganic anions and cations. *Analytical Sciences* **2012,** *28*, 845-852.

2. Nakatani, N.; Kozaki, D.; Mori, M.; Hasebe, K.; Nakagoshi, N.; Tanaka, K., Ion-exclusion/cation-exchange Chromatography with Dual Detection of the Conductivity and Spectrophotometry for the Simultaneous Determination of Common Inorganic Anionic Species and Cations in River and Wastewater. *Analytical Sciences* **2011,** *27*, 499-504.

3. Meng, H. B.; Wang, T. R.; Guo, B. Y.; Hashi, Y.; Guo, C. X.; Lin, J. M., Simultaneous determination of inorganic anions and cations in explosive residues by ion chromatography. *Talanta* **2008,** *76*, 241-245.

4. Nesterenko, P. N., Simultaneous separation and detection of anions and cations in ion chromatography. *TrAC - Trends in Analytical Chemistry* **2001,** *20*, 311-319.

5. Johns, C.; Yang, W.; MacKa, M.; Haddad, P. R., Simultaneous separation of anions and cations by capillary electrophoresis with high magnitude, reversed electroosmotic flow. *Journal of Chromatography A* **2004,** *1050*, 217-222.

6. Kubáň, P.; Karlberg, B., Simultaneous Determination of Small Cations and Anions by Capillary Electrophoresis. *Analytical Chemistry* **1998,** *70*, 360-365.

7. Padarauskas, A.; Olšauskaite, V.; Schwedt, G., Simultaneous separation of inorganic anions and cations by capillary zone electrophoresis. *Journal of Chromatography A* **1998,** *800*, 369-375.

8. Kubáň, P.; Hauser, P. C.; Kubáň, V., A flow injection-capillary electrophoresis system with high-voltage contactless conductivity detection for automated dual opposite end injection. *Electrophoresis* **2004,** *25*, 35-42.

9. Nehmé, R.; Lascaux, A.; Delépée, R.; Claude, B.; Morin, P., Capillary electrophoresis procedure for the simultaneous analysis and stoichiometry determination of a drug and its counter-ion by using dual-opposite end injection and contactless conductivity detection: Application to labetalol hydrochloride. *Analytica Chimica Acta* **2010,** *663*, 190-197.

10. Kubáň, P.; Kubáň, V., Simultaneous determination of inorganic and organic anions, alkali, alkaline earth and transition metal cations by capillary electrophoresis with contactless conductometric detection. *Electrophoresis* **2002,** *23*, 3725-3734.

11. Haumann, I.; Boden, J.; Mainka, A.; Jegle, U., Simultaneous determination of inorganic anions and cations by capillary electrophoresis with indirect UV detection. *Journal of Chromatography A* **2000,** *895*, 269-277.

12. Mai, T. D.; Hauser, P. C., Simultaneous separations of cations and anions by capillary electrophoresis with contactless conductivity detection employing a sequential injection analysis manifold for flexible manipulation of sample plugs. *Journal of Chromatography A* **2012**.

13. Kubáň, P.; Kubáň, V., Simultaneous capillary electrophoretic separation of small anions and cations after complexation with ethylenediaminetetraacetic acid. *Journal of Chromatography A* **1999,** *836*, 75-80.

14. Soga, T.; Ross, G. A., Simultaneous determination of inorganic anions, organic acids and metal cations by capillary electrophoresis. *Journal of Chromatography A* **1999,** *834*, 65-71.

15. Wharton, J. A.; Stokes, K. R., Analysis of nickel-aluminium bronze crevice solution chemistry using capillary electrophoresis. *Electrochemistry Communications* **2007,** *9*, 1035-1040.

16. Bächmann, K.; Haumann, I.; Groh, T., Simultaneous determination of inorganic cations and anions in capillary zone electrophoresis (CZE) with indirect fluorescence detection. *Fresenius' Journal of Analytical Chemistry* **1992,** *343*, 901-902.

17. Reschke, B. R.; Schiffbauer, J.; Edwards, B. F.; Timperman, A. T., Simultaneous separation and detection of cations and anions on a microfluidic device with suppressed electroosmotic flow and a single injection point. *Analyst* **2010,** *135*, 1351-1359.

18. Blanco, G. A.; Nai, Y. H.; Hilder, E. F.; Shellie, R. A.; Dicinoski, G. W.; Haddad, P. R.; Breadmore, M. C., Identification of inorganic improvised explosive devices using sequential injection capillary electrophoresis and contactless conductivity detection. *Analytical Chemistry* **2011,** *83*, 9068-9075.

19. Hutchinson, J. P.; Johns, C.; Breadmore, M. C.; Hilder, E. F.; Guijt, R. M.; Lennard, C.; Dicinoski, G.; Haddad, P. R., Identification of inorganic ions in post-blast explosive residues using portable CE instrumentation and capacitively coupled contactless conductivity detection. *Electrophoresis* **2008,** *29*, 4593-4602.

20. Mai, T. D.; Schmid, S.; Müller, B.; Hauser, P. C., Capillary electrophoresis with contactless conductivity detection coupled to a sequential injection analysis manifold for extended automated monitoring applications. *Analytica Chimica Acta* **2010,** *665*, 1-6.

21. Wang, J.; Chen, G.; Muck Jr, A.; Collins, G. E., Electrophoretic microchip with dual-opposite injection for simultaneous measurements of anions and cations. *Electrophoresis* **2003,** *24*, 3728-3734.

22. Beck, W.; Engelhardt, H., Separation of non UV-absorbing cations by capillary electrophoresis. *Fresenius' Journal of Analytical Chemistry* **1993,** *346*, 618-621.

23. Hopper, K. G.; Leclair, H.; McCord, B. R., A novel method for analysis of explosives residue by simultaneous detection of anions and cations via capillary zone electrophoresis. *Talanta* **2005,** *67*, 304-312.

24. Hutchinson, J. P.; Evenhuis, C. J.; Johns, C.; Kazarian, A. A.; Breadmore, M. C.; Macka, M.; Hilder, E. F.; Guijt, R. M.; Dicinoski, G. W.; Haddad, P. R., Identification of inorganic improvised explosive devices by analysis of postblast residues using portable capillary electrophoresis instrumentation and indirect photometric detection with a light-emitting diode. *Analytical Chemistry* **2007,** *79*, 7005-7013.

25. Sarazin, C.; Delaunay, N.; Varenne, A.; Vial, J.; Costanza, C.; Eudes, V.; Minet, J. J.; Gareil, P., Identification and determination of inorganic anions in real extracts from pre- and post-blast residues by capillary electrophoresis. *Journal of Chromatography A* **2010,** *1217*, 6971-6978.

This chapter has been removed for copyright or proprietary reasons.

Gaudry, A. J.; Breadmore, M. C.; Guijt, R. M.; In-plane alloy electrodes for capacitively coupled contactless conductivity detection in poly(methylmethacrylate) electrophoretic chips. Electrophoresis 2013, 34 (20-21), 2980-2987 comprises the majority of Chapter 3: Microchip manufacture and incorporation of C4D electrodes

# Chapter 4: Polymeric microchip for the simultaneous determination of anions and cations by hydrodynamic injection using a dual channel sequential-injection microchip electrophoresis system

## 4.1 Introduction

Microchip electrophoresis (ME) has been the most successful analytical technique for practical applications of the micrototal analysis system (μTAS) or "lab on a chip" concept.[1] Of critical importance to efficient and repeatable ME separations is repeatable sample injection, relating to both the volume and the shape of the injected sample plug. To maximise the efficiency of the small separation spaces typically available to ME systems, the injected sample plug must be very small and well defined. Electrokinetic injection is by far the most widely employed injection method in ME due to its instrumental simplicity as no pumps or actuators are required,[2, 3] and has been the subject of several reviews.[3, 4] The earliest iterations of ME devices utilised a T intersection injection geometry [5, 6] where variable sample volumes could be electrokinetically transported from a side channel into the separation channel by timed switching of applied voltages (float injection). These T injector chips were found to suffer from sample leakage, in addition to introducing a sample matrix bias by preferentially injecting sample components with a higher electrophoretic mobility reducing applicability to quantitative analysis.[7] The development of the pinched injection approach by Ramsey's group [8] reduced this bias allowing for the injection of minute quantities of sample in a cross-shaped [9] or a double-T shaped [10, 11] fluidic channel, and is now broadly employed in chip-based CE systems. Whilst reducing the sample bias, loading a representative sample onto the intersection depends on the EOF, resulting in long sample loading times under conditions of low EOF. Additionally, pinched injections depend

on the matching ionic strength of the sample and BGE,[12] limiting its suitability for routine analysis of samples of high or variable salinity.

Hydrodynamic injection in ME requires additional instrumentation to control the sample flow, however it has the potential to overcome electrokinetic sample bias and as a result, considerable effort has gone towards the development of efficient and reliable ways to implement this in ME format. Several recent reviews [2, 4] detail the most significant developments including hydrostatic pressure injection,[13] pressure pulse injection,[14-16] negative pressure injection,[17] and positive pressure injection in either valveless, [18, 19] external valve [20-22] and integrated valve [23] configurations. Recently, a hydrodynamic split injection method was employed on a PDMS chip,[18] varying the channel widths at a cross geometry chip to manipulate the sample injection volume. This method bears most in common with the dual channel sequential injection microchip electrophoresis system (DCSI-ME) presented here, however the studies in this chapter demonstrate an external hydrodynamic "split-injection" system, based upon the dual capillary sequential injection capillary electrophoresis system (DC-SICE) presented in Chapter 2.

There are only two examples of simultaneous independent electrophoretic separation from a single sample point in ME. Prest *et al.* reported bidirectional isotachophoresis on a planar chip for the simultaneous analysis of small anions and cations.[24] Reschke *et al.* demonstrated the simultaneous separation of anions and cations on a microfluidic device from a single injection point,[25] although the sample needed to be placed in two separate reservoirs to electrophoretically fill a double-tee channel profile which was cleaned with pressure after the separation. The EOF was suppressed in both microchannels and flow restrictors were fabricated at the entrance of each separation channel to restrict hydrodynamic flow during sample loading. While not in individual

channels, Dual Opposite End-Injection was used for the separation of six ionic explosive and two nerve agent degradation products.[26]

In this work, two approaches are used to control hydrodynamic injection in the DSCI-ME system. Sample is introduced between two parallel "sheath" flows of electrolyte to prevent premature hydrodynamic loading into the separation channels. An external isolation valve is momentarily closed, hydrodynamically forcing a sample plug into the two separation channels. In combination, the injected sample volume can be manipulated by altering the hydrodynamic resistance ratios by varying lengths and internal diameters of PEEK tubing connected to the sampling and separation channels off-chip. Following injection, opposite voltages are applied to the outlets of both separation channels to perform simultaneous cathodic and anodic separations. The DCSI-ME introduced here offers the unique ability to sample from a flow and to easily flush and condition the microchannels, which, in combination with the longevity of the devices, makes this system highly suited for routine and continuous monitoring applications as well as online coupling with other separation techniques for complementary multidimensional or hyphenated analysis.

## 4.2 Experimental

### 4.2.1 Microchip fabrication

The electrophoresis chip is shown in Figure 1 and consists of a PMMA channel plate (50 mm x 75 mm x 1.5 mm, Global 372 Arcylic Pty Ltd., Queensland, Australia), a PMMA cover-plate (50 mm x 75 mm x 1.5 mm), and six PMMA fittings (15 mm x 15 mm x 8 mm). Sample and BGE feeder channels are 500 µm wide, 15 µm deep, and 18 mm long. Separation channels

are 50 µm wide, 15 µm deep, and 106 mm long. The distance to the detection point in both separation channels is 86 mm. The distance to the waste reservoir from the injection cross is 1.5 mm.

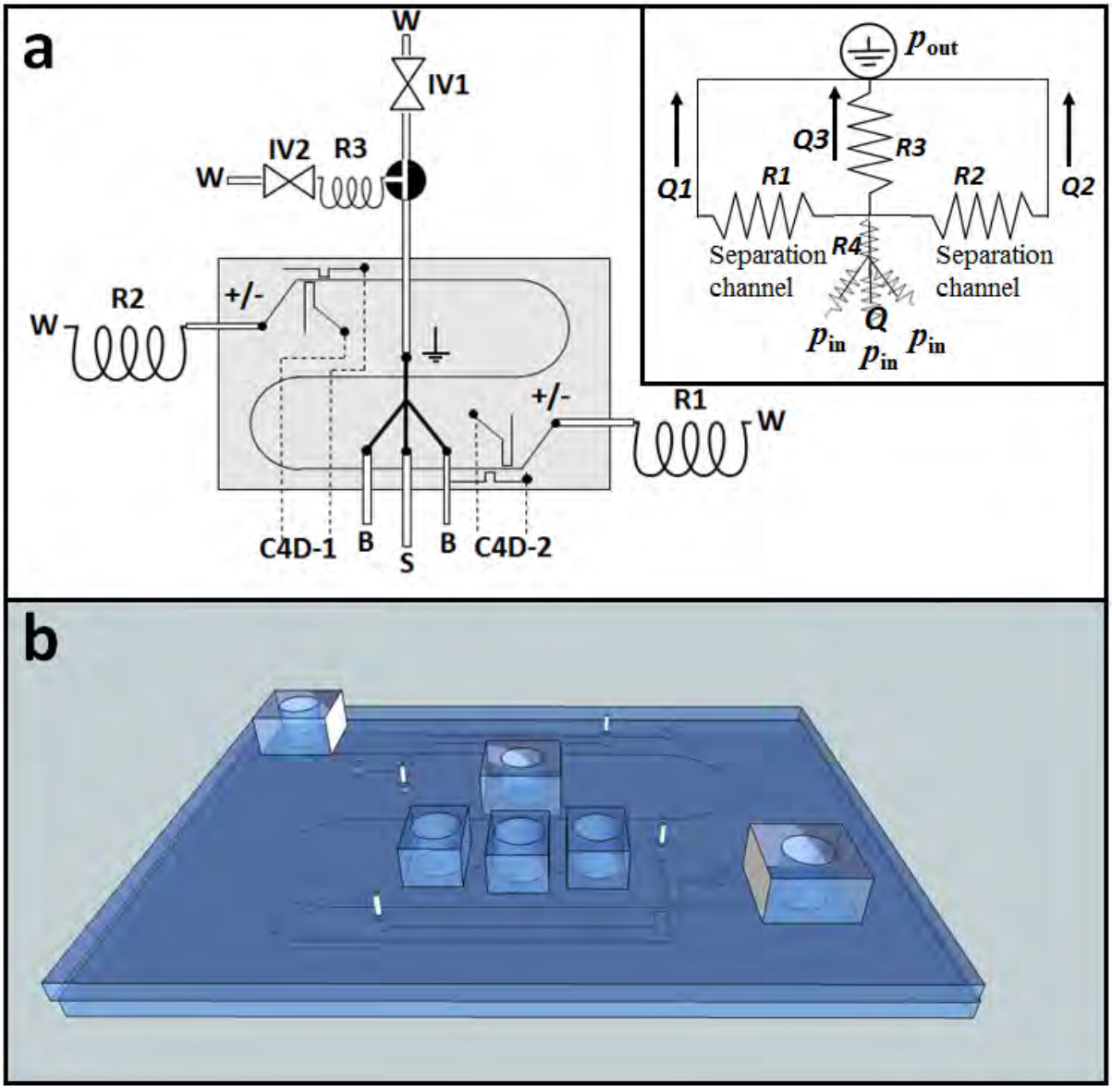


**Figure 4.1:** (a) Microchip schematic; B = buffer input, S = sample input, C4D = capacitively coupled contactless conductivity detection connections, W = waste, IV = isolation valve, R = peek tubing resistors. Inset: equivalent circuit diagram; *R* = Resistances, *Q* = volumetric flow rates, $p_{in}$ = input pressure, $p_{out}$ = atmospheric pressure. (b) Three-dimensional rendering of a dual channel SI-CE micro electrophoretic chip.

The PMMA microchip fabrication procedure, including the method for incorporating in-plane alloy electrodes has been described in detail in Chapter 3. In brief, a positive master embossing stamp of approximately 10 mm thickness was cast in poly(dimethylsiloxane) (PDMS) and was used to hot emboss 1.5 mm thick 50 x 75 mm PMMA plates. These embossed channel plates were thermally bonded to a PMMA plate of identical dimensions containing access holes using a modified office laminator. Detection electrodes were made from Woods metal alloy (Type 160, Micro-Mark, Berkeley Heights, NJ, USA) by drawing the melted alloy through the channel with a syringe. To connect with the detection electronics, 6mm x 0.5 mm Ø lengths of wire were inserted into the reservoirs by temporarily melting the alloy in the reservoir using a soldering iron. Female flat bottom fittings to couple to Upchurch® capillary tubing fittings were produced in house from 6 mm thick PMMA sheets with a 5.5 mm drill bit and tapped with a 1/4-28 thread and were attached by a solvent bonding process with a small amount of 1,2-dichloroethane.

Electrodes for application of the high voltages and ground were constructed from ≈ 100 mm lengths of 1 mm i.d. stainless steel tubing. The hollow electrodes also served as reservoirs and fluidic connections were realised by heat moulding the electrodes to ferrules (P-248, Upchurch Scientific, Oak Harbour, WA, USA) at each end to connect with standard 1/4-28 nuts. All tubing was fitted with 1/4-28 nuts and connected with the appropriate female to female fittings.

### 4.2.2 Microfluidic system

A schematic of the system is given in Figure 4.1 (a). Two channels of a four channel laboratory-built high voltage power supply were utilised for separation, each with a

maximum output voltage of 5 kV. Two Milligat pumps (MG-5, GlobalFIA, Fox Island, WA, USA) were used to deliver BGE and sample to the microchip. The pump supplying BGE was fitted with a Y-piece to split the BGE flow into two equal streams and allow the sample flow to be sheathed. Each pump was fitted with an in-line pressure relief valve rated at 87.1 psi and all feeder tubing was 500 µm i.d. (of insignificant hydrodynamic resistance). Two external isolation valves (HP225K021, NResearch, West Caldwell, NJ, USA) were connected to the outlets of the T-piece (IV1, IV2) connecting with the waste to enable hydrodynamic injection. The maximum response time for the isolation valves is 20 ms to open and 30 ms to close according to the manufacturer's specification. Injection valve 2 (IV2) is not required for the operation of the system, and was only included as fully closed to investigate the effects of external separation channel hydrodynamic resistance, simulating a system without the T-piece installed.

Two commercial $C^4D$ detectors with chip stage connector heads (Tracedec, Innovative Sensor Technologies, Strassahof, Austria) were used; one detector per separation channel. The connector heads were modified with SMA fittings to slip over the pins in the detection electrode wells. Detection parameters used for the study were: frequency high; voltage -6 dB; gain 100%, offset 000; filter: frequency 1/3 and cut-off 0.02. System control and data acquisition were achieved through a LabVIEW program (LabVIEW 2011, National Instruments) and two data acquisition boards (MCC USB-2533 and MCC USB-3105, Measurement Computing Corporation, Norton, MA, USA).

### 4.2.3 Reagents

All reagents were analytical reagent grade obtained from Sigma-Aldrich (NSW, AUS) and were used as supplied unless stated otherwise. Solutions were prepared in 18 MΩ Milli-Q water (Millipore, MA, USA). Given that separations of both anions and cations were conducted simultaneously, standard solutions were prepared from available salts to achieve an approximately equal concentration of all 6 analytes. Standard solutions of 1000 $mgL^{-1}$ were prepared by the dissolution of NaF, $KH_2PO_4$ (BDH, VIC, AUS), and LiCl. Background electrolyte (BGE) solutions of 50 mM acetic acid / 10 mM L-histidine (His) at pH 4.2 were made daily and filtered before use.

### 4.2.4 Electrophoretic procedures

When a new chip was placed in the system, one of the BGE inlets was first connected to fill the main channels with BGE before making the other BGE and sample connections. This was found to eliminate bubbles from being trapped in the channels. Tubing was then connected to the main waste outlet and BGE was pumped until the liquid reached the external isolation valves, again to expel the air from the system. Finally, the separation electrodes/reservoirs were connected to the ends of the separation channels and the isolation valves closed to create sufficient pressure at the intersection to pump BGE through the two separation channels. The separation channels were then conditioned by flushing them with BGE for 30 minutes, before the analysis sequence given in Table 4.1 was started. A discussion of the injection mechanism is given in Sections 4.3.2 – 4.3.5. Separations were conducted at +/- 4.5 kV for anion/cation separations respectively.

**Table 4.1:** Operating procedure for the DCSI ME system.

| | Step | BGE flow rate (µL $s^{-1}$) | Sample flow rate (µL $s^{-1}$) | Time (s) | Volume BGE/Sample (µL) | | Isolation valve 1 | Isolation valve 2 |
|---|---|---|---|---|---|---|---|---|
| 1 | Flush | 4 | 0 | 10 | 40 | 0 | Closed | Closed |
| 2 | Post flush | 4 | 0 | 3 | 12 | 0 | Open | Open |
| 3 | Sample introduction | 3 | 1 | 2 | 6 | 2 | Open | Open |
| 4 | Sample introduction | 2 | 2 | 2 | 4 | 4 | Open | Open |
| 5 | Sample introduction | 1 | 3 | 2 | 2 | 6 | Open | Open |
| 6 | Pre-introduction | 0 | 4 | 1 | 0 | 4 | Open | Open |
| 7 | Injection | 0 | 4 | 0.05 | 0 | varies | Closed | Open/ Closed |
| 8 | Interface cleaning | 4 | 0 | 5 | 20 | 0 | Open | Open |
| 9 | Separation | 1 | 0 | 45 | 45 | 0 | Open | Open |
| | | | Total: | 70.05 | 99 | 16 | | |

## 4.3 Results and discussion

### 4.3.1 Hydrodynamic considerations

The microchip design was based on previous studies of single [27] and dual capillary sequential injection capillary electrophoresis systems described in Chapter 2. The original work employed electrokinetic injection, and it was noted that the BGE flow rate during the separation phase could be increased to approximately 25 µL $s^{-1}$ without affecting the migration times of the analytes. This indicated that the flow resistance of the 50 µm i.d. separation capillaries was sufficiently high to be hydrodynamically isolated from the sequential injection interface. The dimensions of the capillary system were therefore used as a guide in designing the DCSI-ME system. Using the PDMS stamp embossing method,

channel widths of ≤ 30 µm were difficult to achieve (success rate < 50%) and 500 µm channels suffered from significant bowing (to the point of full or partial closure of the feeder channels). The bonding procedure was optimised for the 50/500 µm width ratio that was successful in the CE format and led to a successful bonding rate ≈ 80%.

The use of channel dimensions to regulate flow resistances to control and direct flow was previously studied by Attiya *et al.* who examined the design and performance of glass electrophoretic microchips to semi-continuously sample small volumes from a large flow channel for subsequent electrokinetic injection and electrophoretic separation.[28] Under laminar flow conditions and with the assumption that the pressure gradient along the channel length is uniform, the total volumetric flow rate Q [$m^3$ $s^{-1}$] for the steady-state pressure-driven fluid flow in a circular channel described by Hagen-Poiseuille's law is given as:

$$Q = \frac{\pi r^4}{8\eta}\frac{\Delta p}{L} \quad (1)$$

Where Q is defined as positive for flow from inlet to outlet, $r$ [m] is the circular channel radius, $\eta$ [Pa s] is the fluid viscosity and $\Delta p$ [Pa] is the pressure difference through a finite channel length $L$ [m]. Eqn (1) can be simplified and rearranged to:

$$\Delta p = QR_H \quad (2)$$

where $R_H$ is the hydrodynamic resistance [Pa s $m^{-3}$] of the channels. For circular channels [29] it can be calculated from:

$$R_H = \frac{8\eta L}{\pi r^4} \quad (3)$$

For a channel with rectangular cross-section $R_H$ is well known [29] and for channels of width $w$ [m] and height $h$ [m], the following expression is valid when $h < w$ (low aspect ratio channels):

$$R_H = \frac{12\eta L}{wh^3(1-0.630h/w)} \quad (4)$$

The hydraulic-electric circuit analogy where Hagen-Poiseuille's law corresponds to Ohm's law is well known [29] meaning that the pressure drop is analogous to the voltage drop (V), the volumetric flow rate to the current (I), and the hydraulic resistance to the electric resistance (R).[30] In a network of channels, equivalent resistances can be calculated as for electric circuits: $n$ channels in series have an equivalent resistance of $R_H = R_{H1} + R_{H2} + \ldots R_{Hn}$, and $n$ channels in parallel have an equivalent resistance of $1/R_H = 1/R_{H1} + 1/R_{H2} + \ldots 1/R_{Hn}$.

A schematic overview of the DCSI-ME system is given in Figure 4.1, with an equivalent circuit diagram in the inset of Figure 4.1(a) and a photograph of the system at Figure 4.2.

Using equations (3) and (4) and $\eta$ = 1.002 x $10^{-3}$ (Pa.s), $R_H$ was calculated for the major components of the system (the T-piece, feeder tubing and tubing interconnects were excluded because in this context their resistance can be considered negligible). The results of these calculations are summarised in Table 4.2.

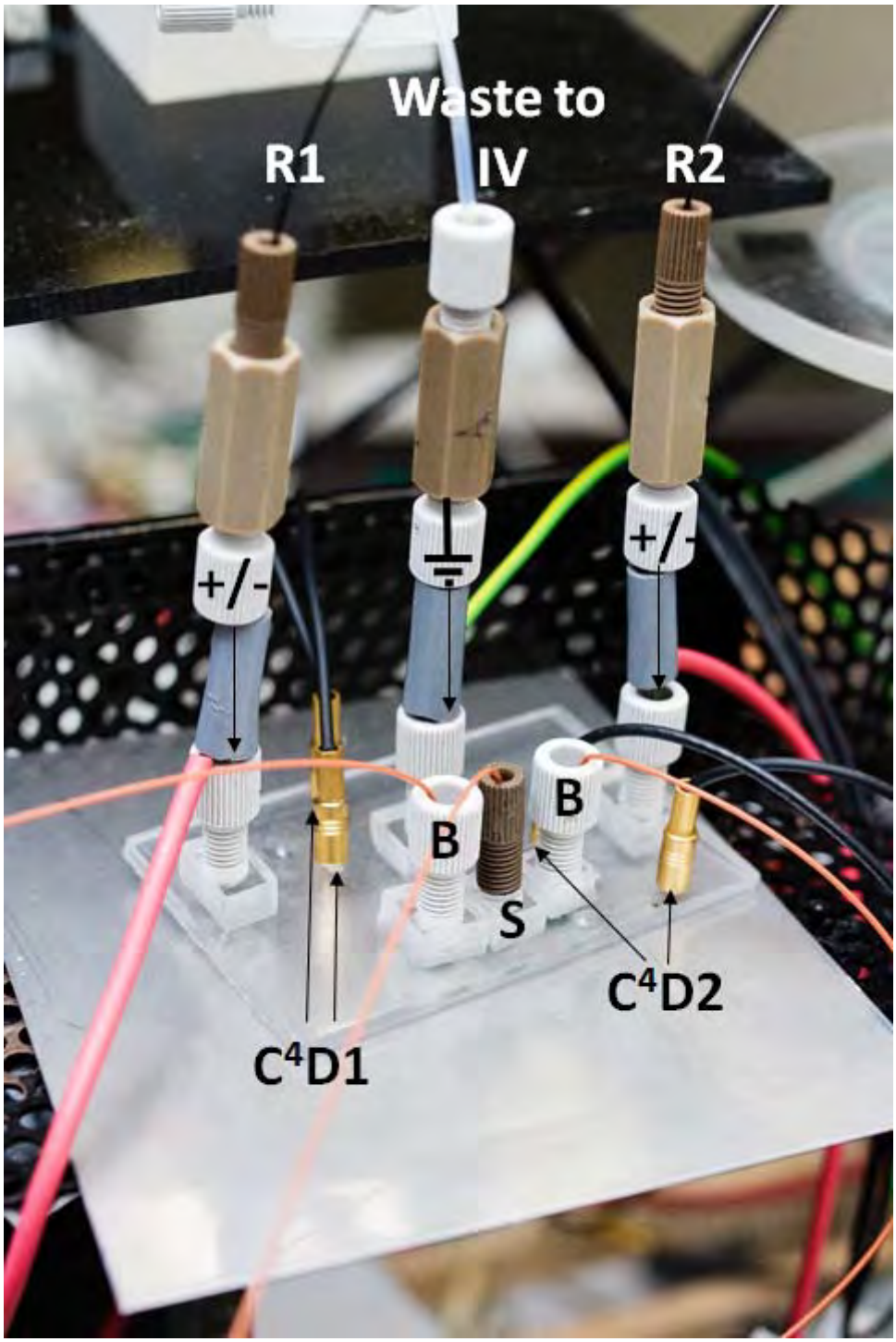


**Figure 4.2:** System photograph; B = buffer input, S = sample input, $C^4D$ = capacitively coupled contactless conductivity detection connections, W = waste, IV = isolation valve, R = peek tubing resistors.

**Table 2:** Values of $R_H$ for system components.

| Serial | Component | $R_H$ [Pa s$^3$ m$^{-1}$] | Serial | Component | $R_H$ [Pa s$^3$ m$^{-1}$] | Serial | External hydrodynamic resistor internal diameters | $R_H$ [Pa s$^3$ m$^{-1}$] (per 10 cm length) |
|---|---|---|---|---|---|---|---|---|
| 1 | Separation channels (50 µm w x 15 µm h x 106 mm) | 9.31 x $10^{15}$ | 6 | Chip holes (1.5mm x 1mm i.d.) | 6.11 x $10^{7}$ | 10 | 65 | 2.29 x $10^{15}$ |
| 2 | BGE feeder channels (500 µm w x 15 µm h x 13 mm L) | 9.44 x $10^{13}$ | 7 | Electrodes (10cm x 1mm i.d.) | 2.55 x $10^{8}$ | 11 | 90 | 6.23 x $10^{13}$ |
| 3 | Sample feeder channel BGE feeder channels (500 µm w x 15 µm h x 10 mm L) | 7.26 x $10^{13}$ | 8 | Ground waste assembly (20 cm x 1mm i.d.) | 5.11 x $10^{8}$ | 12 | 175 | 4.36 x $10^{12}$ |
| 4 | Pre injection channel (500 µm w x 15 µm h x 5 mm L) | 3.63 x $10^{13}$ | | Total Chip $R_H$ without external resistance with IV1/IV2 closed = S4 + (S2 ‖ S3 ‖ S2) + (S1 ‖ S1) | | 13 | 250 | 1.05 x $10^{12}$ |
| 5 | Post injection channel (500 µm w x 15 µm h x 1.5 mm L) | 1.09 x $10^{13}$ | 9 | | 4.69 x $10^{15}$ | 14 | 500 | 6.54x $10^{10}$ |

For a fixed *Δp,* as a result of constant *Q* (controlled by a constant volumetric flow rate supplied by the pumps) and all three waste outlets at atmospheric pressure $p_{atm}$, *Q* will be split proportionally between three paths: the two separation channels [*Q1 = Q2*], each of which has equal $R_H$ of 9.3 x $10^{15}$ Pa s $m^{-3}$ (sum of serials 1, 6 and 7 from Table 4.2 when no external separation channel resistors are fitted) and the main waste outlet leading to the isolation valve (*Q3*) with an $R_H$ of 1.09 x $10^{13}$ Pa s $m^{-3}$ (sum of serials 5, 6, 7 and 8 from Table 4.2). Using the hydraulic-electric circuit analogy we can derive the ratio *Q1*: *Q2*: *Q3* = 1: 1: 855 indicating that 99.677% of the fluid will flow towards the main waste outlet. This ratio is considerably lower than that of the dual capillary system discussed in Chapter 2 where two 50 cm lengths of 50 µm i.d. capillary relative to a 10 cm long, 500 µm i.d. flow path to the main waste outlet yield a volumetric flow ratio of capillary: capillary: waste of 1: 1: 5 x $10^4$ (99.996%). Both of these values lie between the hydrodynamic resistance ratio of $10^5$ where hydrodynamic isolation was observed and 94 where it failed as reported by Attiya *et al*.[28] Thus, experimental evaluation of the design was undertaken to establish its suitability.

### 4.3.2 Sample introduction and hydrodynamic isolation

To examine the effectiveness of the injection interface design with this hydrodynamic ratio, a study of the sample introduction procedure was done by running sample past the interface without closing the isolation valve and effecting injection. Sample injection was made sequentially and typical separation sequence steps are detailed in Table 4.1. A schematic of the sample introduction and injection procedure (corresponding to steps 3 – 9 of Table 4.1) is in Figure 4.3. IV2 is only included to simulate a situation without split

injection and is kept closed during all phases for experiments described in Sections 4.3.2 – 4.3.4.

With both isolation valves closed, the separation channels were flushed (step 1) during which the inline pressure relief valve (87.1 psi) would overflow. IV1 was then opened and the BGE flow rate of 4 µL $s^{-1}$ maintained to equilibrate pressure through the chip (step 2). Sample is then introduced in a way to minimise hydrodynamic leakage and introduce a short well defined and controlled volume of sample. This was achieved by sheathing the sample flow with BGE during sample introduction (steps 3 – 5).

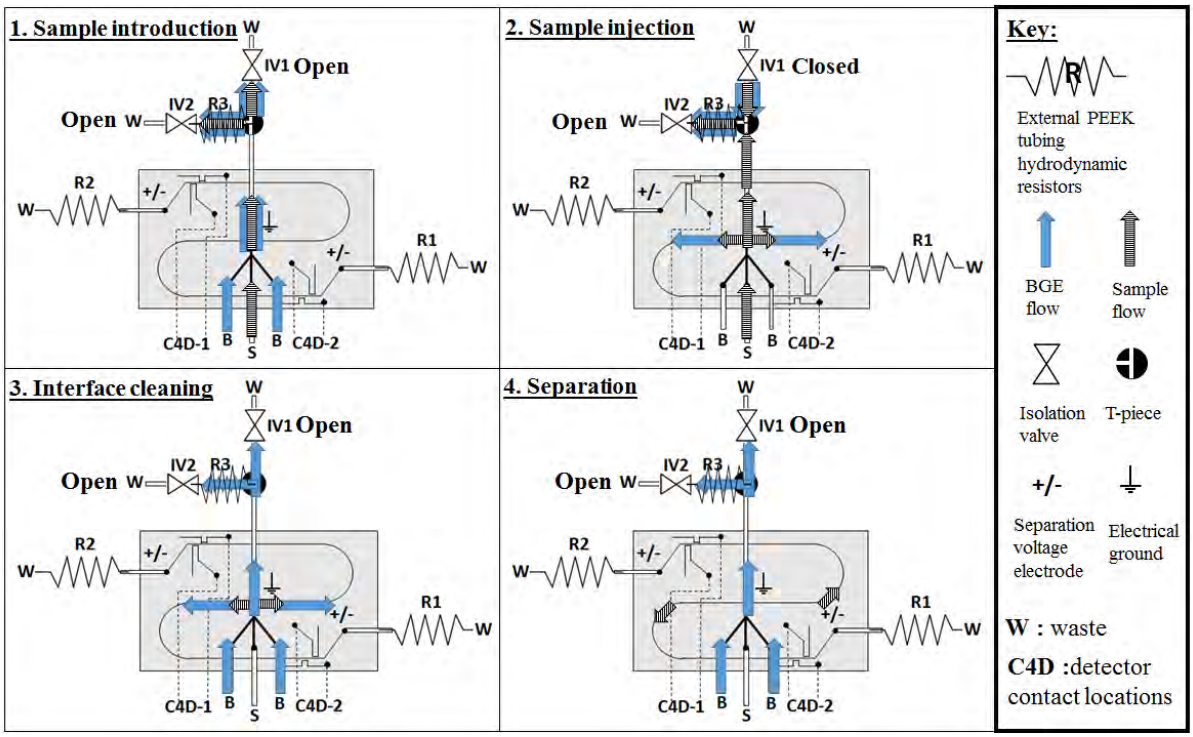


**Figure 4.3:** Sample introduction and hydrodynamic injection mechanism; 1: Sample stream is introduced to the injection interface between two BGE streams at a total flow rate of 4 µL $s^{-1}$. 2: Isolation valve 1 is momentarily closed, splitting *Q* between the three flow paths and forcing sample into both separation channels. 3: IV1 is reopened and BGE used to flush remaining sample away from the injection points at a total flow rate of 4 µL $s^{-1}$. 4: BGE flow rate is lowered to 1 µL $s^{-1}$, + and – 4500 V are applied to either ends of the separation channels for the electrophoretic separation phase.

During this process, there is a risk of bleeding, during the ~1 s where only sample is pumped into the main channel (steps 6 and 7). To examine the extent of hydrodynamic bleed and to ensure no carryover of sample due to incomplete flushing of the interface, control studies were conducted where the pump sequence was conducted as indicated in Table 4.1, without the closure of IV1 for injection (step 7). Theoretically, any hydrodynamic bleed of sample during this ~1 s period would collect as a sample plug at the entrances of the separation channels which could be detected during the separation step (step 9). At flow rates ≥ 7 μL $s^{-1}$, small deviations from the baseline were observed, indicating that the $R_H$ ratio of the DCSI ME system was insufficient to restrict entry of the sample into the separation microchannels. However, at flow rates ≤ 6 μL $s^{-1}$, no changes in the baseline signal could be observed, indicating the sample is introduced only by actuation of IV1 and that there was a sufficiently high difference in hydrodynamic resistance to effectively isolate the separation microchannel during sample introduction.

### 4.3.3 Hydrodynamic control of injection volume

In CE, typically 1-2 % of the capillary length is injected with sample. In order to calculate the amount of sample injected when IV1 is closed, we return to the hydraulic-electric circuit analogy. For all steps in the sequence where the valves are open (filling the interface with sample and during separation), the volumetric flow rate is independent of the pressure drop across the inlet and outlet ports of the microchip and the combined flow from pumps are analogous to the current output from an independent DC current source. However, during the injection phase and at $Q$ ≥ 4 μL $s^{-1}$, $\Delta p$ is controlled by the pump pressure relief valve to 87.1 psi and the system operates as an independent pressure source, which can be

considered to be analogous to a constant DC voltage source. Practically, this means that during injection, $\Delta p$ is constant at 87.1 psi (600.5 kPa, assuming $p_{atm}$ = 0). As the total chip $R_H$ is equal to $R4$ + ($R1 \parallel$ R2) ≈ 4.69 x $10^{15}$ Pa s $m^{-3}$ (Table 4.2), a total volumetric flow rate of $Q = \Delta p / R_H$ = 0.128 µL $s^{-1}$ onto the separation channels. The total injection time as a result of opening and closing the valve cannot be directly determined but can be estimated from the maximal on and off times (20 ms and 30 ms, respectively) giving a maximum injection volume of 6.4 nL. Because this total volume is injected onto the two separation microchannels, the theoretical maximum sample injection volume for each is 3.2 nL, or 4 % of the total separation channel volume (79.5 nL). This value is considerably higher than the recommended 1-2% in CE. To reduce the injected volume and improve the analytical performance of the system, the use of external hydrodynamic resistors was examined and will be discussed in 4.3.4 and 4.3.5.

### 4.3.4 Effect of external hydrodynamic separation channel resistance

To reduce the injected sample volume and evaluate its effect on the separation, external hydrodynamic resistors in the form of readily available pre-cut 30 cm lengths of PEEK tubing were connected to the ends of both separation channels. By using tubing with internal diameters ranging from 65 to 250 µm, the hydrodynamic resistance (*R1* and *R2* in Figures 4.1 (a) and 4.3) could be easily changed.

The additional external hydrodynamic separation channel resistance correlates with an increase in migration time and a decrease in peak height (Figure 4.4), with the effects most noticeable for the smaller resistors (larger diameters). The migration times were found

to increase by 2-4 seconds with the hydrodynamic resistance, principally due to a decrease in hydrodynamic assistance during separation with decreasing resistor diameter.

For all three analytes a 14 – 14.5 % increase in migration times occurred as a result of the addition of the 65 µm resistors as compared to no external hydrodynamic separation channel resistance, indicating a commensurate saving of separation space by the reduction of hydrodynamic assistance during the cleaning and separation steps. Conversely, peak heights decrease with increasing external hydrodynamic separation channel resistance due to smaller sample volumes being injected onto the capillary. The reproducibility of the migration times and peak heights improved with increasing external hydrodynamic separation channel resistance with the average %RSD in migration time for the three analytes decreasing from a maximum of 1.8 % when no external hydrodynamic separation

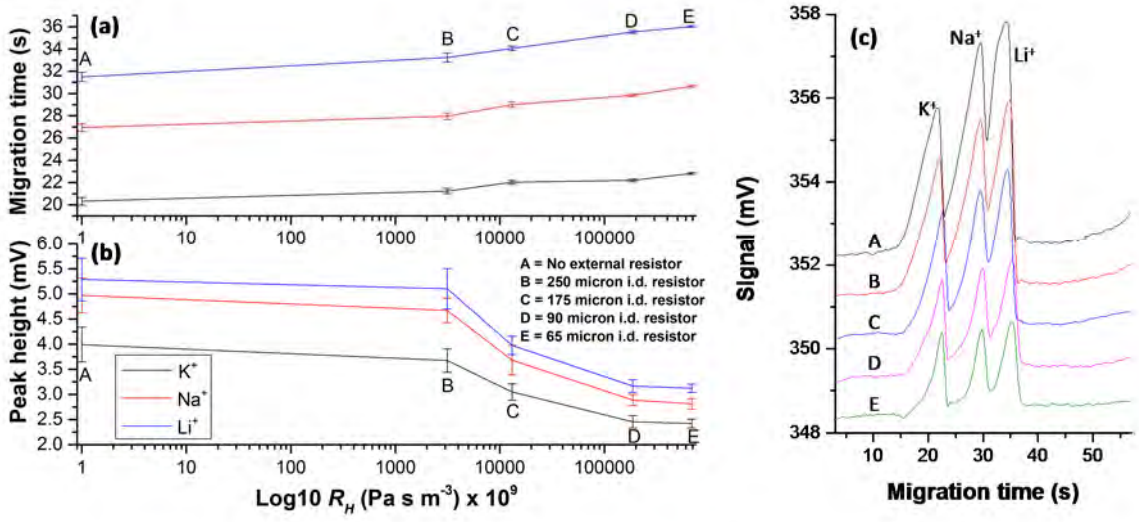


**Figure 4.4:** Effect of external hydrodynamic separation channel resistance through addition of external tubing on migration times (a) and peak heights (b) of a 5 ppm mixture of $K^+$, $Na^+$ and $Li^+$. All resistors were of 30 cm length. Error bars correspond to +/- 1 standard deviation for 5 consecutive runs. The electropherograms shown in panel c have been offset for clarity.

channel resistance was fitted to a maximum of 0.7 % when using the 65 µm tubing. Despite the reduction in injection volume, the injected volume was still too large for CE and the three analytes could not be fully resolved using the hydrodynamic resistors at the separation channel outlets. To further decrease the injection volume, a split injection system was developed, as discussed below.

### 4.3.5 Split injection using external hydrodynamic injection channel resistor

To further reduce injection volumes, a split injection method was developed by the insertion of an additional flow outlet, effectively reducing the $R_H$ of the feeder channel. To this extent, hydrodynamic resistors were fitted to a T piece, as illustrated with *R3* in Figure 4.1 (a) and Figure 4.3, to provide the alternate flow path, *Q3* when IV1 is closed. During injection, the equivalent electrical circuit is analogous to a current divider, reducing the flows Q1 and Q2 in the respective separation channels by Q3.

The T piece was connected with 10 cm long pieces of PEEK tubing with 65, 90, 175 or 250 µm i.d., whilst the separation channels were connected with 30 cm long, 90 µm i.d. PEEK tubing. When IV2 was closed, Q3 equals 0 and this replicates the conditions of the experiments conducted in Sections 4.3.2 – 4.3.4. The effect of reducing R3 of the feeder channel on the analytical performance of the DCSI ME system is given in Figure 4.5. Because $K^+$ was resolved under all conditions, the potassium peak was used to assess the analytical performance based on migration times, peak heights, theoretical plate number and the variability in peak area, as plotted in Figure 4.5(a). Representative electropherograms for external hydrodynamic injection channel resistor values of infinite resistance (IV2 shut = 0 µm i.d.), 65 µm, 90 µm and 125 µm i.d. are given in Figure 4.5(b).

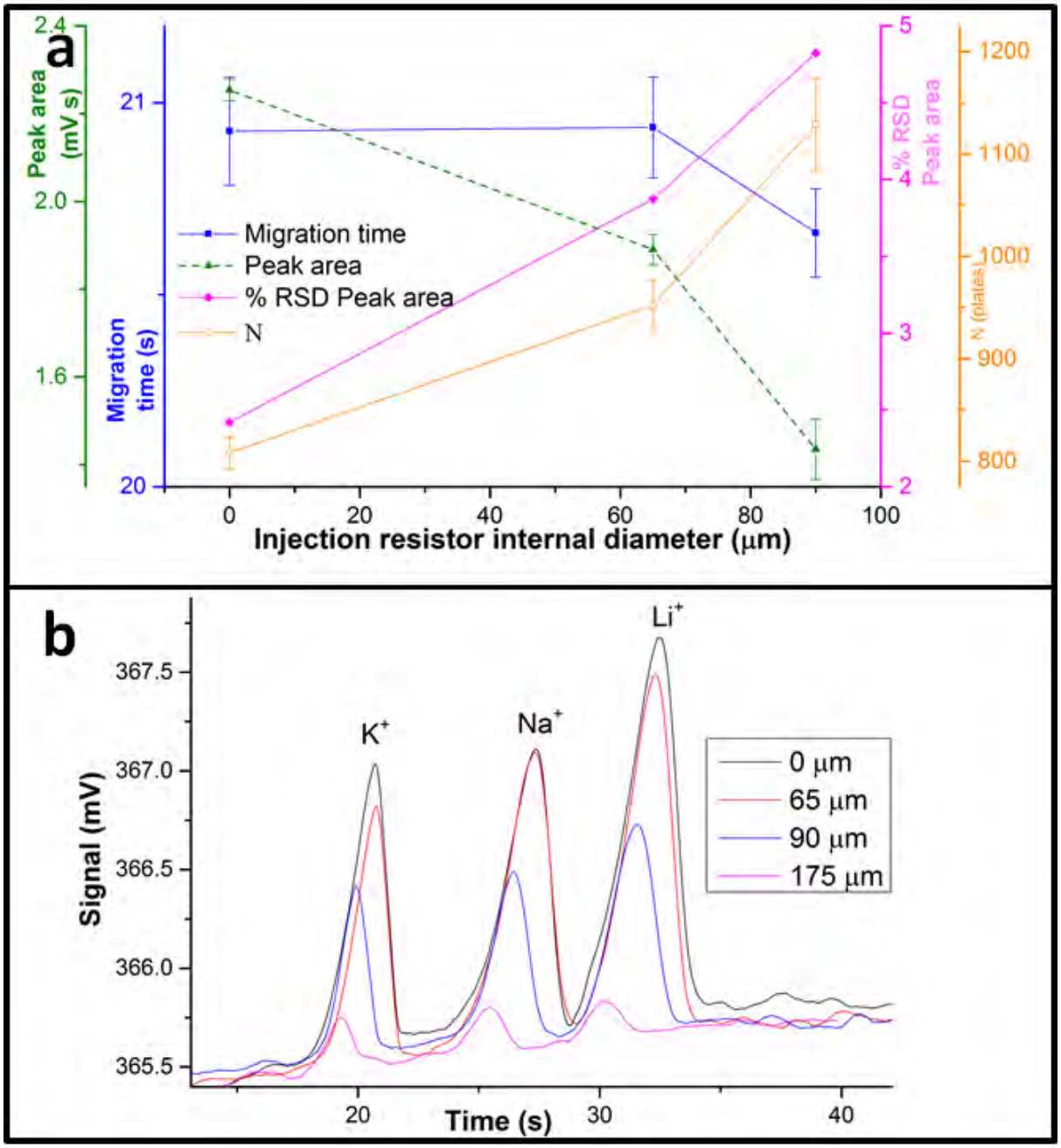


**Figure 4.5:** (a) Effect of the change in external hydrodynamic injection channel resistor internal diameters on migration times and peak heights of $K^+$ at 5 ppm. All resistors were of 10 cm length. Error bars correspond to +/- 1 standard deviation for 5 consecutive runs. %RSD of peak area is calculated for 5 runs. (b) Representative signal trace overlays of separations of 5 ppm $K^+$, $Na^+$, and $Li^+$ with different i.d. hydrodynamic resistors.

With an external hydrodynamic injection channel resistor i.d. of 175 µm, the injection volume was highly variable ( > 50 % RSD) and no injections were observed over 10 consecutive runs when using tubing with an i.d. of 250 µm, hence the values of 175 and 250 µm resistors were omitted from Figure 4.5 (a). As illustrated in the figure, smaller volumes were injected with increasing diameter, as decreasing hydrodynamic resistance *R3* of the external hydrodynamic injection channel resistor increased flow *Q3*. This is demonstrated by the decrease in peak area with increasing external hydrodynamic injection channel resistor internal diameter. The % RSD of peak areas decreased with decreasing internal diameter, with all diameters ≤ 90 µm giving %RSD for peak area < 5% which is similar to the repeatability that is typical for conventional CE. Migration times (and SD) did not change significantly over the resistance ranges examined. The separation efficiencies increased with the smaller injection volumes and while the repeatability decreased, it remained < 5% for the 90 µm i.d. tubing. A maximum efficiency of 1129 plates (13 x $10^3$ plates $m^{-1}$) was observed with the 90 µm i.d. tubing. All three peaks could be baseline resolved when the R1:R3:R2 ratio during injection was ≈ 1:1:870 corresponding to external hydrodynamic separation channel hydrodynamic resistors of 30 cm x 90 µm i.d PEEK tubing and an external hydrodynamic injection channel hydrodynamic resistor of 10 cm x 90 µm i.d.

### 4.3.6 Simultaneous separation of cations and anions

The optimised conditions from Section 4.3.5 were used to run 100 consecutive separations of a mixture comprising $K^+$, $Na^+$, $Li^+$, $Cl^-$, $Fl^-$ and $PO_4^{2-}$ (primarily seen as $H_2PO_4^-$ at pH 4.2). Figure 4.6 shows 10 consecutive separations, with the cations separated in a co-EOF mode in the cation channel, whilst the anions were separated in counter-EOF mode due to the cathodic EOF generated by the PMMA surface, although the magnitude of the EOF is likely

to be low at pH 4.2. A BGE consisting of 50 mM acetic acid / 10mM L-histidine (pH 4.2) was chosen as it has been previously demonstrated as an excellent BGE for the separation of these anionic and cationic targets by Mai *et. al.* [31] and in the DCSI-CE system described in Chapter 2. The choice of BGE has a large impact on the sensitivity of $C^4D$ detection for specific analytes as sensitivity is largely determined by the difference in mobilities between the analyte and the BGE counter ion. This is demonstrated here whereby the LOD of $H_2PO_4^-$ is approximately 20 times higher than that of $Li^+$. Additionally $H_2PO_4^-$ is seen as a negative peak due to the fact that it has a lower mobility than the BGE counter ion (acetate).

Figures of merit were obtained for 20 runs, analysing every 5$^{th}$ run and given in Table 4.3. The %RSD for peak areas ranges from 2.3 to 4.5 %, which compares very well with our previous work using a dual capillary system and electrokinetic injection in Chapter 2 and is comparable to performance data obtained with a conventional commercial CE instrument. Whilst the LODs are about one order of magnitude higher when compared with our previous work in capillaries using the same electronics with the capillary head, the LODs are two orders of magnitude lower than we reported for the in-plane embedded $C^4D$ electrodes in Chapter 3 as a result of modifications in the grounding and shielding of the microchip system. Furthermore, the LODs of the DCSI-ME system are about an order of magnitude lower than those reported for the same analytes using the same electronics in a different electrode arrangement using 45/55 mM MES/His as BGE [32] and slightly better than LODs recently published for in-plane metal $C^4D$ electrodes and a 15 mM MES/His buffer [33] .

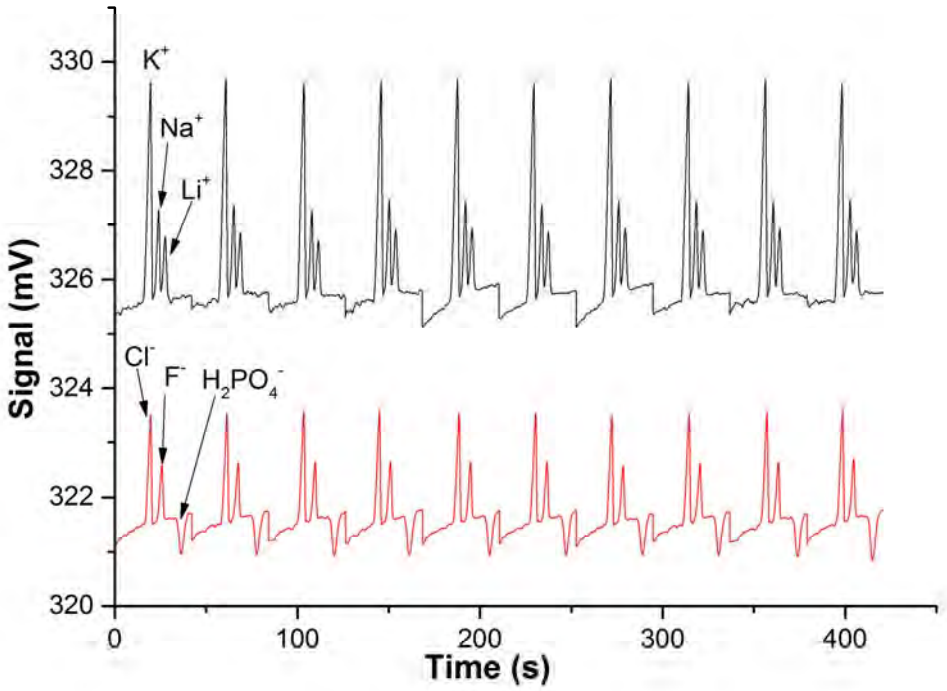


**Figure 4.6:** Ten consecutive simultaneous separations of $K^+$ (10 ppm), $Na^+$ (6 ppm), $Li^+$ (2 ppm), $Cl^-$ (10 ppm), $F^-$ (5 ppm) and $H_2PO_4^-$ (34 ppm). BGE is 50 mM acetic acid / 10 mM His at pH 4.2. Injection conditions are detailed in Table 1. Separations are carried out at +/- 4500 V for anions/ cations respectively.

The efficiencies obtained with the DCSI ME system at a field strength of 450 V $cm^{-1}$ (13.3 x $10^3$ plates $m^{-1}$) are slightly lower than those obtained for the same analytes using electrokinetically pinched injection from a standard injection cross [33] (17.7 x $10^3$ plates $m^{-1}$) using a 15 mM MES/His buffer and a field strength of 250 $Vcm^{-1}$. The lower efficiency can most likely be explained by the loss in separation space to due to hydrodynamic assistance (calculated as approximately 57 % of channel displacement during the ≈ 20 s until the detection of potassium), the parabolic sample plug profile associated with hydrodynamic injection and an increase in diffusion as a result of the curved separation channel, issues

that will be addressed in a future microchip design. However, unlike the pinched injection system, the approach here does not suffer from electrokinetic bias, significantly increasing its suitability for analytical applications. Whilst the sensitivity and separation space of the presented ME system are reduced as compared to the dual channel CE system, the lower sample and reagent consumption volumes (16 µL sample and 99 µL BGE per run for the ME system as compared to 83 µL sample and 232 µL BGE per run) and reduction in run time (70.5 s per analysis for the ME system as compared to 201 s per analysis for the CE system) make this system particularly amenable to initial rapid screening applications.

**Table 4.3:** Figures of merit for 100 consecutive separations of $K^+$, $Na^+$, $Li^+$, $Cl^-$, $F^-$ and $H_2PO_4^-$. BGE is 50 mM acetic acid / 10 mM His at pH 4.2. Injection conditions are detailed in Table 1. Separations are carried out at +/- 4500V for anions/ cations respectively. All results are based on *n* =20 (every 5$^{th}$ run of 100 consecutive runs).

| | MT (s) | MT %RSD | PA %RSD | LOD (S/N = 3) mg $L^{-1}$ / µM |
|---|---|---|---|---|
| **$K^+$** | 20.04 | 0.40 | 2.3 | 0.200 / 5.12 |
| **$Na^+$** | 24.9 | 0.47 | 3.8 | 0.198 / 8.61 |
| **$Li^+$** | 28.53 | 0.44 | 3.9 | 0.110 / 15.9 |
| **$Cl^-$** | 22.17 | 0.63 | 3.4 | 0.317 / 8.95 |
| **$F^-$** | 28.19 | 0.37 | 3.4 | 0.364 / 19.2 |
| **$H_2PO_4^-$** | 38.46 | 0.28 | 4.5 | 2.29 / 23.6 |

## 4.4 Future directions

Whilst the studies in this chapter have demonstrated the potential for simultaneous separations of anions and cations via hydrodynamic injection in the microchip format, they suffer from the same fundamental drawback as the DCSI-CE presented in Chapter 2 and from any dual-opposite end injection method in a single capillary [34, 35] or single [26] or dual micro-channels;[25] the compromise chemistry involved when trying to separate anionic and cationic species in one background electrolyte.

In microfluidic channels, a low Reynolds number dictates a laminar flow regime which enables different liquids to flow alongside one another without mixing other than by diffusion. This property has been effectively used for sample extraction and clean-up since the mid- 1990's.[36] To further study the system developed in this chapter, laminar flow was used to deliver different background electrolytes to the two separation channels.

The same general experimental apparatus and optimised injection conditions as described in this chapter were used, however food dyes (Pillar box red, Yellow, Blue, Queen, Queensland, Australia) were substituted for BGE's and sample. An extra MilliGat pump and in-line relief valve were added for the second BGE input. Flow rates for the BGE as described in Table 4.1 were halved for each individual BGE pump, maintaining the same total BGE flow rates as described in the table.

A microchip of the same design but with 300 µm wide feeder channels and 30 µm wide separation channels instead of the 500 µm/50 µm wide feeder/separation channels reported above was used for the studies; all other channel dimensions specified earlier in this Chapter remained the same. A portable USB microscope (Traveller, Supra, Germany) was used to capture imagery.

Using the same operation procedure as described in table 4.1, both valves are closed for the flushing stage (Step 1) leading to each separation channel being filled exclusively with the BGE closest to the respective BGE feeder channel. The laminar flow allowed for effective isolation of both channels through all operation steps and an image of the injected sample plugs (red dye) just after injection (corresponding to Step 8 in table 4.1) is given in Figure 4.7.

The figure demonstrates both the potential for the dual-BGE separation method and the small size of the hydrodynamically injected plugs. Unfortunately, time constraints did not allow for the further study of the efficacy of this method, in particular, the degree of migration of BGE' counter-ions into opposite separation channels to become unwanted co-ions.

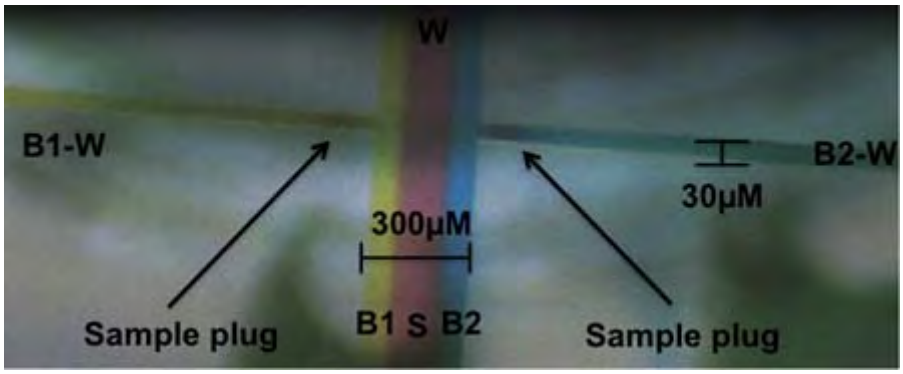


**Figure 4.7:** Photograph of simultaneously injected sample plugs (S, Red) in two separate BGES; BGE 1: B1 (Yellow) and BGE 2: B2 (Blue). W: main waste outlet and solenoid valves. B1-W and B2-W indicate the directions of the anode and cathode waste outlets respectively.

As identified in Section 4.3.4, considerable unwanted hydrodynamic assistance occurred during the flush and separation steps of the DCSI-ME operation sequence. Under the final optimised conditions described in Section 4.3.6, this was calculated as contributing to approximately 57 % of channel displacement during the ≈ 20 s until the separation of potassium. Given the chip manufacturing constraints described in Section 4.3.1, without drastically increasing the external hydrodynamic resistors or increasing the separation channel lengths, reduction of this unwanted hydrodynamic resistance is difficult to practically realise with a 2-dimensional planar chip manufacturing process.

One possible direction forward to increase the hydrodynamic resistance ratio at the injection cross piece (and subsequently reduce hydrodynamic assistance) would be to increase the depth of the main feeder channels relative to the separation channel which would involve two different channel depths on chip. As trialled in Chapter 3, was the production of a directly machined aluminium negative relief master for casting of PDMS positive relief embossing stamps. This method was initially rejected as it resulted in channels of differing depths due to different mounting heights of the two tool pieces required to produce the two different channel widths. This direct machining method could potentially provide a simple means to produce multi-depth channels and simply replace the lithographic negative relief processing step.

## 4.5 Concluding remarks

A new hydrodynamic injection protocol was developed for injection in microchip electrophoresis. Using a dual channel sequential injection interface, one sample could be simultaneously injected into two different separation channels for electrophoretic

separation. Flow conditions were optimised to control the injected sample volume using external hydrodynamic resistors made from commercially available tubing, with the optimised system combining hydrodynamic resistors on the separation channels and also on the waste. Laminar flow was exploited to sheath the sample flow with BGE during sample introduction, preventing hydrodynamic bleed. The analytical performance of the DCSI-ME system is comparable with that of conventional electrokinetic injection methods, with the important improvement that there is no electrokinetic bias during injection. The potential of the DCSI-ME system was demonstrated for the simultaneous analysis of inorganic anions and cations from the same sample in individual separation channels. The continuous flow through the system allows it to operate continuously in a fully automated manner, making it highly suitable for on-line coupling with complementary separations or for applications involving near real-time monitoring. Preliminary results demonstrate great potential for the use of this system with two separate BGE streams, separated due to laminar flow, allowing for individually optimised separation chemistries in both separation channels. Simple modifications to the microchip manufacturing process to allow for multi-depth channels could significantly reduce the amount of unwanted hydrodynamic assistance with a commensurate saving of separation space and considerably improve the analytical performance of the system.

## 4.6 References

1. Manz, A.; Graber, N.; Widmer, H. M., Miniaturized total chemical analysis systems: A novel concept for chemical sensing. *Sensors and Actuators: B. Chemical* **1990,** *1*, 244-248.

2. Saito, R. M.; Coltro, W. K. T.; De Jesus, D. P., Instrumentation design for hydrodynamic sample injection in microchip electrophoresis: A review. *Electrophoresis* **2012,** *33*, 2614-2623.

3. Fu, L. M.; Yang, R. J.; Lee, G. B.; Liu, H. H., Electrokinetic injection techniques in microfluidic chips. *Analytical Chemistry* **2002,** *74*, 5084-5091.

4. Karlinsey, J. M., Sample introduction techniques for microchip electrophoresis: A review. *Analytica Chimica Acta* **2012,** *725*, 1-13.

5. Manz, A.; Harrison, D. J.; Verpoorte, E. M. J.; Fettinger, J. C.; Paulus, A.; Lüdi, H.; Widmer, H. M., Planar chips technology for miniaturization and integration of separation techniques into monitoring systems. Capillary electrophoresis on a chip. *Journal of Chromatography A* **1992,** *593*, 253-258.

6. Seiler, K.; Jed Harrison, D.; Manz, A., Planar glass chips for capillary electrophoresis: Repetitive sample injection, quantitation, and separation efficiency. *Analytical Chemistry* **1993,** *65*, 1481-1488.

7. Slentz, B. E.; Penner, N. A.; Regnier, F., Sampling bias at channel junctions in gated flow injection on chips. *Analytical Chemistry* **2002,** *74*, 4835-4840.

8. Jacobson, S. C.; Hergenröder, R.; Koutny, L. B.; Ramsey, J. M., High-Speed Separations on a Microchip. *Analytical Chemistry* **1994,** *66*, 1114-1118.

9. Harrison, D. J.; Fluri, K.; Seiler, K.; Fan, Z. H.; Effenhauser, C. S.; Manz, A., Micromachining a Miniaturized Capillary Electrophoresis-Based Chemical-Analysis System on a Chip. *Science* **1993,** *261*, 895-897.

10. Effenhauser, C. S.; Manz, A.; Widmer, H. M., Glass Chips for High-Speed Capillary Electrophoresis Separations with Submicrometer Plate Heights. *Analytical Chemistry* **1993,** *65*, 2637-2642.

11. Effenhauser, C. S.; Paulus, A.; Manz, A.; Widmer, H. M., High-speed separation of antisense oligonucleotides on a micromachined capillary electrophoresis device. *Analytical Chemistry* **1994,** *66*, 2949-2953.

12. Shultz-Lockyear, L. L.; Colyer, C. L.; Fan, Z. H.; Roy, K. I.; Harrison, D. J., Effects of injector geometry and sample matrix on injection and sample loading in integrated capillary electrophoresis devices. *Electrophoresis* **1999,** *20*, 529-538.

13. Backofen, U.; Matysik, F. M.; Lunte, C. E., A chip-based electrophoresis system with electrochemical detection and hydrodynamic injection. *Analytical Chemistry* **2002,** *74*, 4054-4059.

14. Solignac, D.; Gijs, M. A. M., Pressure pulse injection: A powerful alternative to electrokinetic sample loading in electrophoresis microchips. *Analytical Chemistry* **2003,** *75*, 1652-1657.

15. Lacharme, F.; Gijs, M. A. M., Single potential electrophoresis microchip with reduced bias using pressure pulse injection. *Electrophoresis* **2006,** *27*, 2924-2932.

16. Lacharme, F.; Gijs, M. A. M., Pressure injection in continuous sample flow electrophoresis microchips. *Sensors and Actuators, B: Chemical* **2006,** *117*, 384-390.

17. Zhang, L.; Yin, X. F., Field amplified sample stacking coupled with chip-based capillary electrophoresis using negative pressure sample injection technique. *Journal of Chromatography A* **2006,** *1137*, 243-248.

18. Gáspár, A.; Koczka, P. I.; Carmona, H.; Gomez, F. A., Split injection: A simple introduction of subnanoliter sample volumes for chip electrophoresis. *Microchemical Journal* **2011,** *99*, 180-185.

19. Lin, Y. H.; Lee, G. B.; Li, C. W.; Huang, G. R.; Chen, S. H., Flow-through sampling for electrophoresis-based microfluidic chips using hydrodynamic pumping. *Journal of Chromatography A* **2001,** *937*, 115-125.

20. Bai, X.; Lee, H. J.; Rossier, J. S.; Reymond, F.; Schafer, H.; Wossner, M.; Girault, H. H., Pressure pinched injection of nanolitre volumes in planar micro-analytical devices. *Lab on a Chip - Miniaturisation for Chemistry and Biology* **2002,** *2*, 45-49.

21. Graß, B.; Neyer, A.; Jöhnck, M.; Siepe, D.; Eisenbeiß, F.; Weber, G.; Hergenröder, R., New PMMA-microchip device for isotachophoresis with integrated conductivity detector. *Sensors and Actuators, B: Chemical* **2001,** *72*, 249-258.

22. Kaniansky, D.; Masár, M.; Bielčiková, J.; Iványi, F.; Eisenbeiss, F.; Stanislawski, B.; Grass, B.; Neyer, A.; Jöhnck, M., Capillary electrophoresis separations on a planer chip with the column-coupling configuration of the separation channels. *Analytical Chemistry* **2000,** *72*, 3596-3604.

23. Büttgenbach, S.; Wilke, R., A capillary electrophoresis chip with hydrodynamic sample injection for measurements from a continuous sample flow. *Analytical and Bioanalytical Chemistry* **2005,** *383*, 733-737.

24. Prest, J. E.; Baldock, S. J.; Fielden, P. R.; Goddard, N. J.; Treves Brown, B. J., Bidirectional isotachophoresis on a planar chip with integrated conductivity detection. *Analyst* **2002,** *127*, 1413-1419.

25. Reschke, B. R.; Schiffbauer, J.; Edwards, B. F.; Timperman, A. T., Simultaneous separation and detection of cations and anions on a microfluidic device with suppressed electroosmotic flow and a single injection point. *Analyst* **2010,** *135*, 1351-1359.

26. Wang, J.; Chen, G.; Muck Jr, A.; Collins, G. E., Electrophoretic microchip with dual-opposite injection for simultaneous measurements of anions and cations. *Electrophoresis* **2003,** *24*, 3728-3734.

27. Blanco, G. A.; Nai, Y. H.; Hilder, E. F.; Shellie, R. A.; Dicinoski, G. W.; Haddad, P. R.; Breadmore, M. C., Identification of inorganic improvised explosive devices using sequential injection capillary electrophoresis and contactless conductivity detection. *Analytical Chemistry* **2011,** *83*, 9068-9075.

28. Attiya, S.; Jemere, A. B.; Tang, T.; Fitzpatrick, G.; Seiler, K.; Chiem, N.; Jed Harrison, D., Design of an interface to allow microfluidic electrophoresis chips to drink from the fire hose of the external environment. *Electrophoresis* **2001,** *22*, 318-327.

29. Oh, K. W.; Lee, K.; Ahn, B.; Furlani, E. P., Design of pressure-driven microfluidic networks using electric circuit analogy. *Lab on a Chip - Miniaturisation for Chemistry and Biology* **2012,** *12*, 515-545.

30. Lee, K.; Kim, C.; Ahn, B.; Panchapakesan, R.; Full, A. R.; Nordee, L.; Kang, J. Y.; Oh, K. W., Generalized serial dilution module for monotonic and arbitrary microfluidic gradient generators. *Lab on a Chip - Miniaturisation for Chemistry and Biology* **2009,** *9*, 709-717.

31. Mai, T. D.; Schmid, S.; Müller, B.; Hauser, P. C., Capillary electrophoresis with contactless conductivity detection coupled to a sequential injection analysis manifold for extended automated monitoring applications. *Analytica Chimica Acta* **2010,** *665*, 1-6.

32. Henderson, R. D.; Guijt, R. M.; Andrewartha, L.; Lewis, T. W.; Rodemann, T.; Henderson, A.; Hilder, E. F.; Haddad, P. R.; Breadmore, M. C., Lab-on-a-Chip device with laser-patterned polymer electrodes for high voltage application and contactless conductivity detection. *Chemical Communications* **2012,** *48*, 9287-9289.

33. Thredgold, L. D.; Khodakov, D. A.; Ellis, A. V.; Lenehan, C. E., On-chip capacitively coupled contactless conductivity detection using "injected" metal electrodes. *Analyst* **2013,** *138*, 4275-4279.

34. Kubáň, P.; Karlberg, B., Simultaneous Determination of Small Cations and Anions by Capillary Electrophoresis. *Analytical Chemistry* **1998,** *70*, 360-365.

35. Padarauskas, A.; Olšauskaite, V.; Schwedt, G., Simultaneous separation of inorganic anions and cations by capillary zone electrophoresis. *Journal of Chromatography A* **1998,** *800*, 369-375.

36. Brody, J. P.; Yager, P., Diffusion-based extraction in a microfabricated device. *Sensors and Actuators, A: Physical* **1997,** *58*, 13-18.

# Chapter 5: Electrophoretic system design and development of an automated multi-purpose microfluidic platform

## 5.1 Introduction

Integration of components is considered as one of the main advantages of miniaturising analytical instrumentation [1] and represents the ultimate goal of the development of platforms with rapid sample-in / answer out capabilities (so-called miniaturized total analysis system, or μTAS).[2] Despite considerable progress, at present microfluidic systems are typically dedicated to one or a few select steps.[3] Ideally, sampling, sample processing, separation and detection are performed on board of a single microfluidic device. The extent to which components including pumps, valves, and injectors and detectors have to be integrated into this device is a key consideration in the development of these systems. A recent review of applications of autonomous microfluidic systems in environmental monitoring by Campos *et. al.* covers the most recent literature and important microfluidic system design considerations as it relates to this field.[4]

In the development of analytical instrumentation, the controlling soft- and hardware manages the operation of components as well as data acquisition and storage. In Figure 5.1, this is schematically illustrated for the sequential injection electrophoresis instruments described in this thesis. The complexity of the components as well as the accuracy and precision required in their operation, in turn, dictate the accuracy and speed at which the control should operate.

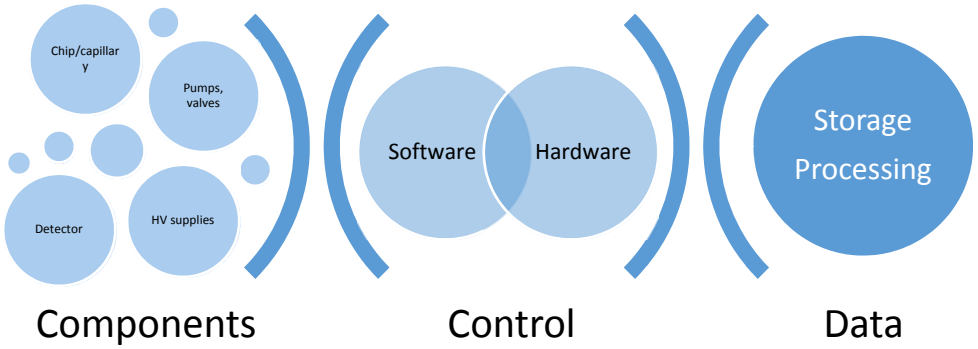


**Figure 5.1:** Component, control and data integration for sequential injection electrophoresis systems.

For identifying the required components, CE is unique in its instrumental simplicity, requiring a narrow bore capillary (or microchannel) and a HV power supply in combination with small (µL-mL) volumes of solutions to achieve high-resolution separations.[5] This instrumental simplicity is one of the most highly cited benefits of CE (and to a lesser extent ME) and makes CE amenable to miniaturisation.[6] The most recent technical advances and commercially available systems in capillary-based portable CE (P-CE) are covered in a recent review.[7]

In this chapter, the considerations made in the design and construction of a multi-purpose microfluidic platform are discussed. This design is informed by the design and performance of other capillary-based systems the author developed over the course of

these studies. The key elements of the development of these capillary-based systems are therefore included in this chapter.

## 5.2 Hardware and Methodology

### 5.2.1 Microchip manufacture

The microchip design and manufacture process is described in Section 4.2.1.

### 5.2.2 Sequential capillary and microchip systems

Major system components of the sequential dual capillary system (Chapter 2), the sequential injection microchip system (Chapter 4) and the multi-purpose microfluidic platform discussed in this chapter are summarised in Table 5.1. Additional systems were developed by the author during the course of this thesis and hardware details are also included in Table 5.1 to provide a more complete picture.

### 5.2.3 Multi-purpose microfluidic system

A schematic and 3D rendering of the multi-purpose microfluidic system developed in this Chapter showing all major hardware components is given in Figure 5.2.

**Table 5.1:** Principal hardware details for developed electrophoretic systems

| Serial | System | HV power supplies | Pumps | Valves | Fittings | Detector | Control board(s) | Software | Application | Reference |
|---|---|---|---|---|---|---|---|---|---|---|
| 1 | **Dual channel SI-CE** | 2 x 30 kV HVPS (CZE 1000/ CZE 2000, Spellman Hauppage, NY, USA) | 1 x double syringe pump (Harvard Apparatus, Model 33, Holliston, MA, USA) *or* 1 x MilliGAT pump with Mforce controller (MG-5, Global FIA,Fox island, WA, USA) and 1 x quaternary gradient HPLC pump (Alltech, Grace Division Discovery Science, Archerfield, QLD, AUS) | 1 x 2-position injector valve (MXP-7980, Rheodyne, Oak Harbour, WA, USA), 1 x isolation valve (HP225K021, NResearch, West Caldwell, NJ, USA). | Standard and Modified COTS. | 2 x $C^4D$ (TraceDec, Innovative Sensor Technolog-ies, Strassahof, Austria) | 1 x DAQ (NI USB-6212, National Instruments, Austin, TX, USA) | LabVIEW 8.1 (NI, Austin, TX, USA) | On-line simultaneous and rapid separation of anions and cations from a single sample using dual-capillary sequential injection-capillary electrophores-is | **Chapter 2** |
| **2** | **Single Channel SI-CE 1** | 1 x 30 kV HVPS (4300, EMCO, CA, USA) | 2 x Peristaltic pumps (PeriWaves, CorSolutions, Ithaca, NY, USA) | 1 x 2-position injector valve (MXP-7980, Rheodyne, Oak Harbour, WA, USA), 1 x isolation valve (HP225K021, NResearch, West Caldwell, NJ, USA). | Standard and modified COTS. | 1 x C4D (TraceDec, Innovative Sensor Technolog-ies, Strassahof, Austria) | 1 x DAQ (NI USB-6212, National Instruments, Austin, TX, USA). | LabVIEW 8.1 (NI, Austin, TX, USA) | On-line sequential-injection capillary electrophores-is for near-real-time monitoring of extracellular lactate in cell culture flasks. | **8** |

**Table 5.1 (continued):** Principal hardware details for developed electrophoretic systems

| Serial | System | HV power supplies | Pumps | Valves | Fittings | Detector | Control board(s) | Software | Application | Reference |
|---|---|---|---|---|---|---|---|---|---|---|
| 3 | **Single Channel SI-CE 2** | 1 x 30 kV HVPS (CZE 1000, Spellman Hauppage, NY, USA) | 3 x MilliGAT pumps with Mforce controllers (MG-5, Global FIA,Fox island, WA, USA) | 1 x 2-position injector valve (MXP-7980, Rheodyne, Oak Harbour, WA, USA), 1 x isolation valve (HP225K021, NResearch, West Caldwell, NJ, USA). | Standard COTS. | 1 x $C^4D$ (TraceDec, Innovative Sensor Technolog-ies, Strassahof, Austria) | 1 x DAQ (NI USB-6008, National Instruments, Austin, TX, USA) and in-house constructed dual channel 2 x Op amplifier. | LabVIEW 2011 (NI, Austin, TX, USA) | Hyphenated IC-CE analysis of complex samples | Publication in progress |
| **4** | **Single Channel SI-CE 3** | 1 x 33 kV HVPS (4330, EMCO, CA, USA) | 3 x MilliGAT pumps with Mforce controllers (MG-5, Global FIA,Fox island, WA, USA) | 1 x 2-position injector valve (MXP-7980, Rheodyne, Oak Harbour, WA, USA), 1 x isolation valve (HP225K021, NResearch, West Caldwell, NJ, USA). 1 x 3-way valve (HP225K031, NResearch, West Caldwell, NJ, USA) | Standard COTS. | 1 x C4D (TraceDec, Innovative Sensor Technolog-ies, Strassahof, Austria) | 1 x DAQ (NI USB-6212, National Instruments, Austin, TX, USA) | LabVIEW 2011 (NI, Austin, TX, USA) | Pre-blast screening of inorganic explosive anions | Publication in progress |

**Table 5.1 (continued):** Principal hardware details for developed electrophoretic systems

| Serial | System | HV power supplies | Pumps | Valves | Fittings | Detector | Control board(s) | Software | Application | Reference |
|---|---|---|---|---|---|---|---|---|---|---|
| 5 | **Dual channel SI-DC - MCE** | 1 x custom +/- 5 kV 4 Channel reversible power supply | 2 x MilliGAT pumps with Mforce controllers (MG-5, Global FIA,Fox island, WA, USA) | 2 x isolation valves (HP225K021, NResearch, West Caldwell, NJ, USA). | Modified COTS. | 2 x $C^4D$ (TraceDec, Innovative Sensor Technologies, Strassahof, Austria) | 2 x DAQ (MCC USB-2533 and MCC USB-3105, MCC, Norton, MA, USA) | LabVIEW 2011 (NI, Austin, TX, USA) | Simultaneous determination of anions and cations by hydrodynamic injection on a polymer microchip. | **Chapter 4** |
| **6** | **Multi-purpose micro-fluidic platform** | 2 x +/- 8 kV custom reversible power supplies | 4 x MilliGAT pumps with Mforce controllers (MG-5, Global FIA,Fox island, WA, USA) | 4 x isolation valves (HP225K021, NResearch, West Caldwell, NJ, USA), 1 x 3-way valve (HP225K031, NResearch, West Caldwell, NJ, USA) | Modified COTS. | 2 x custom C4D detectors | 1 x DAQ (NI USB-6212, National Instruments, Austin, TX, USA) | LabVIEW 2011 (NI, Austin, TX, USA) | Multiple. | Publication in progress |

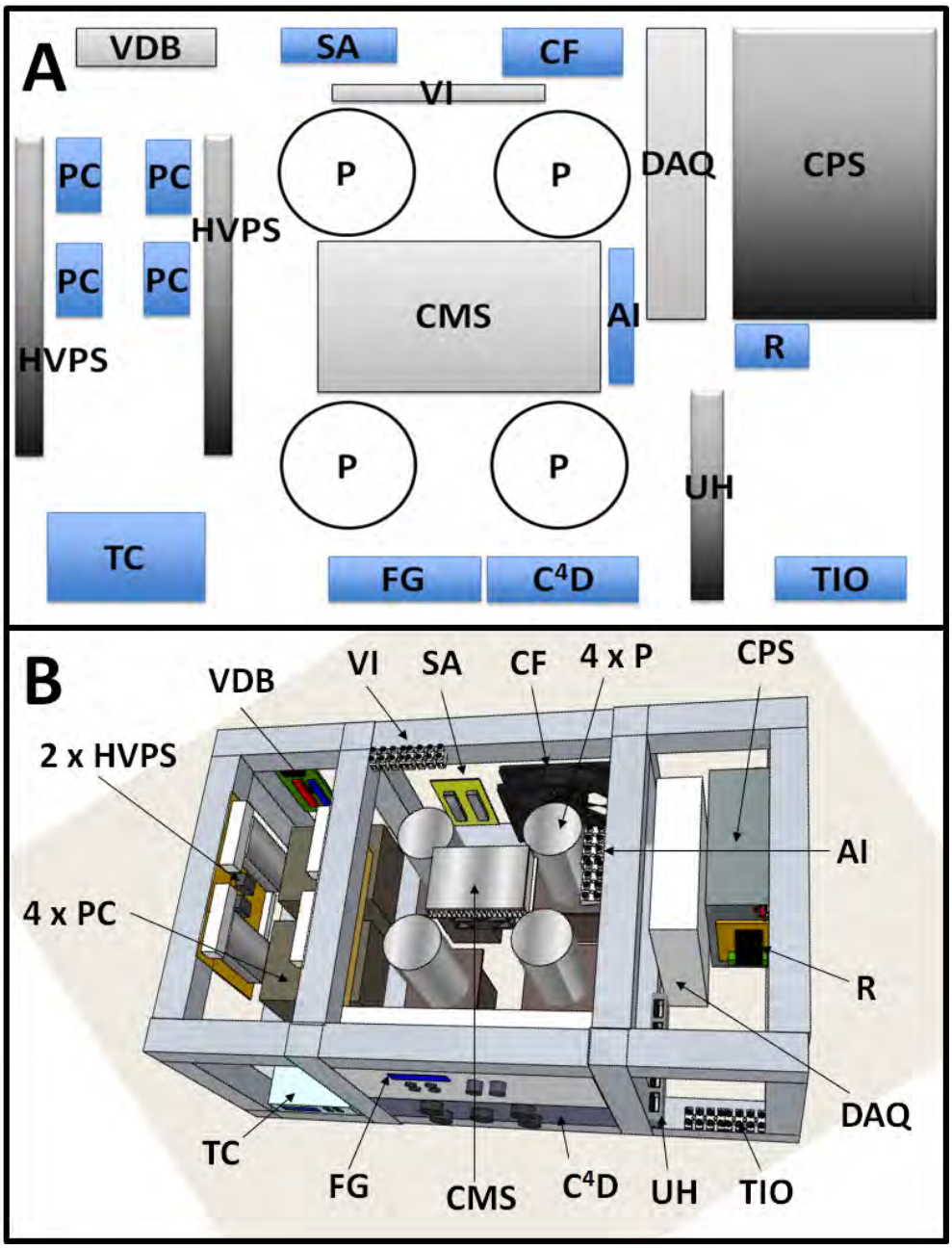


**Figure 5.2:** A: Schematic of major hardware components and B: 3D rendering of the multi-purpose microfluidic system. VDB: valve driver board, PC: pump controller, HVPS: custom reversible high voltage power supply, VI: valve input terminal block, SA: two channel signal amplifier, CF: cooling fan, P: pump, CMS: chip mounting stage, FG: two channel digital function generator, TC: temperature controller, C4D: two channel $C^4D$ unit, DAQ: data acquisition board, AI: analogue input/ 5V DC power supply terminal block, CPS: computer power supply, UH: USB hub, R: 12V two position relay, TIO: Terminal input/output block.

Two separate reversible high voltage power supplies (HVPS) were manufactured in house by coupling two opposite polarity 8000 V regulated supplies (C80P/C80N EMCO, Sutter Creek, CA, USA) and fitting enabling and output relays to allow computer control and provide component protection. A photograph of a HVPS is given in Figure 5.3.

Four MilliGAT pumps (P) (MG-5, GlobalFIA, Fox Island, WA, USA) were positioned in close proximity to the chip mounting stage with MForce pump controllers (PC) mounted in a separate compartment in the unit. All pumps were fitted with in-line pressure relief valves.

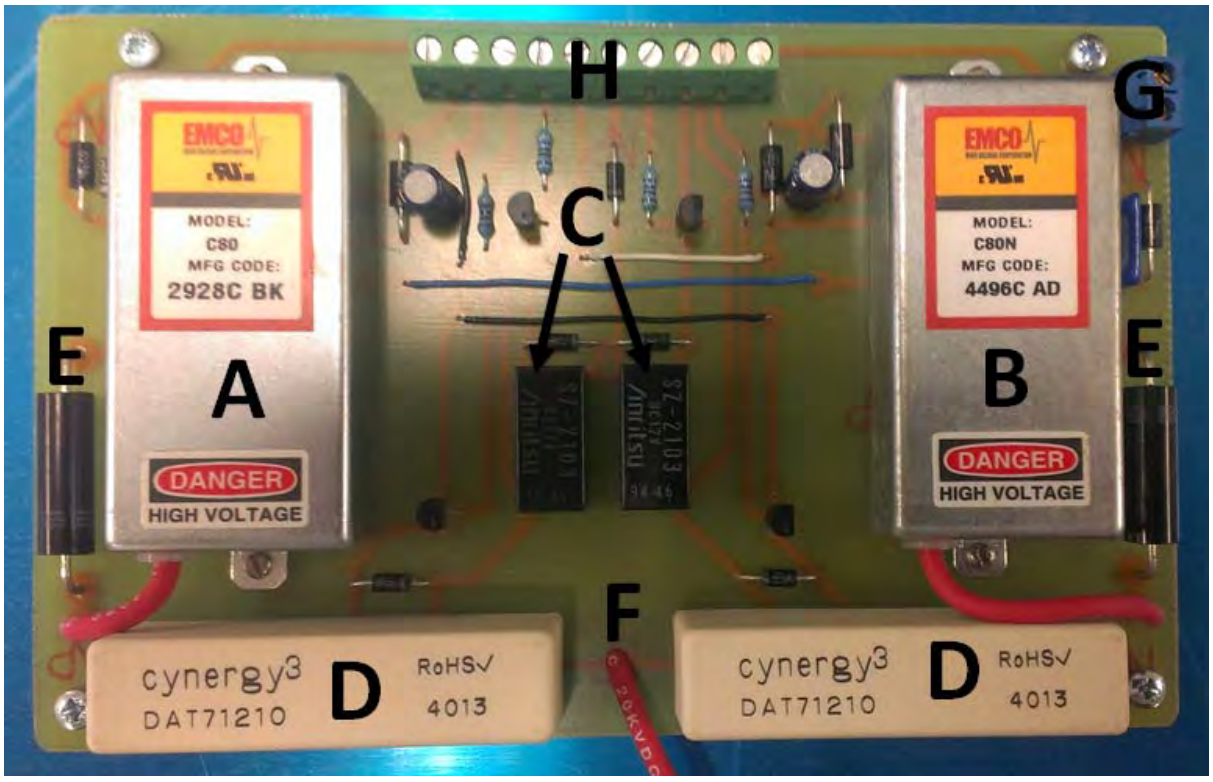


**Figure 5.3:** Custom reversible +/- 8000V HVPS. A: + 8000V HVPS, B: - 8000V HVPS, C: 12V DC enabling relays, D: High Voltage output relays, E: Voltage protection diodes, F: HV output, G: Common HVPS ground and H: Input / output terminal block.

A valve driver board (VDB) (648D5X12, NResearch, West Caldwell, NJ, USA) was extended to a terminal block (VI) to allow for the connection of up to 5 isolation and/or 3 way valves (HP225K021/HP225K031, NResearch, West Caldwell, NJ, USA).

For capacitively coupled contactless conductivity detection ($C^4D$), a two channel digital function generator (FG) (UDB1305S, Shanghai, dealextreme, AUS) was amplified though an in-house manufactured two channel buffering power supply. Manual control of the function generator and signal amplifier is achieved via controls mounted on the front panel of the unit. A two channel custom-built $C^4D$ unit was mounted to the front panel of the unit with manual control for signal gain and offset enabled. The analog voltage output signal from the $C^4D$ unit was passed through a NI USB-6212 data acquisition device (DAQ) (National Instruments, Austin, TX, USA) and a low-pass filter programmatically applied.

The DAQ device enabled control of all pumps, valves, HVPS, and triggers and enabled signal acquisition from the two $C^4D$ units, two additional analogue inputs and current return for the two HVPS via a custom LabVIEW program (LabVIEW 2011, National Instruments, Austin, TX, USA).

A 5 port USB hub (Gadget Geek, Brisbane, QLD, Australia) was mounted to the front-panel of the unit and was used to allow PC communication to the USB DAQ and control of the pumps. The DAQ was connected to two separate terminal blocks; AI to allow for 2 analogue voltage signal inputs in order to accommodate alternate and/or additional detection inputs and TIO to allow for two 5 V triggered outputs and one 5 V triggering inputs to allow for coupling to other devices. Additionally, a constant 5 V power source was taken directly to terminal block AI to allow for powering of ancillary devices such as Arduino boards, and a 12 V two position relayed (R) output to a terminal block (TIO) to allow for direct programmatic control of 12 V devices.

A Chip Mounting Stage (CMS) consisting of a Peltier (12 W direct to air heat pump, Laird Technologies, RS components, Melbourne, Australia) mounted to a stainless steel plate (110 mm x 90 mm x 1 mm) was located centrally. A 90 mm x 70 mm x 5 mm piece of thermally conductive polymer (T-FLEX$^{TM}$ 3100, Laird Technologies, RS components, Melbourne, Australia) was placed on the CMS. The Peltier was configured for both heating and cooling and was manually controlled by a temperature controller (TC) (ir33, Carel, RS components, Melbourne, Australia) mounted to the front panel of the unit. Movable aluminium straps and wing nut assemblies for retaining microfluidic devices were fitted to the stainless steel plate of the CMS.

All system components were powered from a Computer Power Supply (CPS) (Earthwatts 430, Antec, Fremont, CA, USA) enabling consolidation of all +/- 12 V and 5 V requirements of the various hardware components. The system has one 240 V AC power supply and one USB input to connect to a PC.

### 5.2.4 Reagents

All reagents and preparation procedures utilised in these studies are detailed in Chapters 2 through 4.

### 5.2.5 Electrophoretic procedures

Electrophoretic procedures used for these studies are described in Chapter 4.

## 5.3 Design considerations

### 5.3.1 General hardware considerations

The system was designed to be a flexible, portable multi-purpose platform with the potential to perform a range of microfluidic functions relevant to chemical analysis such as electrophoresis and mixing. In the design of the instrument, flexibility means that interoperability with other external devices including detectors should be fast and straightforward, while portability stipulates a relatively small form factor and weight.

To realise this, weight and size were a significant consideration in the selection and/or modification of all components. Most reports of commercial and experimental CE and MCE systems only list the weight and dimensions of the system, excluding the external computer control and data recording/processing. Whilst it is possible to increase compactness and portability by embedding the control and data acquisition into the system, this comes at a cost to system flexibility and possibly performance. Regardless of the decision to embed the control system into the platform, having a flexible software interface is essential for flexibility in operation and functionality.

The approach described in this thesis is unique in its ability to sample from a stream rather than from a discrete sample vial. As discussed in Chapter 2, this ability allows the application of the system for long-term monitoring of changes in the chemical fingerprint of a sample without the need for manual intervention to load sample and/or reagents. The autonomous character of the system, however, also puts a different perspective on the design requirements for the system. First, whilst disposable microchips are widely regarded as being ideal for diagnostics,[9-12] this approach is not suitable for continuous monitoring applications. Instead, the devices must be rugged and designed for long-term use. Second,

the flow injection interface imposes high-pressure conditions, challenging the fluidic interconnects.[13] Third, ruggedness of the system is critical to its functioning outside a laboratory, allowing sacrifices to be made to increase ruggedness to the expense of increasing the size from truly portable or hand-held to field-deployable.

### 5.3.2 High voltage power supplies

Both CE and MCE require the use of a HVPS for the application of the high electric field required for the separation. Whilst electrophoretic separations can be carried out in constant voltage (CV) or constant current modes, CV is by far the most commonly utilised in CZE.[14]

As separation speed and resolution are ultimately determined by the electric field strength, theoretically one could say the higher the field strength, the better. A number of practical reasons such as minimisation of Joule heating, detector isolation and shielding (especially for $C^4D$) and safety, however, limit the maximum field strength that is useful in CE, hence most CE apparatus are equipped with HVPSs in the 25 – 30 kV range.[14] All capillary-based CE systems built as part of this research utilised regulated HVPS with maximum outputs of 30 kV (serials 1-3 of Table 5.1) or 33 kV (serial 4). The choice of HVPS was primarily dictated by the required form factor, with smaller supplies preferred due to the requirement to be fitted inside temperature controlled enclosures (serials 2 and 4 of Table 5.1).

When scaling down to microchips, the reduction in the separation length allows for an equivalent reduction in demands for the high voltage power supply (HVPS) when aiming at equivalent field strengths during separation. One should realise that in practice, however,

the reduction in size, weight and power by as result of the use of smaller HVPS[6] in ME, is often offset by the requirement for multiple HVPS (typically four) to realise gated or pinched electrokinetic injection. Additionally, the operation of multiple HVPS significantly increases the demands on the control soft- and hardware as the independent supplies have to be controlled in the kV range with millisecond switching times, necessitating the use of high-voltage relays.[15] The studies conducted in Chapter 3 on the traditional cross-injection design chips required the use of a pinched injection mechanism and hence an extant custom built four channel HVPS capable of timed positive, negative, ground or float conditions was used. The implementation of hydrodynamic injection on microchips allows for the elimination of the 2 HVPS used for the pinching/pullback voltages. Two channels from this HVPS were used for the separations with hydrodynamic injection conducted in Chapter 4 (serial 4 of Table 5.1).

For the multi-purpose microfluidic platform, two small (14 cm x 8 cm x 2.5 cm) reversible power supplies were assembled, with the detail about their control described in Section 5.2.3. Both custom HVPS were tested using a multimeter fitted with a high voltage probe and found to be > 1% accurate through programmatic control over the working ranges +/- 0 V - +/-8000 V. The use of hydrodynamic injection does increase the demands on hardware and/or hardware control (discussed in several reviews [16, 17] and Section 4.1) including pumps and valves.

### 5.3.3 Pumps

Pumps are essential for sequential injection systems, with the main considerations including maximum operating pressure, linear flow rate range, size and mass, chemical

resistance/compatibility and power consumption. The maximum operating pressure of all developed systems was set at 100 psi with all pumps and hardware components selected to meet this requirement. As indicated in Table 5.1, syringe, peristaltic and MilliGAT pumps were used for the different systems built as part of this project, and all were found to provide sufficiently smooth flows over required operating flow rates (Chapters 2 and 4).[8]

The SI-DCE system described in Chapter 2 employed a dual syringe pump system, the capacity of which was insufficient for extended autonomous application. To enable this experiment, two lines of a quaternary pump were used to mix sample and internal standard, while a MilliGAT pump was used to provide BGE to the system (serial 1 of Table 5.1).

For the SI-CE system developed for use by *Alhusban et al* [8] for monitoring of cell culture and fermentation media, peristaltic pumps were used to avoid the sample solution coming into contact with the pump internals (serial 2 of table 5.1). Cell culture broths contain lipids, proteins and cell debris that could adhere to the pump causing contamination and blockages. When using a peristalitic pump, blockages can be simply removed by replacing the flexible tubing.

For all other systems MilliGAT pumps were used. The multi-purpose microfluidic platform included 4 pumps, with the control hardware currently supporting the addition of a fifth pump and allowing for the expansion up to a total of 25 MilliGAT pumps. The ability to run so many pumps from one platform (controlled through one program) enables multiplexing as well as conducting a number of functions such as sampling, mixing, extraction, pre-concentration, separation and coupling/hyphenation to other flow systems.

### 5.3.4 Valves and fluidic connections

To direct the flows in the systems, a combination of hydrodynamic resistance and valves was used (Chapter 4). The choice of the valves was dictated by the functional requirements of the system and the maximum operating pressure. For the capillary-based CE systems (serials 1 – 3 of Table 5.1), a two position switching valves commonly used for injection in HPLC enabled delivery of BGE or sample to the separation systems while small isolation valves positioned behind the flow-through interface were employed for system cleaning and/or hydrodynamic injection. For several systems, three way valves were used to provide a small, low cost alternative (serials 4 and 6 of Table 5.1) for alternate flow delivery.

For the microchip system developed in Chapter 4, the two position switching valves were no longer required as flow sheathing was used to introduce, gate and alternate BGE and sample flow (serial 5 of Table 5.1). Small isolation valve were still used at the outlet to enable the system to operate in either flow or pressure-controlled mode, as explained in further detail in Chapter 4.

To connect the capillaries and the fluidic control system, unmodified custom off the shelf (COTS) HPLC fittings were used for all CE systems, with the exception of the modified injection interfaces which are described in Chapter 2 and other publications.[8, 18] The SI-MCE system described in Chapter 4 utilised a combination of COTS, modified COTS and custom developed fittings to meet the demands of the device. For example, female flat bottom fittings were produced in house from 6 mm thick PMMA sheets with a 5.5 mm drill bit and tapped with a 1/4-28 thread and attached to the chip reservoirs using a small amount of 1,2-dichloroethane (DCE) to interface with capillary tubing using Upchurch® fittings. These connections were also used to connect flow-through electrodes to the waste and ends of

the separation channels. The flow-through electrodes were made from ≈ 100 mm lengths of 1 mm i.d. stainless steel tubing, heat moulded to ferrules (P-248, Upchurch Scientific, Oak Harbour, WA, USA) to connect with COTS 1/4-28 nuts. Corresponding female-to-female fittings were used to connect the electrodes with tubing fitted with 1/4-28 nuts. The valves were interfaced with similar 1/4-28 fittings.

### 5.3.5 Detectors

In the development of a portable analytical system, the selection of the detection method requires careful consideration. Optical detection methods, predominantly fluorescence, are the most frequently used in microfluidic devices.[19, 20] With this work initially targeting inorganic ions, $C^4D$ was selected as the detection method for the reasons outlined in Chapter 1.[21]

$C^4D$ detectors were sourced from TraceDec®, with the exception of the multi-purpose microfluidic system, where a small, customised 2 channel $C^4D$ detector was developed. Whilst $C^4D$ was selected as the detection method for study in this Chapter, the design of the system allows for the incorporation of alternative detection systems via two +/- 10 V AI lines. The performance of the custom $C^4D$ detector was examined with the results discussed in Section 5.4.1.

### 5.3.6 Separation device

For serials 1-4 (Table 5.1), fused silica capillary (either coated or uncoated) with an i.d. of 50 or 25 µm was used for the electrophoretic separations. The inherent flexibility in design of MCE devices provides many options in terms of geometry and size of the channels and

device, material as well as the level of integration. As discussed, the aim here was to develop a flexible microfluidic platform, hence only a low level of on-chip integration of functionalities was desired. Based on access to facilities, hot embossing in PMMA was selected as the microfabrication method for the production of hard plastic devices. The size of the PMMA devices complied with the research group standard of 50 x 75 mm, allowing sharing of resources across projects. The chip was designed to have a wide, central feeder channel in combination with two narrow separation channels to maximise the difference in hydrodynamic flow resistance and therefore limit hydrodynamic bleed into the separation channels (discussed in detail in Chapter 4). The hot embossing and bonding processes were optimised and using the process discussed in Chapter 4, with a 80 % success rate for embossing and bonding of device with 50 µm wide separation channels and a 500 µm wide feeder channel.

Whilst in CE the separation efficiency is determined by the field strength, time, and therefore length are required to achieve this separation, provided the injected sample zone does not exceed 1-2% of the separation channel length. The size of the detector cell is also an important determinant of the resolution that should be achieved, as for example a detector with a 0.5 mm cell length cannot distinguish two peaks that are separated by 0.1 mm. Serpentine channel geometries allow for the introduction of significant channel lengths on a small footprint, but it is well known that curves compromise the separation efficiency as a result of the so-called race track effect.[22, 23] The proposed chip design integrates two 106 mm long separation channels on a 75 (L) x 50 (W) mm substrate using a single, wide curvature to minimise band broadening while allowing for sufficient separation space.

The extent of integration of detectors is an interesting discussion as higher levels of integration avoid alignment issues and enhance sensitivity, but also complicate the microfabrication process. Here, we developed a simple approach to electrode integration allowing for the combination of economical microfabrication with high precision positioning of the electrodes (Chapter 3).

### 5.3.7 Temperature control

The electrophoretic mobility of an ion varies with temperature through its dependence on the dynamic viscosity, making the ability to control temperature critical for reliable migration times in electrophoretic separations.[24] In Chapter 2, temperature was identified as a significant contributor to variance in migration time and this was addressed by placing the electrophoretic apparatus into a temperature controlled enclosure in subsequently built CE systems.[8] For the multi-purpose microfluidic system, temperature control was an important consideration as the system may be expected to operate in the field for environmental monitoring applications. A Peltier was directly incorporated in the chip mounting stage for compact and efficient temperature control of the microfluidic system.

### 5.3.8 Data acquisition and control hardware

The hardware requirements of the system proper dictate the minimum requirements of the data acquisition and programming hardware, in particular, the number and nature of analogue I/O (A I/O) channels, the number of digital I/O (D I/O) channels and the requisite resolution of the captured data signal. For most systems built during the course of this thesis (serials 1, 2, 4 and 6 of Table 5.1) the NI USB-6212 DAQ proved a suitable solution

principally due to the capability of providing 2 x 0 – 10 V AO, critical to achieving full-scale programmatic control of the HVPS used. A NI USB-6008 DAQ (2 x 0 – 5 V AO max.) was used to provide a suitable lower cost solution (≈ 10 % of the price of the NI USB-6212) when coupled with a custom dual channel 2 x Op Amplifier for the system described in serial 3 of Table 5.1.

To enable programmatic control of the four channel HVPS required for the pinched injection experiments carried out in Chapter 3, a DAQ board capable of time independent control of 8 x 0 – 10 V AO was required (each HV channel consisted of two relayed +/- HVPS) and a MCC 3105-USB board was used for this task. The AI functions (differential return voltage and current monitoring of each HVPS) and D I/O functions for HVPS relaying, solenoid valve operation and safety functions were carried out using the MCC 2533-USB board (serial 5 of Table 5.1).

### 5.3.9 Programming

Often neglected from scientific literature as it pertains to custom built systems, are details related to programming. Few, if any other details beyond the listing of the requisite interfacing hardware and programming language are given.

The general programming sequence for systems 1 through 4 of Table 5.1 were identical except for the provision of a hydrodynamic and electrokinetic injection mechanism for systems 2 through 4 inclusive. For systems 5 and 6 an open timed sequence was used allowing for individual flow rates, valve positions and HVPS states to be set for any period of time in the operating sequence loop.

A screen shot of the graphical user interface (GUI) of the multi-purpose microfluidic platform is given at Figure 5.3. The program has 14 discrete timed steps with individual control over the 4 x pump flow rates, 5 x valve positions, 12 V power enable, 2 x 5 V triggers, 2 x HVPS enable, polarity and a common power supply output voltage. This degree of programming control makes for a very flexible control interface capable of performing multiplexed functions. A summary of the microfluidic system capabilities is given in Table 5.2.


**Figure 5.3**: Portion of the LabVIEW GUI for the multipurpose microfluidic platform program.

**Table 5.2**: Overview of capabilities of the multi-purpose microfluidic system

| HVPS | Pumps | Valves | Fittings | Detector support | External interfacing support | Temperature Control | Size and Weight |
|---|---|---|---|---|---|---|---|
| 2 x Reversible +/- 8000V power supplies | 4 x MilliGAT pumps (plug and play for 5 and expandable to 25). 100 PSI maximum operating pressure, Linear flow rates from 0.6 - 20 µL $s^{-1}$ | Capability to directly control 5 x isolation/3 way valves. 100 PSI maximum operating pressure. | Fluidic lines from pumps are standard COTS | Custom 2 channel $C^4D$ detector. Each channel with a maximum of 80 $V_{pp}$ and 0.01 Hz to 5 MHz range. Manual offset and gain control of each channel and integrated data readback and capture through custom software. Two additional +/- 10 V analogue input lines with readback and capture are also supported for alternate detectors. Return current readback for HVPS'. 16 bit resolution for all readback channels. | 2 x 5V output triggers and 1 x 5V input trigger (Software controlled). 2 position relay for 12 V power output (Software controlled). 1 x 5V power output. | A custom Chip Mounting Stage (CMS) consisting of a Peltier capable of heating and cooling functions over the temperature range 0 -60 °C (optimised for operation between 20 - 30 °C) | 40 cm (L) x 22 cm (W) x 22 cm (H). Total weight ≈ 9 kg. |

### 5.3.10 Frame

The multi-purpose microfluidic system frame was constructed from 1'' hollow square aluminium connected with low cost commercial polymer fittings and the system was clad in 1-2 mm thick aluminium sheet. The system was divided internally into three compartments to allow for vertical mounting of components and to make efficient use of available space (Figure 5.1). Hardware placement was primarily dictated by the requirement to have the four heaviest components (pumps) as central and close to the chip mounting stage as possible to centralise mass for stability and to minimise the length of feeder lines to the microfluidic device to reduce sample and reagent consumption.

Active and passive heat control strategies were applied through the placement of high heat generating components (pumps, pump controllers and signal amplifier) to ensure isolation, sinking and active cooling via the inclusion of an exhaust fan in the central internal compartment. Finally, spacing of high voltage and sensitive electronic components was applied in order to minimise the likelihood of arcing and/or electrical interference. Front and rear profile views of the system are given in Figure 5.4. A photograph of the front panel showing manual controls is at Figure 5.5. System dimensions are ≈ 40 cm (L) x 22 cm (W) x 22 cm (H, excluding lid). Total weight is ≈ 9 kg.

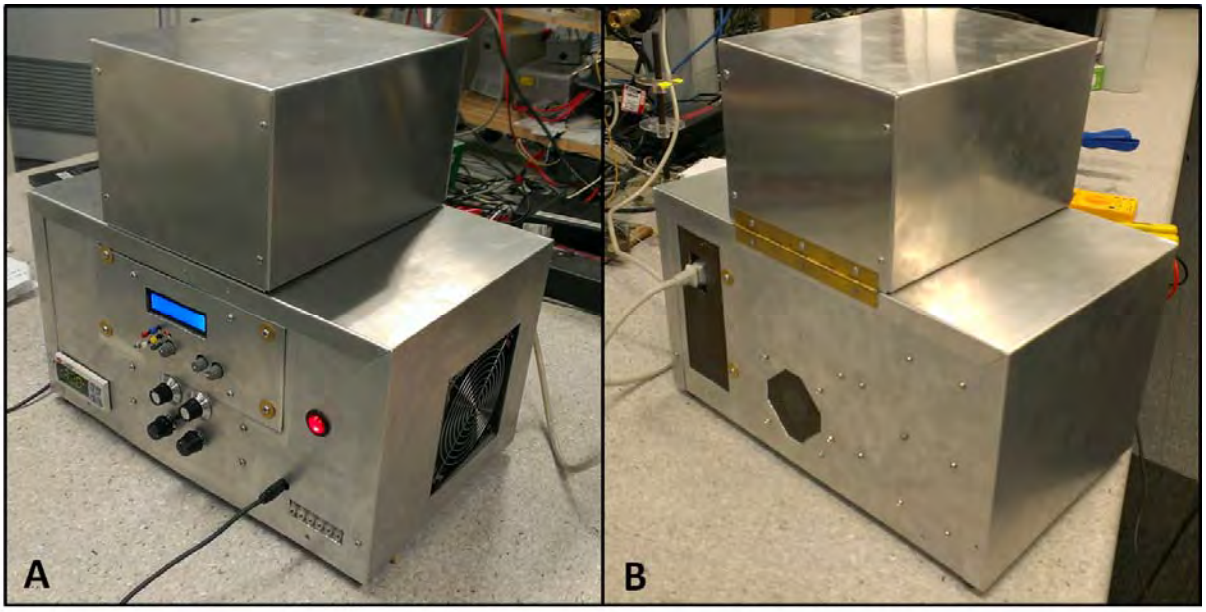


**Figure 5.4:** Multi-purpose microfluidic platform; A: Front view showing manual control panel and USB input. B: Rear view showing power input.

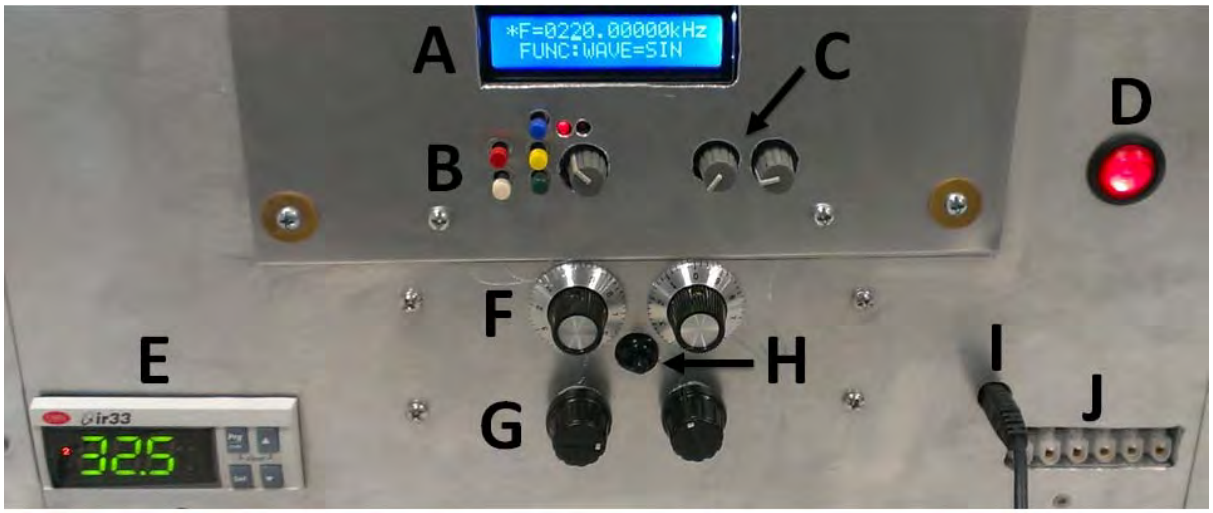


**Figure 5.5:** Front panel controls; A: Function generator display, B: Function generator control cluster, C: Two channel signal amplifier, D: System on/off switch, E: Temperature controller, F: Two channel $C^4D$ gain controls, G: Two channel $C^4D$ offset controls, H: $C^4D$ Detector on/off switch, I: USB input and J: TIO terminal block (Two relayed 12V power outputs, common ground, two triggered 5V outputs and one 5V input trigger).

## 5.4 Results and discussion

### 5.4.1 $C^4D$ performance studies

During the early stages of studies examining the performance of the custom $C^4D$ detectors it was noted that significant interference to the return signal was caused by the temperature control system. This interference manifested itself as sudden significant rises or falls in the baseline signal as the temperature controller relays switched between heating/cooling phases and also as considerable baseline oscillation over an approximately 45 second peak to peak period as a result of change in conductivity of the background electrolyte responding to slight changes in the temperature (+/- 0.1 °C ) as the temperature controller oscillated around the set temperature. To alleviate both of these problems a piece of thermally conductive polymer was added to isolate the microchip from the ground interference of the Peltier (eliminating the relay interference spikes) and to provide increased thermal mass to reduce the magnitude and frequency of baseline oscillation to an imperceptible level.

Previous studies in Chapters 3 and 4 with microchips containing embedded in-plane electrodes utilised TraceDec ® detectors, which could not be optimised with regards to the excitation frequency. In order to study the effect of excitation frequency on the embedded in-plane electrode geometry, electrophoretic chips of the same design as studied in Chapter 4 were assessed using the same electrophoretic procedures but conducted entirely upon the newly constructed microfluidic platform using the integral dual channel $C^4D$.

Gain for both detector channels was set to one, signal voltage was 40 $V_{pp}$ and the same separation channel on the same microchip was used for all studies. Results were averaged from 3 electrophoretic runs at each frequency setting and peak height to noise

ratios for $K^+$, $Li^+$ and $Na^+$ were determined over the excitation frequency range 100 – 650 kHz with the results given in Figure 5.5.

At lower excitation frequencies, signal response is reduced primarily due to the relatively high impedance of the insulating layer separating the electrode from the separation channel resulting in reduced current flowing to the detector. Conversely, at higher excitation frequencies, stray capacitance reduces the S/N ratio. However, at higher frequencies the main limitation to increased signal response is due to a reduction of gain from the operational amplifier as a result of input capacitance. These results showed that the optimum signal frequency for the embedded in-plane electrode geometry using the custom detectors was between ≈ 180 – 220 kHz.

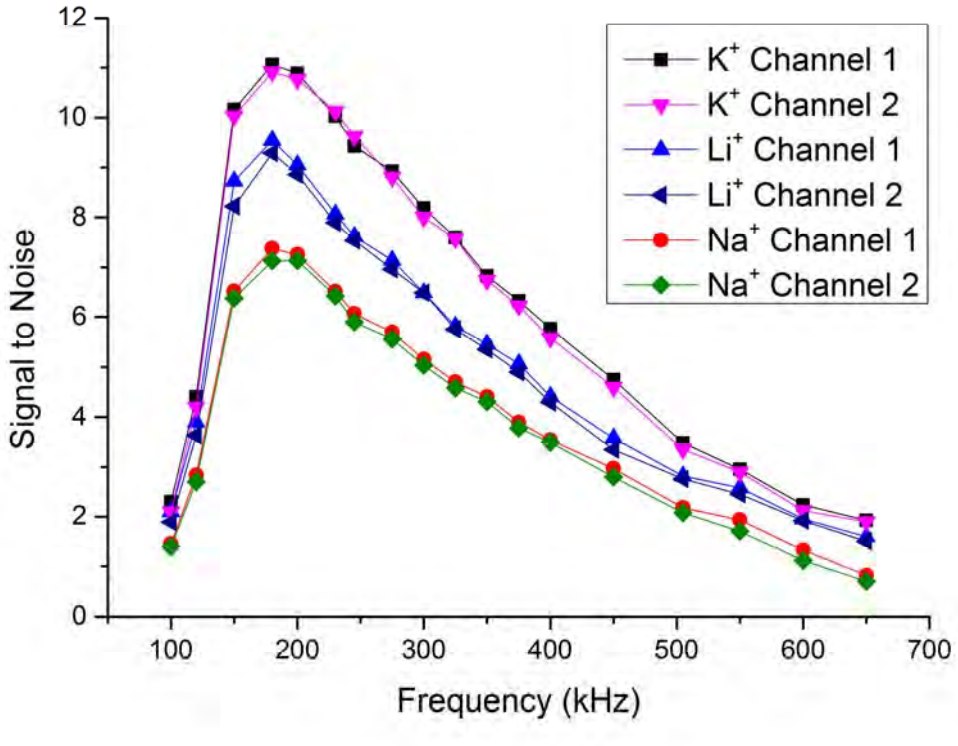


**Figure 5.5:** Effect of actuation frequency upon signal to noise ratio of electrophoretically separated $K^+$, $Li^+$ and $Na^+$ ions. $V_{pp}$ = 40 V for all experiments. S/N results are averaged from 3 runs.

Increasing the excitation voltage can also lead to improved signal to noise ratios [25, 26] and better detector performance when carefully matched to the detector electronics. Detailed studies of optimum excitation voltages were not conducted however, as in practice close optimisation of the excitation voltage could be quickly achieved via manual adjustment of the excitation voltage over the course of several automated runs and the main focus of these detector studies was to compare the detector performance to the previously used commercial TraceDec ® detector and not to necessarily optimise conditions for the chip detector cell geometry. A value of $V_{pp}$ = 40 V was chosen based upon manual optimisation of the S/N of electrophoretic separations conducted at 200 kHz and these detector conditions were kept for all subsequent experiments, adjusted only by offset and minor gain adjustments.

The same experimental conditions as described in Section 4.3.6 were used and LODs of $K^+$, $Na^+$, $Li^+$, $Cl^-$, $F^-$ and $H_2PO_4^-$ were averaged for 5 electrophoretic runs using the microfluidic system. It was found that the custom $C^4D$ unit had an average 21.1% reduction in sensitivity as compared to the results obtained with the commercial TraceDec ® detector and the experimental apparatus described in Chapter 4. These results are summarised in Table 5.3.

**Table 5.3:** LOD comparison of $K^+$, $Na^+$, $Li^+$, $Cl^-$, $F^-$ and $H_2PO_4^-$ using commercial TraceDec ® and custom $C^4D$ detection units.

| | **TraceDec ® system LOD (S/N = 3) mg $L^{-1}$ / µM (n=20)** | **Custom $C^4D$ unit LOD (S/N = 3) mg $L^{-1}$ / µM (n=5)** | **% difference** |
|---|---|---|---|
| **$K^+$** | 0.200 / 5.12 | 0.241 / 6.17 | 20.5 |
| **$Na^+$** | 0.198 / 8.61 | 0.234 / 10.19 | 18.3 |
| **$Li^+$** | 0.110 / 15.9 | 0.131 / 19.4 | 19.2 |
| **$Cl^-$** | 0.317 / 8.95 | 0.392 / 11.08 | 23.8 |
| **$F^-$** | 0.364 / 19.2 | 0.455 / 23.98 | 24.9 |
| **$H_2PO_4^-$** | 2.29 / 24.1 | 2.75 / 28.9 | 20.1 |
| | | **Average % difference** | 21.1 |

Whilst these results were conducted on different hardware systems and used different microfluidic chips, they provide a practical estimation of the custom detector sensitivity and indicate that the overall system performance agrees well with the results obtained in Chapter 4.

### 5.4.2 Electrokinetic injection

Whilst hydrodynamic injection in the CE and ME format is useful for eliminating sample matrix bias, electrokinetic injection can still be a very useful tool and is essential where stacking or electrokinetic extraction methods are required. By altering the programming parameters, it was found that simple electrokinetic injection was possible using the same experimental conditions and dual channel polymer chips used in Section 5.3.3. For the hydrodynamic injection, the same injection conditions given in Section 4.3.6 were used, however 5 ppm solutions of $NH_4^+$, $Na^+$, and $Li^+$ (as chloride salts) were used with only the

cations studied due to time constraints. Representative electropherograms of both the hydrodynamic and electrokinetic injections run sequentially are given in Figure 5.6.

For the electrokinetic injections, the same injection procedure as for the hydrodynamic injection was used but instead of rapidly shutting and reopening the injection valve, +/- 1.5 kV was applied on either separation channel for 2 seconds (in the same manner as the DC-SICE mechanism in Chapter 2) with all flow rates and other steps remaining the same.

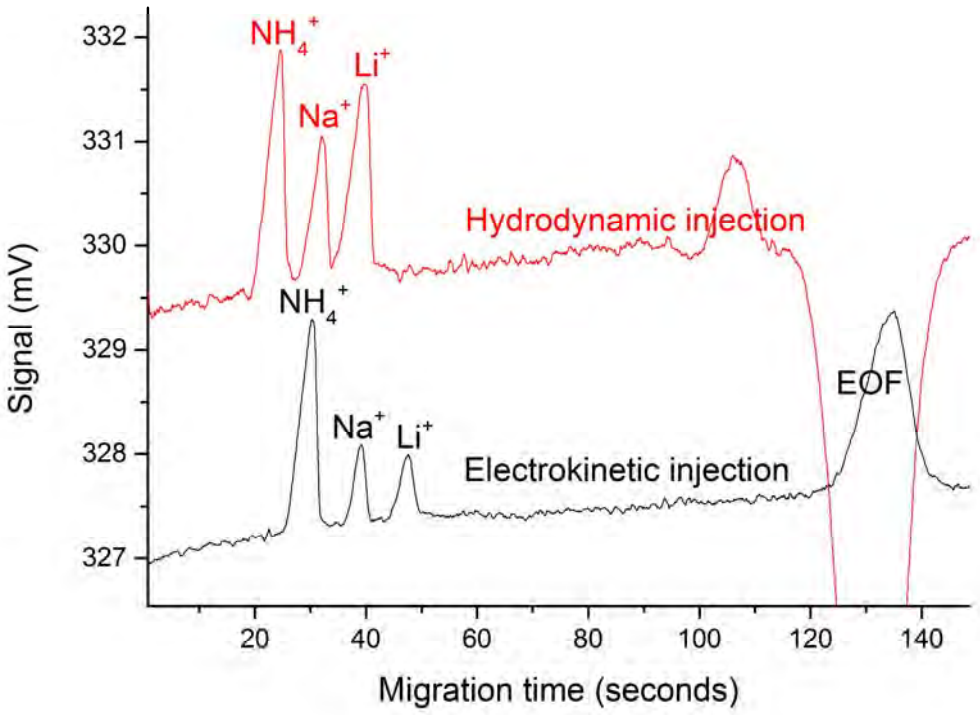


**Figure 5.6:** Hydrodynamic and electrokinetic separations of 5 ppm $NH_4^+$, $Na^+$ and $Li^+$ using the multipurpose microfluidic platform.

No optimisation or quantitative studies were performed on the electrokinetic injection mechanism but these results demonstrate electrokinetic injection can be effected by the multi-purpose microfluidic platform.

## 5.5 Concluding remarks

In this chapter, the design and construction of a multi-purpose microfluidic platform has been discussed alongside the design and construction of a number of other CE and ME systems developed by the author during the conduct of these thesis studies. Previous system designs have guided the construction of the multi-purpose microfluidic platform, which has also been designed with a future outlook to accommodate potential future applications including hyphenation to other flow systems, extended autonomous operations, sample extraction and pre-concentration functions and the ability to run multiplexed separations.

Custom built low-cost reversible HVPS and $C^4D$ detectors were evaluated along with the potential for electrokinetic injection in order to enable stacking and electrokinetic extraction functions. The system featured temperature control and programming capable of enabling simultaneous and/or multiplexed functions. Where achievable, priority was given to low-cost and small form factor components with a total system weight of only 9 kg.

## 5.6 References

1. Johnson, A. S.; Selimovic, A.; Martin, R. S., Integration of microchip electrophoresis with electrochemical detection using an epoxy-based molding method to embed multiple electrode materials. *Electrophoresis* **2011,** *32*, 3121-3128.

2. Culbertson, C. T.; Mickleburgh, T. G.; Stewart-James, S. A.; Sellens, K. A.; Pressnall, M., Micro total analysis systems: Fundamental advances and biological applications. *Analytical Chemistry* **2014,** *86*, 95-118.

3. Wu, A.; Wang, L.; Jensen, E.; Mathies, R.; Boser, B., Modular integration of electronics and microfluidic systems using flexible printed circuit boards. *Lab on a Chip - Miniaturisation for Chemistry and Biology* **2010,** *10*, 519-521.

4. Campos, C. D. M.; Da Silva, J. A. F., Applications of autonomous microfluidic systems in environmental monitoring. *RSC Advances* **2013,** *3*, 18216-18227.

5. Kubáň, P.; Nguyen, H. T. A.; Macka, M.; Haddad, P. R.; Hauser, P. C., New fully portable instrument for the versatile determination of cations and anions by capillary electrophoresis with contactless conductivity detection. *Electroanalysis* **2007,** *19*, 2059-2065.

6. Breadmore, M. C., Capillary and microchip electrophoresis: Challenging the common conceptions. *Journal of Chromatography A* **2012,** *1221*, 42-55.

7. Ryvolová, M.; Macka, M.; Brabazon, D.; Preisler, J., Portable capillary-based (non-chip) capillary electrophoresis. *TrAC - Trends in Analytical Chemistry* **2010,** *29*, 339-353.

8. Alhusban, A. A.; Gaudry, A. J.; Breadmore, M. C.; Gueven, N.; Guijt, R. M., On-line sequential injection-capillary electrophoresis for near-real-time monitoring of extracellular lactate in cell culture flasks. *Journal of Chromatography A* **2014,** *1323*, 157-162.

9. LaCroix-Fralish, A.; Clare, J.; Skinner, C. D.; Salin, E. D., A centrifugal microanalysis system for the determination of nitrite and hexavalent chromium. *Talanta* **2009,** *80*, 670-675.

10. Xi, Y.; Templeton, E. J.; Salin, E. D., Rapid simultaneous determination of nitrate and nitrite on a centrifugal microfluidic device. *Talanta* **2010,** *82*, 1612-1615.

11. Zou, Z.; Jang, A.; MacKnight, E.; Wu, P. M.; Do, J.; Bishop, P. L.; Ahn, C. H., Environmentally friendly disposable sensors with microfabricated on-chip planar bismuth electrode for in situ heavy metal ions measurement. *Sensors and Actuators, B: Chemical* **2008,** *134*, 18-24.

12. Kalish, H.; Phillips, T. M., Assessment of chemokine profiles in human skin biopsies by an immunoaffinity capillary electrophoresis chip. *Methods* **2012,** *56*, 198-203.

13. Sen, A. K.; Darabi, J.; Knapp, D. R., A fluidic interconnection system for polymer-based microfluidic devices. *Microsystem Technologies* **2010,** *16*, 617-623.

14. Blanes, L.; Coltro, W. K. T.; Saito, R. M.; Van Gramberg, A.; Lucio do Lago, C.; Doble, P., High-voltage power supplies to capillary and microchip electrophoresis. *Electrophoresis* **2012,** *33*, 893-898.

15. Revermann, T.; Götz, S.; Künnemeyer, J.; Karst, U., Quantitative analysis by microchip capillary electrophoresis - Current limitations and problem-solving strategies. *Analyst* **2008,** *133*, 167-174.

16. Saito, R. M.; Coltro, W. K. T.; De Jesus, D. P., Instrumentation design for hydrodynamic sample injection in microchip electrophoresis: A review. *Electrophoresis* **2012,** *33*, 2614-2623.

17. Karlinsey, J. M., Sample introduction techniques for microchip electrophoresis: A review. *Analytica Chimica Acta* **2012,** *725*, 1-13.

18. Blanco, G. A.; Nai, Y. H.; Hilder, E. F.; Shellie, R. A.; Dicinoski, G. W.; Haddad, P. R.; Breadmore, M. C., Identification of inorganic improvised explosive devices using sequential injection capillary electrophoresis and contactless conductivity detection. *Analytical Chemistry* **2011,** *83*, 9068-9075.

19. Myers, F. B.; Lee, L. P., Innovations in optical microfluidic technologies for point-of-care diagnostics. *Lab on a Chip - Miniaturisation for Chemistry and Biology* **2008,** *8*, 2015-2031.

20. Mogensen, K. B.; Kutter, J. P., Optical detection in microfluidic systems. *Electrophoresis* **2009,** *30*, S92-S100.

21. Gencoglu, A.; Minerick, A. R., Electrochemical detection techniques in micro- and nanofluidic devices. *Microfluidics and Nanofluidics* **2014**.

22. Jacobson, S. C.; Hergenröder, R.; Koutny, L. B.; Warmack, R. J.; Michael Ramsey, J., Effects of Injection Schemes and Column Geometry on the Performance of Microchip Electrophoresis Devices Stephen C. Jacobson, 1 Roland Hergenröder, 1 Lance B. Koutny, 1 R. *Analytical Chemistry* **1994,** *66*, 1107-1113.

23. Molho, J. I.; Herr, A. E.; Mosier, B. P.; Santiago, J. G.; Kenny, T. W.; Brennen, R. A.; Gordon, G. B.; Mohammadi, B., Optimization of turn geometries for microchip electrophoresis. *Analytical Chemistry* **2001,** *73*, 1350-1360.

24. Evenhuis, C. J.; Haddad, P. R., Joule heating effects and the experimental determination of temperature during CE. *Electrophoresis* **2009,** *30*, 897-909.

25. Lichtenberg, J.; de Rooij, N. F.; Verpoorte, E., A microchip electrophoresis system with integrated in-plane electrodes for contactless conductivity detection. *Electrophoresis* **2002,** *23*, 3769-3780.

26. Kubáň, P.; Hauser, P. C., Effects of the cell geometry and operating parameters on the performance of an external contactless conductivity detector for microchip electrophoresis. *Lab on a Chip - Miniaturisation for Chemistry and Biology* **2005,** *5*, 407-415.

# Chapter 6: Conclusion and future directions

A novel DCSI-CE system was developed and successfully demonstrated for the rapid simultaneous separation of small anions and cations from a single sample using $C^4D$ detection. The system leveraged the instrumental flexibility and simplicity of the CE technique to allow for simultaneous determinations of both positively and negatively charged species by means of a simple cross injection interface and a reconfiguration of the standard grounding and application voltage arrangement. By multiplexing the anion and cation separations, the total analysis time was reduced, whilst retaining high resolution and low LODs. The two capillary approach presented the possibility for further system flexibility by allowing for separate EOF conditions for anionic and cationic separations and was examined. Three BGEs were examined in order to optimise the separations of a target set of common small environmental ions. Finally, the system was simply modified to allow for extended autonomous operations including inter-run cleaning and the autonomous addition of anionic and cationic standards with controllable dilution and a 2 day study of tap water was conducted. The system was proven suitable for a range of applications and was capable of simultaneously separating at least 11 anions and 12 cations within a total analysis time of 3.5 min with LODs for the target analyte set in the range 0.005- 0.061 mg $L^{-1}$.

To enable a move towards a micro-chip system, simple low cost techniques for the manufacture of polymer microchips and the incorporation of detection electrodes were developed using limited resources. Aluminium embossing master templates were trialled but found to suffer from variation in channel depths due to the template machining method. Soft lithography techniques were then pursued to produce positive PDMS master embossing templates. The embossing procedure was optimised and these templates were

found to produce high quality channel plates in PMMA. Several chip bonding methods were trialled including vacuum oven bonding and solvent bonding which were found to be either non-reproducible or unachievable. A low cost lamination bonding method was finally developed and optimised for the bonding of chips used in all further studies.

A simple, low cost method for incorporating contactless metal electrodes was developed by incorporating electrode channels into the channel plate. To incorporate the electrodes, the bonded chip was taken to 80$^{o}$ C, above the melting point of the alloy (≈ 70 $^{o}$C) and below the glass transition temperature of the PMMA (≈ 105 $^{o}$C), and the molten alloy drawn into the electrode channels with a syringe before being allowed to cool and harden. A 0.5 mm diameter stainless steel pin was then inserted into the alloy filled reservoirs of the electrode channels to provide external connection to the C$^{4}$D detector electronics. This advance provides for a quick and simple manufacturing process and negates the need for integrating electrodes using costly and time-consuming thin film deposition methods. No additional detector cell mounting structures were required and connection to the external signal processing electronics was achieved by simply slipping commercially available shielded adaptors over the pins. With a non-optimised electrode arrangement consisting of a 1 mm detector gap and 100 µm insulating distance, rapid separations of ammonium, sodium and lithium (< 22 s) yielded LODs of approximately 1.5 – 3.5 ppm. These LODs were significantly reduced in later experiments through the use of improved shielding arrangements but future optimisation of the electrode geometry, particularly the electrode length, the distance between the electrodes along the separation channel and the thickness of the insulating layer, will likely significantly improve these LODs even further.

Having demonstrated a viable on-line autonomous DCSI-CE system and developed a method for producing PMMA microfluidics with integrated $C^4D$ electrodes, a translation from the CE system described in Chapter 2 to the micro-chip format was made. Notably, it was desirable to incorporate a hydrodynamic injection mechanism to remove sample matrix bias effects and improve the quantitative performance of the system. Using the DCSI-CE dimensions as a starting point, we developed PMMA microchips incorporating the integral in-plane contactless conductivity detection electrodes developed in Chapter 3. A novel, hydrodynamic "split-injection" method utilised BGE sheathing to gate the sample flows, whilst control over the injection volume was achieved by balancing hydrodynamic resistances using external hydrodynamic resistors. The developed system was very robust, with individual microchips used for up to two thousand analyses with lifetimes limited by irreversible blockages of the microchannels. Injection was realised by a unique flow-through interface, allowing for automated, continuous sampling for sequential injection analysis by microchip electrophoresis. The unique dual channel geometry was demonstrated by the simultaneous separation of three cations and three anions in individual microchannels in under 40 s with LOD's ranging from 1.5 – 24 µM. From a series of 100 sequential injections the % RSDs were determined for every fifth run, resulting in % RSDs for migration times ranged from 0.3 – 0.7 (n=20), and 2.3 – 4.5 for peak area (n=20). This system offers low limits of detection, a high degree of reproducibility and robustness while the hydrodynamic injection eliminates electrokinetic bias during injection, making it attractive for a wide range of rapid, sensitive and quantitative online analytical applications. Whilst the system displayed advances in autonomy, repeatability and robustness, it was found that considerable unwanted hydrodynamic resistance was still extant under the optimised conditions, leading to a reduction in separation space and analytical performance. This was

due primarily to the geometry restraints of the 2D microchip manufacture method. It is proposed that a direct machining method briefly trialled in Chapter 3 for the production of the microchip negative relief master templates will enable the production of a PMMA chip with two different channel depths to improve the hydrodynamic ratios at the injection interface, leading to a significant reduction in hydrodynamic assistance. Additionally, like the DCSI-CE system presented in Chapter 2, the DCSI-ME system relied upon the use of one BGE for the separation of small anions and cations. To overcome this limitation, brief experiments with dyes to visualise the flow mechanism within the DCSI-ME chip system were conducted to examine the viability of simultaneously using two different BGEs separated by laminar flow for optimal separation chemistry of both anions and cations. Initial experiments indicated the viability of this approach with no instrumental, programming or microchip design modifications required, however, more work is required to realise this advance.

Having developed the DCSI-ME system and a number of other CE based systems, a small form factor multipurpose microfluidic platform for the conduct of advanced future studies of interest to the research group was designed and constructed. The design of this system was informed by the developments of all previous systems and was intended to leverage the benefits of both the instrumental simplicity and flexibility of CE with the reductions in analysis time of ME. The system was designed to be able to simultaneously perform a number of common microfluidic functions such as sample extraction and pre-concentration pre- or post-column derivatisation, electrophoretic separation and coupling to other flow or sequential injection systems. Evaluation of custom hardware components was conducted and testing of small, low cost custom $C^4D$ detectors showed only a ≈ 20% decrease in sensitivity as compared to high-end commercial $C^4D$ systems. The system,

however, is forward compatible with alternative detection methods including laser induced fluorescence detection (LIF). The developed system shows considerable potential for integrating multiple functions on or off-chip and is particularly suited for on-line multiplexed electrophoretic separations.